UNIVERSITY OF CINCINNATI

November 22 , 20 02

I, Alison B. Moore **,**

hereby submit this as part of the requirements for the degree of:

Doctor of Philosophy

in:

Chemistry

It is entitled:

CHARACTERIZING THE BINDING INTERACTION BETWEEN DICYANOGOLD (I) AND HUMAN SERUM ALBUMIN

Approved by:

Dr. Richard C. Elder, chair

Dr. Katherine Tepperman

Dr. William B. Connick

Dr. Apryll M. Stalcup

CHARACTERIZING THE BINDING INTERACTION BETWEEN DICYANOGOLD (I) AND HUMAN SERUM ALBUMIN

A dissertation submitted to the

Division of Research and Advanced Studies
of the University of Cincinnati

in partial fulfillment of the
requirements for the degree of

DOCTORATE OF PHILOSOPHY (Ph.D.)

in the Department of Chemistry
of the College of Arts and Sciences

2002

by

Alison B. Moore

B.S., Transylvania University, 1998
M.S., University of Cincinnati, 2000

Committee Chair: Richard C. Elder, Ph.D.

Abstract

Gold-based drugs have been used in the treatment of rheumatoid arthritis for over 60 years, yet the mechanism of action or these drugs is not understood clearly. This study focuses on an early step in the transport mechanism of gold drugs, namely the interaction of dicyanogold(I) (a common bio-transformation product of gold drugs) with human serum albumin (the most abundant protein in blood serum). These binding studies involve both qualitative and quantitative characterization of the binding interaction between dicyanogold(I) and two forms of human serum albumin (HSA): HSA with cysteine-34 in the native form and HSA with a blocking group bound to the sulfur of cysteine-34 (HSA•AA). The blocked protein is HSA treated with iodoacetamide so that cysteine-34, a known binding site for gold drugs, is prevented from participating in other covalent interactions.

Each form of HSA was characterized using two mass spectrometry techniques. FT-ICR-MS with electrospray ionization uses an acidic environment to add up to 60 protons to the HSA, lowering the mass to charge ratio to a value that can be detected easily by the mass spectrometer so that the intact protein can be characterized. MALDI-TOF-MS forms predominantly singly charged ions, thus it is necessary to perform an enzymatic digest of the HSA before analysis. Subsequently, individual fragments were studied yielding information about the form of cysteine-34 (native vs. blocked).

A series of experiments were conducted in which the effect of changing the conditions of the system on the equilibrium constant, Keq, was studied. These experiments include varying the initial concentration of dicyanogold(I) used, the ionic strength of the buffer solution and the incubation temperature of the system. Additionally, a series of experiments that tested the reversibility of this binding were conducted. Reversed phase ion-pairing chromatography was

used to determine that the gold species released from the protein after establishing equilibrium was dicyanogold(I). Throughout these experiments, both HSA and HSA•AA were used. Comparing the results of these experiments using different forms of the protein shows that there is a relationship between the binding site for dicyanogold(I) on HSA and cysteine-34, though covalent binding is not observed.

To my family

Acknowledgments

In the course of completing my graduate work, I have encountered people that have been a tremendous help to me. First, I thank my Ph.D. advisor Dick Elder for support when I needed it, for guidance when it was necessary and for encouraging me to develop as an individual. I also want the members of my Ph.D. committee, Katherine Tepperman, Apryll Stalcup and Bill Connick, to know how much I have appreciated their input and suggestions throughout my graduate career.

At times during my life as a graduate student, it seemed that my committee included most of the Department of Chemistry, and thus I wish to single out a few people who made themselves available when I had questions, concerns or issues with my project. Pat Limbach, thank you for everything; though your contributions are too numerous to count, without your expertise in mass spectrometry, or your students hours of labor, my dissertation would be a completely different entity. Bruce Ault, thank you for the impromptu physical chemistry discussions. Brian Halsall, thank you for giving me a biochemist's point of view when I needed it most.

The graduate experience for each student is unique. My experience at the University of Cincinnati has been shaped by my interaction with the entire department. I am a Ph.D. chemist because of the support and guidance I have received from the entire department. Specifically, I wish to thank the rest of the Elder group (especially Nathan, who makes the impossible happen), the Connick group, the Baldwin group, the Limbach group and that random organic guy, I hope each of you know how much I gained from you friendship and I wish you the best of luck in finishing your graduate work.

Finally, without the support of all of my friends (you know who you are) and family (i.e. the 2 Georges and my grandparents), I would have gone completely insane long ago…

Table of Contents

Chapter 2. Experimental

Chapter 3. Results and discussion

List of figures

page #

List of Tables

Chapter 1:

Introduction

Throughout history it has often been the case that effective drugs were discovered by accident. Similarly, drugs that were initially intended for the treatment of a specific ailment were found to be equally, if not more, effective in the treatment of a different condition. In these situations, the drug discovery comes first and the mechanism of action is determined later. The driving force behind this approach is that, while patients are effectively treated, new generations of similar drugs can be developed that are more effective and less expensive to produce than the original drug. It is the aim of this research to study a portion of the mechanism of action of anti-rheumatic gold drugs. Specifically, the binding interaction between dicyanogold(I), a common bio-transformation product of all gold drugs, and human serum albumin, the most abundant protein in blood serum, in the context of drug transport in blood will be addressed.

In this work two types of experiments have been designed to study the binding interaction between dicyanogold(I) and human serum albumin. The first type of experiment involves perturbing the equilibrium and analyzing the gold species released by the protein. Experiments of this type have been designed so that the gold that is released from the protein can also be quantified. Data gathered during these experiments are used to determine the nature, whether covalent or electrostatic, of the binding interaction. The second type of experiment focuses on the determination of the binding constant, K_{eq}, under a series of different conditions. These experiments were designed to study the change in the amount of dicyanogold(I) that binds to human serum albumin under different equilibrium conditions. In both types of experiments two forms of the protein are used, normal HSA (the form found in blood serum) and blocked HSA (protein that has been treated to alkylate cysteine-34). The data from each set of experiments are used to determine the change in binding as a result of altering a single amino acid in the protein

sequence, and thus the influence of this amino acid (cysteine-34) on the binding of dicyanogold(I) to HSA can be determined.

During the course of this research it was determined that a significant portion of the protein, as it is found in the purchased sample, contains an extraneous cysteine bound to the protein through a disulfide linkage with cysteine-34. Therefore, it was necessary to pre-treat the protein to restore cysteine-34 to the form that can be found circulating in blood plasma. The method selected for reduction of this disulfide was chosen so that the native disulfide linkages found in serum albumin remained intact. Thus it was possible to use homogenous protein samples throughout these experiments.

A. Rheumatoid arthritis

Rheumatoid arthritis is a systemic inflammatory disease that affects the synovial membranes located within joints. This disease is characterized by inflammation and deterioration of the joint. A likely autoimmune disease, RA leads to immune system attack on the synovial membranes and the cartilage found within the joint ultimately leading to fusion of the bones and loss of function of the joint. Rheumatoid arthritis affects 1-2% of the general population, and currently, there is no cure. Traditional treatment of RA involves administration of NSAIDs (non-steroidal anti-inflammatory drugs which relieve pain and inflammation. A second class of drugs, known as DMARDs (disease-modifying anti-rheumatoid drugs), is known to slow the progression of the disease and, in some cases, cause remission. Gold-based drugs prescribed for the treatment of rheumatoid arthritis fit into the latter category. (This and other information about rheumatoid arthritis is available through publications provided by the Arthritis Foundation or by visiting their website at http://www.arthritis.org.)

B. Gold drugs

Like most DMARDs, gold drugs were not initially intended for use in treating rheumatoid arthritis. In fact, gold drugs were first administered over 100 years ago as a treatment for tuberculosis. It was not until the mid-1930's gold drugs were first being used for rheumatoid arthritis.[1] Currently there are three gold drugs in use including myochrysine (gold(I) thiomalate), solganol (gold(I) thioglucose) and auranofin (triethylphosphinegold(I) tetraacetylthioglucose). (Figure 1) Of these drugs, only auranofin is taken orally, the other two are injectable drugs.

Generally, DMARDs are slow-acting and use must be continued for several weeks before any benefit is noted. Gold drugs are no exception to this rule. Although gold drugs have been shown to be effective in approximately 50% of patients, side effects are often severe enough to require cessation of treatment.[2]

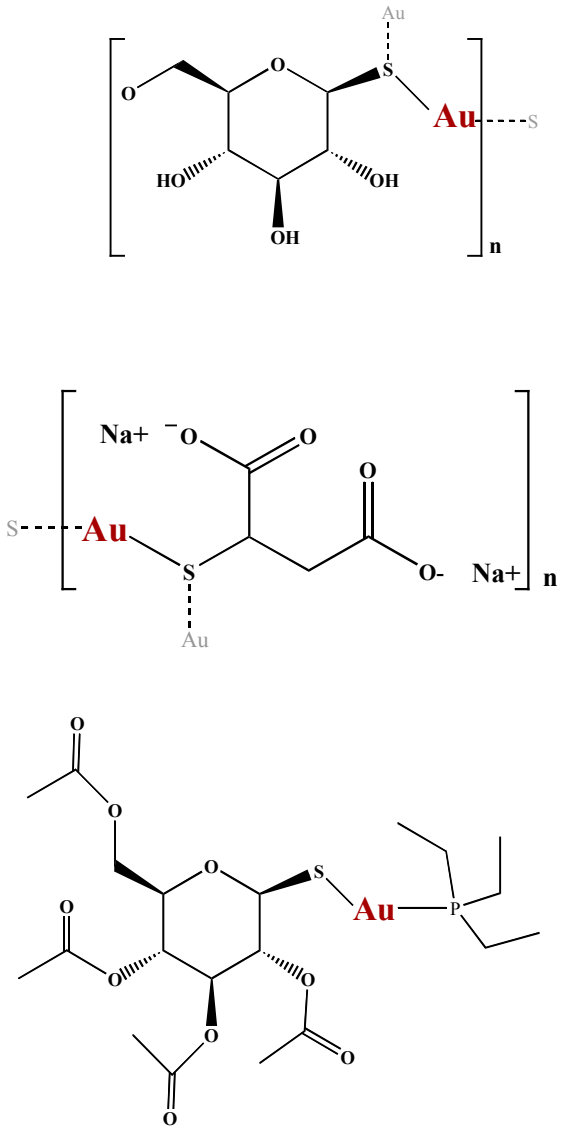

Figure 1. The gold drugs currently in clinical use are, from top, Solganol, Myochrysine and Auranofin.

Gold drugs are prodrugs, drugs that change form once inside the body. These gold drugs are known to interact with human serum albumin at cysteine-34. Each of the gold drugs contains a single gold(I) atom coordinated by two ligands, at least one of which is bound to the gold through the sulfur atom. The parent compounds undergo a ligand exchange reaction upon binding to serum albumin, exchanging the sulfur of the ligand in the drug with the sulfur of

cysteine-34.[11] (Figure 2) *In vitro* studies involving the uptake of gold drugs by red blood cells have determined that of the two types of drugs, injectable or oral, only the oral drug Auranofin appeared to cause the accumulation of gold in the RBC lysate in significant amounts.[3] It may be significant to note here that after studying the results of 66 clinical trials, Auranofin was shown to be somewhat less effective than its injectable predecessors.[4]

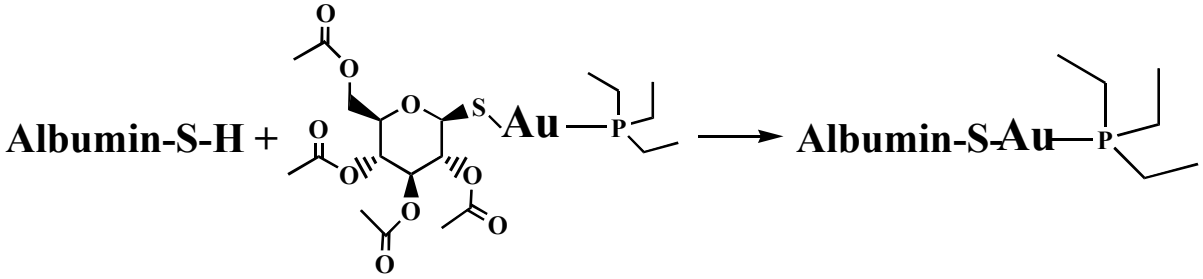

Figure 2. Reaction of Auranofin with cysteine-34 of serum albumin.

In studies of blood and urine samples from patients receiving gold therapy, none of the parent gold compounds could be detected.[5] Instead, it was found that most of the gold in circulation had become protein bound or was taken up by red blood cells.[3, 5] The small molecule gold left in plasma that could be identified was the dicyangold(I) anion. (Figure 3) The concentration of (free) dicyanogold(I) found in patient blood samples ranges from 0.7 ppb up to 15 ppb.[5, 6]

Figure 3. The dicyangold(I) anion has a 5 atom linear structure.

C. Dicyanogold(I)

Dicyangold(I) is a linear anion that carries a negative charge and is a bio-transformation product common to all of the gold drugs mentioned above.[5] Shaw and coworkers have shown that dicyanogold(I) binds in significant amounts to bovine serum albumin.[15] The ability of this anion to inhibit the oxidative burst of PMN (polymorphonuclear leukocytes) has led to the hypothesis that formation of this species, *in vivo*, may slow the progression of rheumatoid arthritis.[7] It is known that red blood cells actively take up dicyanogold(I).[3, 8] Due to this behavior, as well as the ability to interfere with the oxidative burst, dicyanogold(I) is believed to play an important role in the mechanism of action of gold drugs. *In vitro* studies of the efflux of gold from Auranofin-treated[8] and dicyanogold(I)-treated[3] red blood cells have shown that serum albumin successfully competes with RBC's for Auranofin but not for dicyanogold(I), suggesting two different binding interactions with serum albumin, i.e. one mechanism for drug binding and another mechanism for anion binding. In trying to elucidate the transport mechanism of this common product, various groups have focused on the interaction between dicyanogold(I) and serum albumin, the most abundant protein found in blood serum.

D. Serum albumin

Serum albumin, as mentioned above, is the most abundant protein found in blood serum. It is a carrier protein with a number of metal binding sites, fatty acids sites as well as sites for other molecules.[9] The tertiary structure of serum albumin is primarily defined by the 17 disulfide bonds which keep the protein tightly wound even under widely variable conditions. In general, serum albumin has three forms that vary with pH keeping the disulfide bonds intact until the pH is below 2.5, at which point the protein denatures.[10(p. 65)] In addition to the 34 cysteine residues that participate in disulfide bonding, there is a single cysteine that does not, this cysteine is called cysteine-34 as it is the 34th amino acid in the structure of albumin.

Serum albumin, either human or bovine, is isolated from whole blood. During the purification process a significant portion of the thiol of cysteine-34 becomes blocked with another cysteine forming a cystine disulfide.[11] (Figure 4) The amount of albumin available commercially that is found in the free thiol form varies between 30 and 50%, depending on the

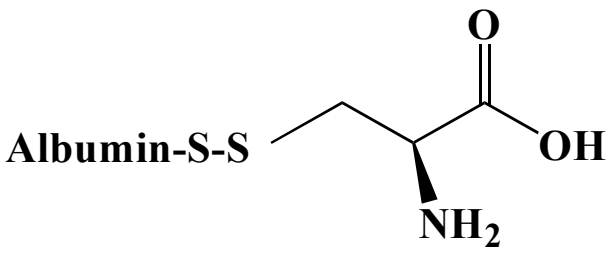

Figure 4. Serum albumin blocked by cystine formation at cysteine-34.

particular lot and is a side effect of the purification process. It is reported by Sadler, *et al,* that less than 10% of the thiol of human serum albumin in circulation is blocked in this manner.[11] In

general, the thiol content of commercially available bovine serum albumin (BSA) is believed to be more consistent from lot to lot and therefore is often used as a substitute for the human protein without treatment to restore the thiol at cysteine-34. Additionally, the two albumins are structurally similar, both containing 17 disulfide bonds and one free thiol, of cysteine-34. The calculated molecular mass for HSA is 66438 Daltons, while the calculated molecular mass for BSA is 66411 Daltons[10 (p. 25)]. Except for the comparison of techniques for binding constant determination where bovine serum albumin was used, the protein being studied here was human serum albumin.

Because of the variation in the amount of free cysteine-34 in different lots of albumin, binding studies require steps to produce a more uniform protein preparation in order to successfully study the interaction of serum albumin with other molecules. This becomes extremely important, in cases such as this, where the binding site could actually be dramatically different from one lot to the next. There are a number of methods available for the reduction of protein disulfides. The most widely used reducing agent, dithiothreitol, is known to reduce all of the disulfide bonds of serum albumin under certain conditions.[12] As a result, it becomes difficult to protect the internal disulfides while fully reducing the cystine disulfide of cysteine-34. Because cysteine-34 is the most exposed of the 35 cysteine residues, it is possible to use milder reducing agents to fully reduce the cystine disulfide of cysteine-34. Though it is located near the surface of the protein, the environment of cysteine-34 is restricted so that the binding of large molecules to cysteine-34 is accompanied by a local conformational change. In this respect, the cystine disulfide present at cysteine-34 is easily reduced by reaction with glutathione (GSH), a reducing agent milder than dithiothreitol. Because of its size, glutathione is too bulky to easily react with cysteine-34 to form a protein-glutathione disulfide. In this reaction, glutathione

preferentially forms a mixed disulfide with the non-native cysteine.[13] (Figure 5) The albumin species referred to as HSA throughout this work is human serum albumin that has been pre-treated with glutathione to restore cysteine-34 to its native conformation.

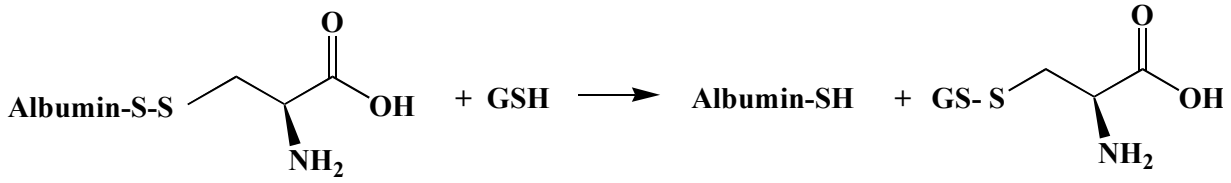

Figure 5. Serum albumin, blocked by cystine formation at cysteine-34, reacts with glutathione to yield a mixed disulfide and an albumin molecule with a free thiol at cysteine-34.

E. Cysteine-34

Cysteine-34 is part of the loop of amino acids between helices h2 and h3 and is located near the surface of the protein. Though it is near the surface, cysteine-34 lies within a hydrophobic crevice 9.5-10 Å deep that protects the thiol from oxidation. [10 (p. 54), 11] It has been determined by Sadler, et al, that upon ligand binding to cysteine-34, the protein undergoes a conformational change consistent with the widening of the crevice and the "flip out" of cysteine-34.[11] The pK of free cysteine is normally ~8.5, though the thiol of cysteine-34 of serum albumin has a pK value closer to 5. Therefore, at the pH of blood (7.40), the majority of cysteine-34 in circulation is present as the thiolate form, which carries a negative charge.[10 (p. 53)] Using an estimated pK of 5.5, the ratio of thiolate to thiol can be calculated for pH 7.4 using equation 1. The calculated ratio is 0.013 SH/S^-, or 1.3% of the protein is in the thiol form.

$$pH = pK + \log (SH/S^-) \qquad \text{(eq. 1)}$$

F. Characterization of serum albumin

1. UV-visible spectroscopy

The UV-visible spectrum of serum albumin is featureless in the visible range and has one useful band near 280 nm as shown in Figure 6. In human serum albumin, the absorption at 280 nm ($\varepsilon = 36600\ M^{-1}cm^{-1}$)[14] can be used to determine the concentration of albumin in solution.

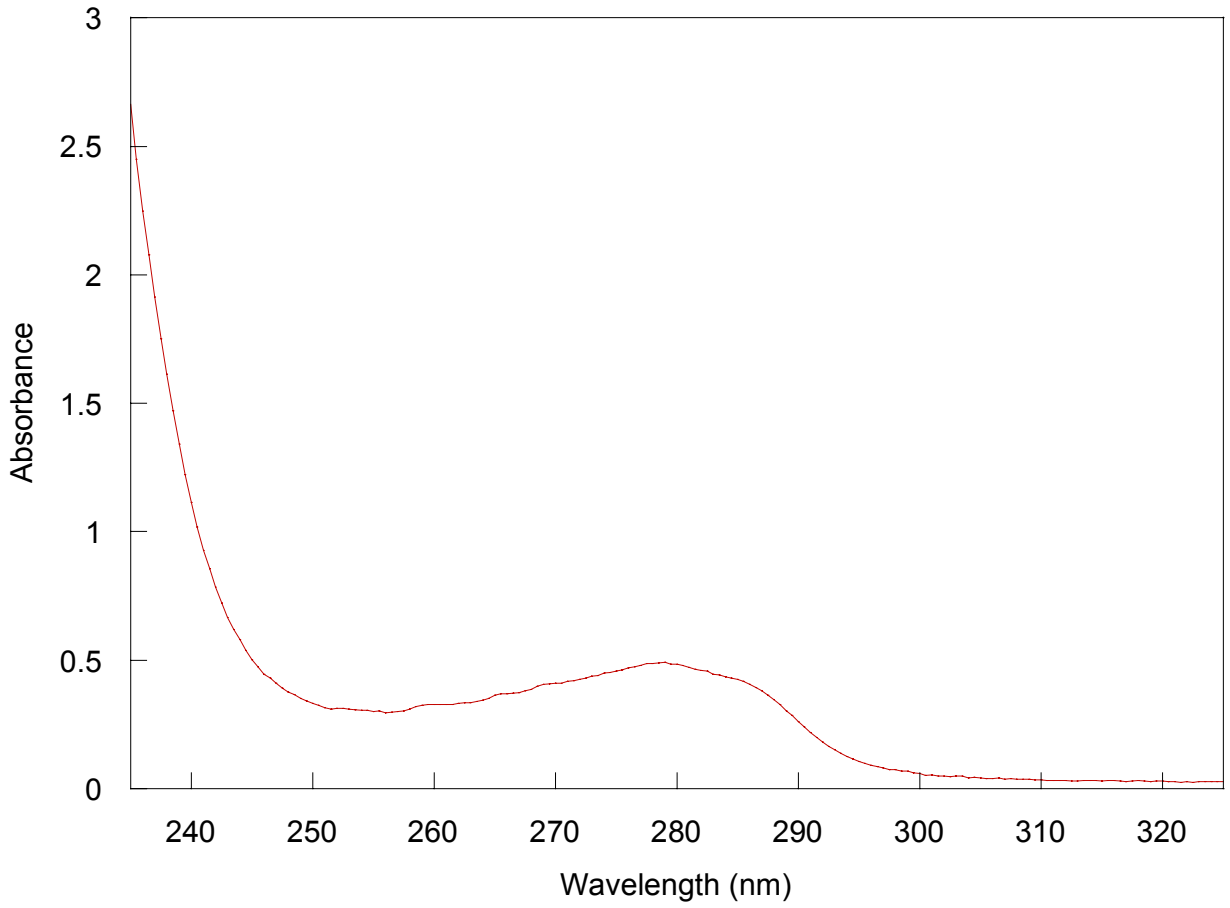

Figure 6. UV-visible spectrum of human serum albumin in water.

2. FT-ICR-MS

Mass spectrometry can also be used to characterize HSA. In order to study the intact molecule the m/z ratio must be within the limits of the detector. Fourier transform ion cyclotron resonance mass spectrometry (FT-ICR-MS) can detect ions with m/z in the range of 400-2500. Using electrospray ionization, it is possible to generate molecular ions with 60 or more positive charges on HSA in an acidic environment.[24] (Figure 7) It is important to note here that de-salting protein samples is necessary because the calculation of protein mass assumes that all of the charged species added to the protein are protons, not sodium or potassium ions. Calculation of both the charge state of the protein and the mass of the protein in Daltons is explained further in the results section. Though FT-ICR-MS allows us to look at the unfragmented protein, the resulting peaks are average mass peaks rather than the isotopic distribution of peaks seen with smaller molecules. The limitation of FT-ICR-MS lies with the ability of the instrument to resolve adjacent peaks.[24] Currently, with the instrumentation available at the University of Cincinnati, peaks arising from a difference of at least 45 Daltons can be distinguished easily from one another.

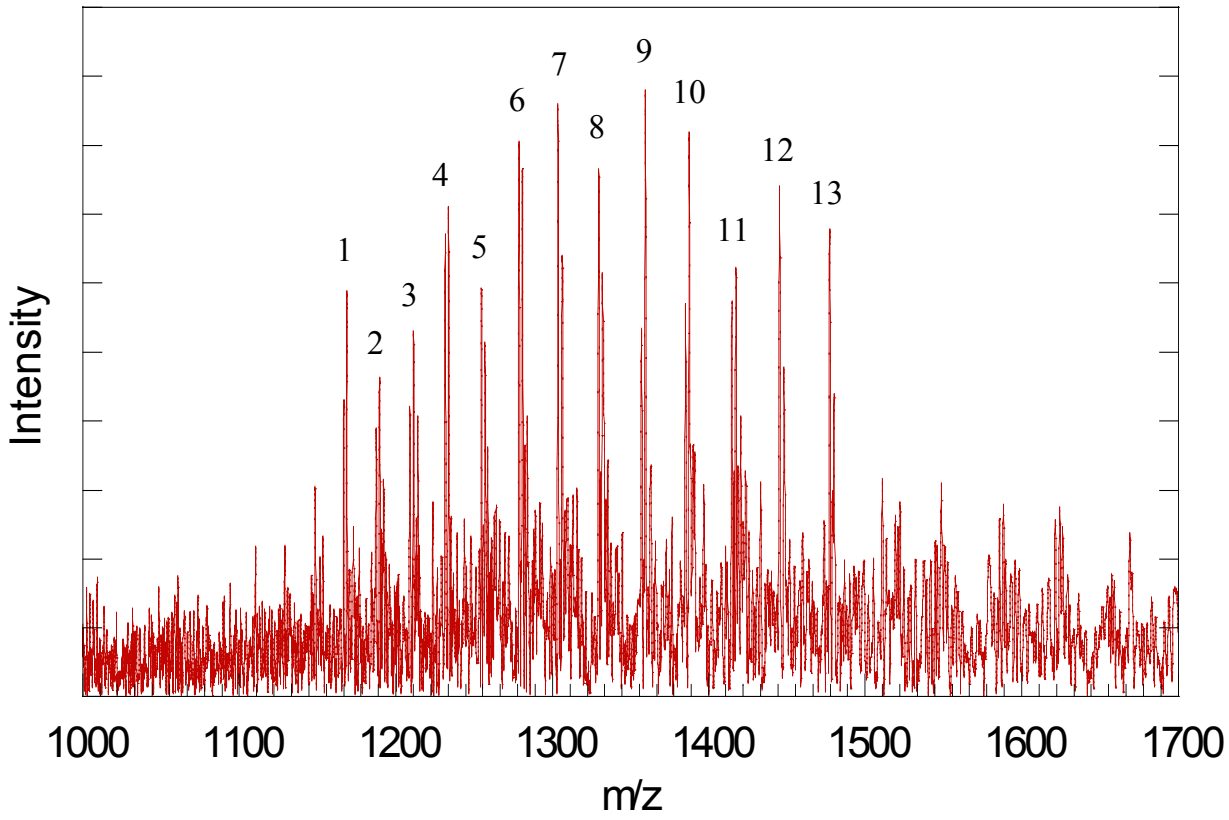

Figure 7. Representative FT-ICR-MS (normal HSA, not treated with glutathione) prepared in 50/50 acetonitrile/water with 1% formic acid. Masses of HSA (first) peak of each group and calculated charge state: 1) 1166.5907 (57+), 2) 1187.3496 (56+), 3) 1208.8545 (55+), 4) 1231.3476 (54+), 5) 1254.5338 (53+), 6) 1278.6712 (52+), 7) 1303.5879 (51+), 8) 1329.7828 (50+), 9) 1356.8374 (49+), 10) 1385.1490 (48+), 11) 1414.6300 (47+), 12) 1445.3826 (46+), 13) 1477.3656 (45+).

3. MALDI-TOF-MS

Matrix assisted laser desorption ionization time-of-flight mass spectrometry (MALDI-TOF-MS) is also widely used in the characterization of proteins. This method forms predominantly singly charged ions, though in more concentrated samples doubly and even triply charged ions may be seen. The mass limit of MALDI-TOF-MS is approximately 40000 Daltons, at which point resolution, precision and accuracy suffer greatly.[25] The utility of MALDI-TOF-MS lies with the ability to look at the well-characterized enzymatic digests that are used to break the protein into manageable pieces rather than at the entire protein molecule.[26] In this work trypsin, which cuts on the C-terminal side of arginine and lysine, is used to digest HSA so that covalent interactions at cysteine-34 can be studied specifically. Typically in a tryptic digest, the disulfide bonds of a protein are reduced with dithiothreitol and subsequently alkylated to prevent oxidation back to the disulfide before digestion.[25] Because we are looking specifically at the fragment that contains cysteine-34 and no other cysteine residues, reduction and alkylation of the disulfide bonds are unnecessary. (Figure 8)

K/ALVLIAFAQYLQQCPFEDHVK

Figure 8. The resulting amino acid sequence ranging from ala-21 to lys-41 containing cysteine-34 of HSA after digestion by trypsin is represented by the one-letter code for amino acids.[10]

The calculated mass of the fragment represented in Figure 8, 2433.9 Da[26], can be used to determine the expected masses of fragments of HSA that have been modified at cysteine-34

through covalent bond formation. Through MALDI-TOF-MS, it is possible to determine if modifications of HSA, intended for reaction with cysteine-34, have taken place at the expected site.

G. The binding interaction between dicyanogold(I) and serum albumin

Investigating the behavior of the dicyanogold(I)-HSA system at physiologically relevant concentrations was the main focus of this project. Recall that dicyanogold(I) is a small, linear anion. There are two possible mechanisms for interaction between dicyanogold(I) and serum albumin that retain a two-coordinate gold(I): covalent or electrostatic. A covalent binding mechanism similar to that observed for gold drugs would involve the loss of a cyanide ligand in order to bind to the sulfur of cysteine-34. (Figure 9) In an electrostatic binding mechanism, the dicyanogold(I) anion would bind intact to some positively charged region of the protein. (Figure 10)

Figure 9. Covalent interaction between dicyanogold(I) and serum albumin.

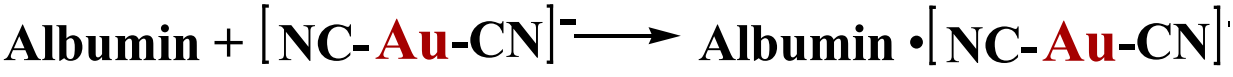

Figure 10. Electrostatic interaction between dicyanogold(I) and serum albumin.

Because cysteine-34 is a known binding site for gold drugs, the investigation of the binding interaction between dicyanogold(I) and serum albumin focuses on this site. The most obvious course of action is to render cysteine-34 incapable of forming a covalent bond, as is observed with gold drugs, without otherwise altering the protein. A direct method for accomplishing this is simply to alkylate the thiol of cysteine-34. Recall that, in MALDI-TOF-MS, treatment of the disulfide bonds of proteins with dithiothreitol is often followed by alkylation of the cysteine residues to prevent oxidation back to the disulfides. The same approach used in MALDI-TOF-MS can be used to alkylate the thiol of cysteine-34. Without treating serum albumin with dithiothreitol, there is only one thiol available for alkylation, cysteine-34. As a result, some of the cysteine-34 of the protein is blocked with cysteine while the rest is blocked with the alkylating agent.

A small alkylating agent, iodoacetamide, is often used after reaction with dithiothreitol as well as for the specific purpose of alkylating cysteine-34 in serum albumin.[15] Iodoacetamide was chosen for use in this study because it is a small but selective alkylating agent that reacts quickly with cysteine-34.[13,16] (Figure 11) Other larger groups that could be used include *N*-ethylmaleimide and acrylonitrile, among others.[10 (p. 53)] Evidence presented in the results section for MALDI-TOF-MS analysis shows that reaction with iodoacetamide does not replace the non-native cysteine bound to cysteine-34, but this reaction adds an acetamide to albumin molecules that are not already blocked. Thus, commercial albumin, containing a mixture of blocked and unblocked cysteine-34 contains two different groups bound to cysteine-34 when reacted with iodoacetamide. Therefore, to generate a uniform population, it is necessary to pretreat the protein with glutathione to remove the excess bound cysteine before alkylation.

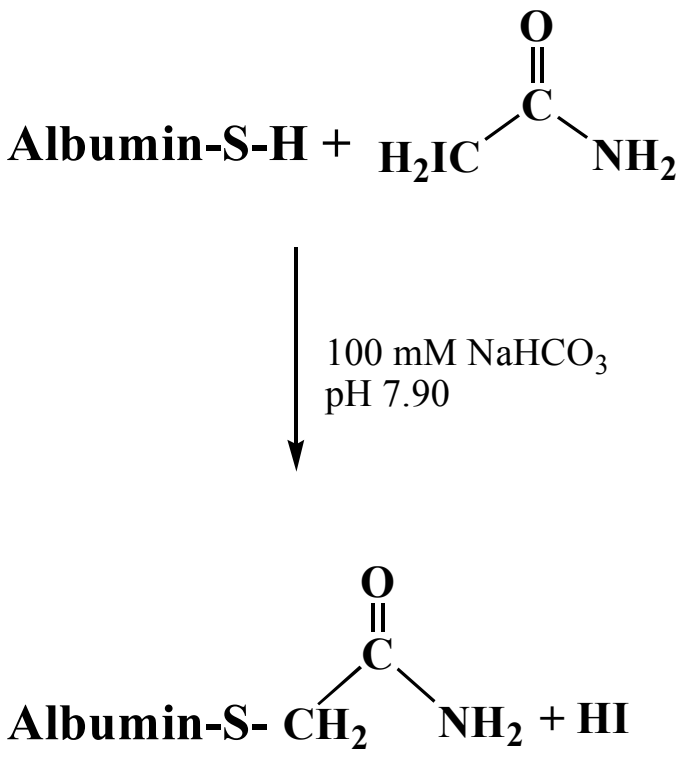

Figure 11. Reaction of serum albumin with iodoacetamide, a common alkylating agent.

Though blocking cysteine-34 through formation of a cystine disulfide is, in fact, commonly used as a method for blocking, it has been conspicuously left out of this discussion thus far. The reason for this omission is specific to this study. It is known that cyanide, like dithiothreitol, reduces disulfide bonds of proteins.[13] Cyanide, unlike other reducing agents, forms a covalent bond with the sulfur of cysteine, so that the net result is an exchange of cyanide for cysteine.[16] Because dicyanogold(I) solutions contain some small, equilibrium amount of free cyanide, the cyanide in the solution has the potential to react with the readily reducible cystine disulfide of

cysteine-34. For this reason, all serum albumin used for these experiments was treated with glutathione to restore the thiol of cysteine-34. The albumin species referred to as HSA•AA is human serum albumin that was pre-treated with glutathione to restore cysteine-34 to its native form followed by alkylation with iodoacetamide.

H. Studying the binding interaction

Throughout this work the binding interaction between dicyanogold(I) and serum albumin is compared to the binding interaction between dicyanogold(I) and serum albumin that is blocked at cysteine-34 with acetamide. Equilibrium is established between albumin-bound dicyanogold(I), free dicyanogold(I) and free albumin. (Figure 12)

$$\text{Albumin} + \text{Au(CN)}_2^- \underset{}{\overset{K_{eq}}{\rightleftharpoons}} \text{Albumin} \bullet \text{Au(CN)}_2^-$$

Figure 12. Chemical equation representing the equilibrium established in the dicyanogold(I)-HSA system.

The binding interaction between dicyanogold(I) and serum albumin is studied through experiments that vary the incubation conditions of the system. Varying the incubation conditions effects a change in the binding constant of the system. Through careful

monitoring of the incubation conditions, much can be learned about the binding interaction between these two molecules. The equilibrium constant, K_{eq}, measures the strength of the binding interaction between dicyanogold(I) and serum albumin. I needed to determine consistently the binding constant after incubation under different conditions. The following equation is used to calculate K_{eq}.

$$K_{eq} = \frac{[\text{albumin}\bullet Au(CN)_2^-]_{eq}}{[\text{albumin}]_{eq}\,[Au(CN)_2^-]_{eq}} \qquad \text{(eq. 2)}$$

Since the initial concentrations of both the albumin and dicyanogold(I) can be determined directly, only one of the terms from the above equation must be measured in order to calculate the three equilibrium values and thus the binding constant. Two methods of binding constant determination have been explored during this project, though only one, ultrafiltration, will be discussed here. A discussion of the second method, Penefsky chromatography, can be found in appendix A.

I. Binding constant determination using ultrafiltration

Determining the binding constant of the dicyanogold(I)-HSA system necessarily requires measurement of some quantity at equilibrium. Specifically, one needs to measure the equilibrium concentration of the albumin-dicyanogold(I) complex, the free dicyanogold(I) or the free albumin as well as the initial free dicyanogold(I) and free albumin concentrations in order to calculate K_{eq}. Ideally, one would be able to directly measure the equilibrium concentration of the albumin-dicyanogold(I) complex by monitoring a change in the UV-visible spectrum of albumin upon dicyanogold(I) binding, but there is no detectable change in the spectrum. It was therefore necessary to measure the concentration of free dicyanogold(I) and to achieve this I needed to separate the components of the incubation solution so that the equilibrium established among the three species in solution was maintained. These separations were accomplished using ultrafiltration.

Ultrafiltration uses centrifugal force and a filtration membrane to separate components of a solution based on the molecular weight of the molecules in solution. Each ultrafilter has three main components: sample reservoir, receiver tube and filtration membrane. (Figure 13) The filtration membrane is a porous material that restricts the passage of molecules based on molecular weight. As a result, smaller molecules are allowed to pass through into the receiver tube while larger molecules are retained in the sample reservoir. The proper membrane for a given system will have a nominal molecular weight limit (NMWL) that lies between the molecular weights of the components being separated. For example, the separation of serum albumin (~66,400 Da) from dicyanogold(I) (249 Da) is easily accomplished with a 30,000 NMWL filtration membrane.

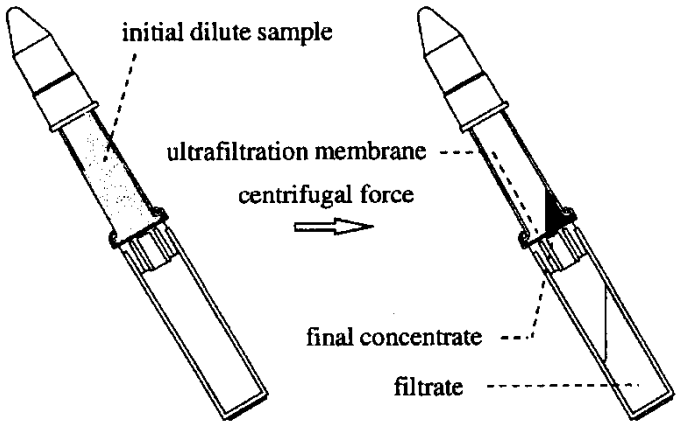

Figure 13. Typical ultrafilter before and after centrifugation.

Ultrafiltration is a method that works well for this separation because the equilibrium of the system is maintained throughout centrifugation.[17] The net result of ultrafiltration is concentration of the high molecular weight species, i.e. both gold-bound and free albumin. In this case, both protein species are concentrated ; however, their concentration ratio remains constant in the retentate. Thus the equilibrium is maintained as long as free dicyanogold(I) passes through the filter without changing concentration. This is demonstrated mathematically through algebraic manipulation of equation 1 used for calculating K_{eq}.

$$K_{eq} = \frac{[albumin \bullet Au(CN)_2^-]_{eq}}{[albumin]_{eq}\,[Au(CN)_2^-]_{eq}} \qquad \text{(eq. 2)}$$

Separating the terms of this equation we get:

$$K_{eq} = \frac{[albumin \bullet Au(CN)_2^-]_{eq}}{[albumin]_{eq}} \times \frac{1}{[Au(CN)_2^-]_{eq}} \qquad \text{(eq. 2)}$$

The revised equation shows that in order for K_{eq} to remain constant while the protein components are being concentrated, the concentration of dicyanogold(I) in solution must also remain constant. Since the concentration of dicyanogold(I) in the solution does not change during separation, the concentration of dicyanogold(I) in the filtrate is the equilibrium concentration of dicyanogold(I) for the system. (Figure 14)

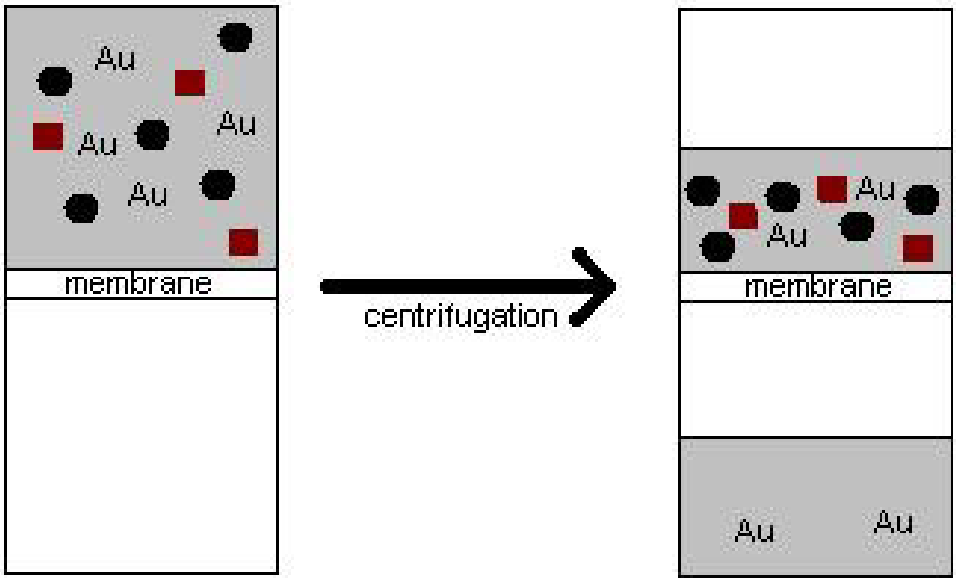

Figure 14. The concentration of dicyanogold(I) remains constant throughout ultrafiltration.
● -represents free albumin, ■-represents albumin with gold bound, **Au**-represents free dicyanogold(I)

At this point, the concentration of free dicyanogold(I) at equilibrium can be measured directly by analyzing the gold content of the filtrate. Both the equilibrium concentration of the albumin-gold complex and the equilibrium concentration of free albumin can be calculated from

the initial concentrations of dicyanogold(I) and albumin and the equilibrium concentration of free dicyanogold(I).

$$[\text{albumin}\bullet\text{Au(CN)}_2^-]_{eq} = [\text{Au(CN)}_2^-]_{initial} - [\text{Au(CN)}_2^-]_{eq} \quad \text{(eq. 3)}$$

$$[\text{albumin}]_{eq} = [\text{albumin}]_{initial} - [\text{albumin}\bullet\text{Au(CN)}_2^-]_{eq} \quad \text{(eq. 4)}$$

The values calculated from these equations can be substituted into the expression for K_{eq}, and the binding constant for the system can now be calculated.

J. Gold specific detection and Inductively Coupled Plasma Mass Spectrometry

In the work done by Shaw, et al, the concentration of gold in individual samples was determined by Flame Atomic Absorption Spectroscopy (F-AAS).[15] In general, the quantitative range of F-AAS is between 0.1 and 100 parts per million (1 ppm = 1 x 10^{-6} g Au/g of solution).[18] In this work, gold concentrations are determined exclusively using Inductively Coupled Plasma Mass Spectrometry (ICP-MS) which has a linear, quantitative range between 0.1 and 100 parts per billion (1 ppb = 1 x 10^{-9} g Au/g of solution). The quantitative range represents the range of concentrations that can be determined without making additional dilutions or taking extra measures to reduce the elemental background. The sensitivity of ICP-MS is such that a physiologically relevant concentration of dicyanogold(I) can be studied, which was not possible with F-AAS. Another attribute of ICP-MS is that the instrument can easily be interfaced with an

HPLC system to provide not only quantitative analysis of specific elements, but also provide a method for speciation. A full discussion of HPLC with ICP-MS detection of gold-containing compounds can be found in Chapter 1 of the doctoral dissertation of Yafei Zhang, University of Cincinnati.[6]

K. Reversibility of dicyanogold(I) binding

Evidence gathered by Shaw, et al., supports an electrostatic binding mechanism between dicyanogold(I) and bovine serum albumin. Using ^{13}C NMR spectroscopy of the associated dicyanogold(I)-BSA complex, it has been shown that the dicyanogold(I) anion remains intact in both BSA and BSA•AA, so that the reaction of dicyanogold(I) with BSA does not involve ligand exchange with the loss of a cyanide.[15] Studies using Mössbaur spectroscopy have been interpreted to show that upon binding to BSA, dicyanogold(I) remains linear and 2-coordinate.[19] However, it should be noted that both of the above studies used much higher binding levels of dicyanogold(I) than are obtained under physiologically relevant conditions. Thus, if the physiologically relevant binding site held a very minor portion of the bound dicyanogold(I), then the nature of the gold species at that site would be totally unknown. In fact, equilibrium studies indicate that there are other binding sites with different binding affinities that come into play under high dicyanogold(I) to albumin ratios.

Of the two possible binding mechanisms for the interaction between dicyanogold(I) and serum albumin, only the non-covalent mechanism is expected to be reversible under these experimental conditions, where excess dicyanogold(I) and cyanide have been removed. In an

environment that contains excess cyanide, it is possible for the covalent mechanism to appear as reversible, intact binding, so that the net result of such a "reversible" interaction would be cyanide exchange.

Using a combination of techniques, it is possible to analyze the gold-containing species released by the protein after establishing equilibrium. Two experiments which I performed explored the reversibility of the binding interaction between dicyanogold(I) and HSA; each provided evidence to support the electrostatic binding mechanism.

In the first of these experiments, the amount of gold released from the HSA was studied. In order to force the release of bound gold by the protein, the free dicyanogold(I) present at equilibrium was removed. This was accomplished by placing the incubated solution in a Penefsky size exclusion column that removes small molecules from the solution. (see Appendix for a full discussion of the technique) After the free dicyanogold(I) was removed from the solution, the equilibrium was re-established between dicyanogold(I), HSA and HSA•$Au(CN)_2^-$. Any free gold that was present in the re-equilibrated solution was gold that has been released from the protein. (Figure 15) The re-equilibrated solution could be separated using ultrafiltration and the equilibrium constant, $K_{re\text{-}eq}$, for the re-equilibrated solution could be determined. It was necessary, before ultrafiltration, to re-measure the total concentrations of albumin and dicyanogold(I) in order to establish new initial concentrations of these species.

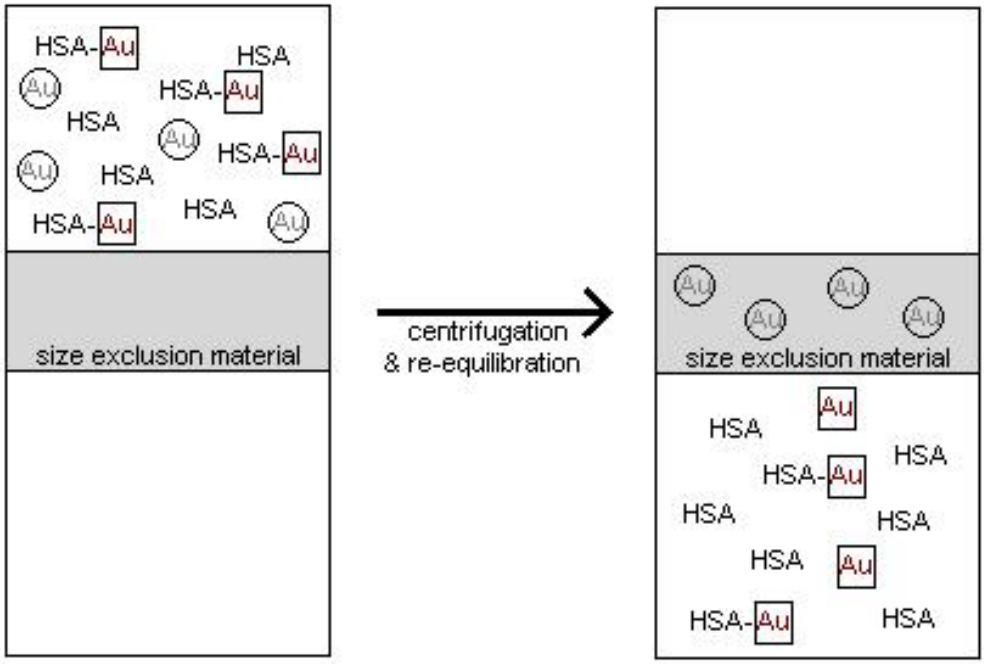

Figure 15. Distribution of free gold before and after Penefsky chromatography. The circled gold represent free gold after the initial equilibrium is established and squared gold represents gold that is/was bound to HSA.

In the second of these experiments, the gold that was released by the HSA was analyzed to determine the chemical species. Speciation of the gold compounds using reverse phase ion-pairing chromatography (RP-IPC) with ICP-MS detection has been thoroughly explored by previous group members. (For a complete discussion of the techniques developed refer to chapter 3 of the doctoral dissertation of Yafei Zhang.[6]) In this experiment the ultrafiltrate from the re-equilibrated solution was analyzed first for total gold content, then analyzed via RP-IPC to determine the chemical form of the gold.

Since it is possible that the gold species may undergo a chemical change upon binding to HSA, it is also possible that a "new" gold species will be fully retained by the chromatographic column. Thus, it is necessary to quantify the amount of gold that is represented by the chromatographic peaks. The species that is expected is dicyanogold(I), so standard solutions that contain known concentrations of dicyanogold(I) can be chromatographed and subsequently used to construct a calibration line. In order to do this, the area of the peaks is compared to one another. The process used to quantify the area of the peaks is described in Chapter 3. This made it possible to determine that all of the gold released by the HSA upon re-equilibration was dicyanogold(I), which supports a reversible, electrostatic binding mechanism.

L. Changing the equilibrium conditions of the dicyanogold(I)-HSA system

The binding constant, K_{eq}, of the dicyanogold(I)-HSA system is affected by changes in the incubation conditions. Figure 16 illustrates the simplified chemical equilibrium assumed for this study. Information about the binding interaction between dicyanogold(I) and HSA can be collected by monitoring the change in K_{eq} with respect to specific factors that perturb the equilibrium. It is important to keep in perspective the conditions that have been altered throughout these experiments. First, the ratio of dicyanogold(I) to HSA found *in vivo* is very low (Introduction, section A), so the ratio in the incubated samples must also be very low. The concentrations of dicyanogold(I) and HSA are typically held constant, with much more HSA than dicyanogold(I) present, so that the same binding interaction is under investigation as each parameter is changed. This method applies to two of the experiments discussed in this section, the variation of the ionic strength and of the temperature. The first experiment discussed in this section, varying the initial concentration of dicyanogold(I), requires non-physiological concentrations of dicyanogold(I).

$$\mathbf{Albumin + Au(CN)_2^-} \underset{}{\overset{\mathbf{K_{eq}}}{\rightleftharpoons}} \mathbf{Albumin \bullet Au(CN)_2^-}$$

Figure 16. Chemical equation representing the equilibrium established in the dicyanogold(I)-HSA system.

1. Varying the initial concentration of dicyanogold(I)

The binding interaction between dicyanogold(I) and HSA is influenced by many factors. The effect of one of these factors, the initial concentration of dicyanogold(I), on the binding constant of the system was explored in this set of experiments. In order to isolate the effect of the dicyanogold(I) concentration on binding, the concentration of the albumin solution was held constant and the amount of gold added to each set of samples was varied. Also, the ratio of gold to HSA was kept below 1 for each experiment. Ideally, by keeping the ratio below 1, there was only enough dicyanogold(I) available to bind to the main site. This allowed more complete exploration of the binding sites available at low dicyanogold(I) to HSA ratios.

The data from these experiments were analyzed in two ways. First, the binding constants at several gold to protein ratios were determined. If a single binding site was being populated as the ratio of dicyanogold(I) to HSA approached 1, K_{eq} should have remained constant. Conversely, if two binding sites were being populated, K_{eq} should have changed as the ratio of dicyanogold(I) to HSA changes. In fact, K_{eq} should approach the value of the second binding site.

The second method used for analyzing the data from these experiments involved constructing a Scatchard plot.[20] The Scatchard method of analysis is a graphical method from which the binding constants and number of binding sites can be estimated. The quantities calculated for this type of analysis were similar to those calculated to determine the binding constant for the system via ultrafiltration. Namely, the equilibrium concentration of free dicyanogold(I) was measured and the ratio of bound dicyanogold(I) to total HSA was calculated. The plot was constructed using the ratio of bound dicyanogold(I) to total HSA (B) on the x-axis and the equilibrium concentration of free dicyanogold(I) divided by that ratio ($[Au]_{free}/B$) on the

y-axis. A line of best fit was drawn through the data. The slope of that line is the negative of the binding constant, K_{eq}. The x-intercept of this line is the number of binding sites of a particular kind per molecule of HSA. (See Appendix B for a discussion of Scatchard and reciprocal plots.) If a single site is being populated as the initial ratio of dicyanogold(I) to HSA approaches 1, then the data are expected to fall on a single line. If multiple sites are being populated as the ratio approaches 1, then the data should fall on multiple lines. The latter behavior has been observed for the dicyanogold(I)-bovine serum albumin system and indicates that there are at least two kinds of sites that are being populated as the dicyanogold(I) to BSA ratio increases, though in that study, ratios approached 5.[15]

2. Varying the ionic strength of the solution

Another factor that influences the binding interaction between a protein and a small molecule is the ionic strength of the system under investigation. At low ionic strengths fewer counter-ions are available, so that the screening effect of the counterions present is much less. (Figure 17) At high ionic strengths many counterions are available to balance the charge of the protein, and the electrostatic interactions are effectively screened. (Figure 18) Additionally, at high ionic strength, the electrostatic interaction between macromolecules in solution is weaker than in low ionic strength conditions.[21]

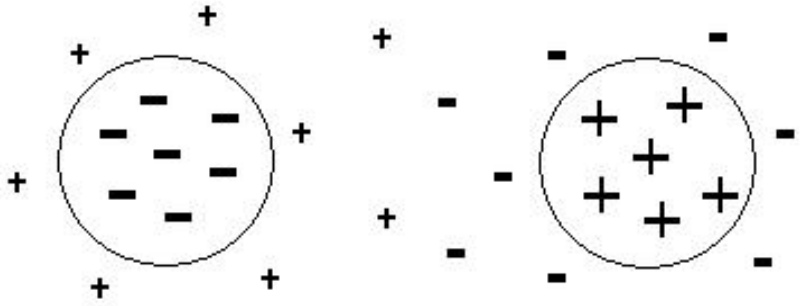

Figure 17. At low ionic strength, electrostatic interactions are ineffectively screened.

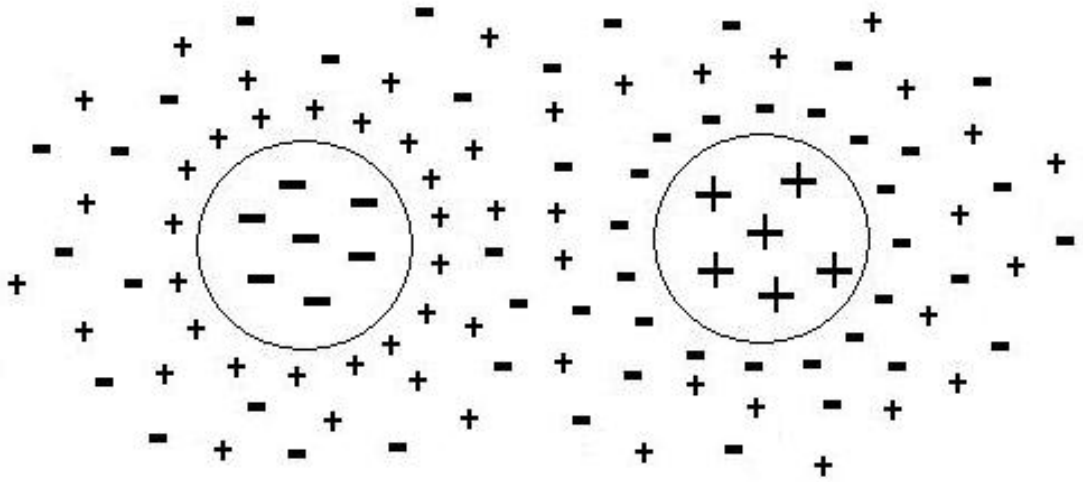

Figure 18. At high ionic strength, the counterions present effectively screen electrostatic interactions.

In this set of experiments, the amount of dicyanogold(I) and HSA was held constant while the ionic strength of the buffer solution was varied. In each case, the same buffer was used with increasing amounts of added salt (NaCl). The concentration of ions in all solutions was much greater than the concentration of either HSA or dicyanogold(I), so there should be no changes in the tertiary structure of the protein that may lead to a change in the binding interaction between the two species. The dependence of the binding interaction on ionic strength

is evaluated by determining the binding constant, K_{eq}, for each ionic strength tested. The binding constants are expected to be affected by a change in the ionic strength of the solution if the predominant interaction is electrostatic in nature. If there is a covalent interaction, then the binding constant should be largely unaffected by changing the ionic strength. The ionic strengths tested during this experiment include no salt added, 50 mM salt added and 100 mM salt added to the 100 mM $NaHCO_3$ buffer at pH 7.40.

3. Varying the incubation temperature of the samples

The temperature at which the HSA plus dicyanogold(I) samples are incubated is a factor that has an effect on the value of the binding constant, K_{eq}. In this series of experiments, the concentrations of HSA and dicyanogold(I) were held constant while the incubation/centrifugation temperature was varied. The binding constants were determined for HSA and HSA•AA at each temperature via ultrafiltration followed by a gold analysis using ICP-MS. The temperature of centrifugation was held consistent with the incubation temperature. Since the equilibrium must be maintained throughout centrifugation, and the equilibrium is established rapidly, changing the temperature during centrifugation of the ultrafilters would also change the equilibrium conditions. A comparison of these values for HSA and HSA•AA is also useful is determining a relationship between the binding sites of the two forms of HSA.

The van't Hoff equation relates the equilibrium constant, K, to the change in free energy of the system upon binding.[18] The Gibbs free energy relates to the enthalpy and entropy at any temperature. By determining K at multiple temperatures, it is possible to determine the change in enthalpy, ΔH, and entropy, ΔS, upon binding of dicyanogold(I) to HSA. Rearranging the van't Hoff equation (eq. 5),

$$\ln K = -(\Delta G/RT) \quad \text{(eq. 5)}$$

$$\Delta G = -RT\,(\ln K)$$

Introducing the equation for Gibbs free energy:

$$\Delta G = \Delta H - T\Delta S \quad \text{(eq. 6)}$$

Setting these equations equal to each other and solving for lnK, the following equation results.

$$-RT\,(\ln K) = \Delta H - T\Delta S$$

$$\ln K = (-\Delta H/R)(1/T) + (\Delta S/R) \quad \text{(eq. 7)}$$

Using the relationship between lnK and 1/T, a plot can be constructed and a line of best fit can be drawn through the data.[18] From equation 7 both the enthalpy and entropy of binding for the dicyanogold(I)-HSA system can be determined using the mathematical relationships below[18].

$$-\Delta H/R = \text{slope}$$

$$\Delta S/R = \text{y-intercept}$$

The binding constant of the system reveals whether or not the forward reaction is favorable. Determining the values of ΔH and ΔS for the dicyanogold(I)-HSA system gives more insight into the specific characteristics of the binding interaction between the two species. In order for a process to be spontaneous, the free energy change (ΔG) upon binding must be

negative. A positive change in enthalpy upon binding is disfavored since it causes ΔG to become more positive. In this case, if the process is to remain favorable, then the entropy change upon binding must be sufficiently favorable (ΔS greater than 0) so that the magnitude of the -TΔS term of equation 6 becomes greater than ΔH. In a system that behaves in this manner, the binding interaction is endothermic. In the opposite situation, where ΔH is negative, the reaction is favored with respect to ΔH. The change in entropy upon binding in this system can be either positive or negative in order to maintain a negative value for ΔG, though if -TΔS is greater than the magnitude of ΔH, the reaction will become non-spontaneous.

Chapter 2:

Experimental

A. Equipment and buffers

Bovine and human serum albumins were obtained from Sigma chemicals. Gluthathione was obtained from Fisher Scientific. Iodoacetamide was obtained from Aldrich. Potassium dicyanogold(I) was synthesized in-house by Nathan Coker. (A complete description of the synthesis of potassium dicyanogold(I) can be found in the Ph.D. dissertation of Nathan Coker[24]). ICP-MS gold standard was purchased from Alfa Aesar. UV-visible measurements were made using an Olis Cary-14 Spectrophotometer and 1.0 cm matched quartz cuvettes from Fisher. The HPLC system included a Spectra-Physics SP8800 pump, a Rheodyne injector, an Alltima 7.5mm C18 guard column, and a Microsorb-MV 25 cm C18 reverse phase analytical column. An Elan 6000 Inductively Coupled Plasma Mass Spectrometer was used for gold-specific detection. Ultrafilters were purchased from Millipore. Centricon (2 mL sample capacity) and centriplus (15 mL sample capacity) ultrafilters have 30000 NMWL regenerated celluose filtration membranes. Samples were centrifuged using a Sorvall RC-R5 centrifuge manufactured by DuPont; an SS-34 rotor was used for all centrifugation of both types of ultrafilters. Buffers were made using ACS reagent grade chemicals and nanopure water. Buffer A (100 mM $NaHCO_3$, pH 7.90) was made in 100 mL batches by dissolving 0.84 g (10 mmol) $NaHCO_3$ in distilled water and adjusting the pH to 7.90 by dropwise addition of HCl (10% solution). Buffer B (10 mM Na_2HPO_4, pH 7.40) was made in 1 L batches by dissolving 1.42 g (10 mmol) Na_2HPO_4 in 1 L distilled water and adjusting the pH to 7.40 by dropwise addition of NaOH (10% solution) and HCl (10% solution). Buffer C (100 mM $NaHCO_3$, 50 mM NaCl, pH 7.40) was made in 100 mL batches by dissolving 0.84 g (10 mmol) $NaHCO_3$ and 0.29 g (5 mmol) NaCl in 100 mL distilled water and adlusting the pH to 7.40 by dropwise addition of HCl (10% solution). Buffer

D (10 mM $NaHCO_3$) was made in 500 mL batches by dissolving 0.42 g (5 mmol) $NaHCO_3$ in distilled water and adjusting the pH to 7.40 by dropwise addition of HCl (10% solution).

B. Reconstitution of cysteine-34 with glutathione

The reduction of the cystine formed by cysteine addition to cysteine-34 was conducted by reaction with glutathione under an argon atmosphere. Approximately 40 mL of water was deoxygenated by bubbling argon through it for 30 minutes. The following quantities were for preparation of an albumin solution from which 10-1 mL protein aliquots were taken. Approximately 0.5 g (7.58×10^{-6} moles) of HSA was weighed and dissolved in 20 mL of the deoxygenated water. The resulting solution was placed in a 3-neck flask and sealed with rubber septa. The flask was partially evacuated and refilled with argon 5-6 times. The protein solution cannot be deoxygenated by bubbling argon through the solution because the solution forms gas-filled bubbles and becomes foam-like, leading to denaturation of the protein. A ten-fold molar excess (0.023 g) of glutathione was dissolved in 5 mL of the deoxygenated water. Argon was bubbled through the glutathione solution for 5 minutes before adding it to the HSA solution. The glutathione solution was added through one opening of the flask while argon flowed through the flask. The flask containing the HSA/glutathione mixture was re-sealed with a rubber septum and partially evacuated and refilled with argon 4-5 times. The sealed flask was placed in a circulating water bath at 37°C for 1 hour 45 minutes. The reaction vessel was removed from the water bath and excess glutathione was removed using the following wash procedure. The flask was opened to air and the contents (ca. 25 mL) were poured into two 15 mL ultrafilters (30000 NMWL, regenerated cellulose membrane), diluted with the addition of 5 mL distilled water to each filter and centrifuged for 1 hour 30 minutes at 4000 rpm (2500 x g). The filtrate

was discarded while the concentrated protein (ca. 3 mL) was diluted with distilled water (total volume ca. 15 mL)` and the ultrafilters were centrifuged again. The process was repeated one more time with water. The concentrated protein was diluted with the desired buffer and the ultrafilters were centrifuged for 1 hour 30 minutes as described above. The filtrate was discarded and the concentrated protein was diluted with buffer again. The protein solution was centrifuged a total of three times with buffer and was diluted finally to the desired volume (10 mL) with the appropriate buffer (either pH 7.40 for incubation with gold, or pH 7.90 for reaction with iodoacetamide). There was minimal protein loss during this process. This solution was stored at 5°C until it was used.

C. Alkylation of cysteine-34 with iodoacetamide

The alkylation of cysteine-34 of HSA with iodoacetamide was done in air. Buffer A (100 mM $NaHCO_3$, pH 7.90) was used for this alkylation. HSA, 0.25 g (3.76×10^{-6} moles), was dissolved in 10 mL of distilled water. Alternatively, the glutathione-treated HSA was used by diluting 5 mL of the solution prepared in the previous section to 10 mL with buffer A. A 100-fold excess, 0.07 g (3.78×10^{-4} moles), iodoacetamide was dissolved in 4 mL of buffer A. The HSA and iodoacetamide solutions were mixed thoroughly with gentle agitation and allowed to incubate at room temperature for 45 minutes. After incubation, the excess iodoacetamide was removed from solution and the resulting protein was washed via ultrafiltration. The incubated mixture was divided between two 15 mL ultrafilters and the contents of each ultrafilter was diluted to 15 mL with distilled water. The ultrafilters were centrifuged for 1 hour 15 minutes at 4500 rpm (2500 x g) and 25ºC. The filtrate was discarded, the concentrated protein (ca. 3 mL)

was diluted to 15 mL with distilled water and the ultrafilters were centrifuged for 1 hour 15 minutes as described above. This step was repeated two more times with water. After the last centrifugation with water, the HSA in each ultrafilter was diluted to 15 mL with an appropriate buffer at pH 7.40. The process was repeated by adding pH 7.40 buffer two more times. The final concentrated protein was removed from the ultrafilters, combined into a plastic vial and diluted to 5 mL with pH 7.40 buffer. This solution was stored at 5°C until used.

D. FT-ICR-MS

Before analysis using FT-ICR-MS, protein samples must be made free of extraneous salts. This was accomplished using a variation of the method previously described for removing small molecules via ultrafiltration. Samples were prepared by dissolving 1 mg of HSA in distilled water. This solution was placed in a 2 mL ultrafilter (30000 NMWL, regenerated cellulose membrane) and centrifuged at approximately 1200 rpm for 40 minutes. The filtrate was discarded, the protein was diluted with distilled water and the ultrafilter was centrifuged again. This process was repeated two more times (4 spins total). The final concentrated protein was diluted to 1 mL and filtered through a 0.22 μm syringe filter, then stored in a 1.5 mL plastic vial. Each of four HSA solutions were prepared in this way: HSA as purchased, HSA as purchased and reacted with iodoacetamide, HSA treated with glutathione, and HSA treated with glutathione and reacted with iodoacetamide. The final protein concentration in all cases was approximately 1 mg/mL. For FT-ICR-MS analysis, the protein solutions were diluted 2:3 with a 50/50 acetonitrile/water, 1% formic acid solution. The injection flow rate is 30 μL/hour. The mass

spectrometer was set to collect 32k data points at a data collection frequency of 1 MHz. The instrument used was an Ion-Spec 99 FT-ICR-MS with electrospray ionization and was available through the Mass Spectrometry facility at the University of Cincinnati.

E. MALDI-TOF-MS

Sequence grade modified trypsin from Promega of Madison, WI was used in this experiment. The stock trypsin (1 mg/mL) was prepared by dissolving 200 μg of trypsin in 200 μL of 50 mM acetic acid. The digestion buffer was prepared by dissolving 4.8 g (0.08 mol) urea and 0.316 g (0.04 mol) NH_4HCO_3 in 10 mL of distilled water.[27] The HSA solution, prepared in distilled water, was de-salted and diluted to 1 mg/mL with distilled water. The digestion mixture contained 10 μL of protein (HSA) plus 20 μL of the digestion buffer. The digestion mixture was now diluted to 2 M urea and 0.1 M NH_4HCO_3 by adding 50 μL of distilled water. Approximately 5 μL of the stock enzyme (trypsin) was added to the protein solution so that the final concentration of protein was 25 times greater than the concentration of enzyme.[27] The digestion solution was mixed thoroughly and placed in an incubator at 37°C for 24 hours.[27] The digestion was stopped by freezing, but alternatively could be stopped by adding 3% TFA in water. The samples were then submitted to the Mass Spectrometry facility at the University of Cincinnati for MALDI-TOF-MS analysis, and the protein fragments in each sample were extracted from the digest mixture using a C18 Zip-tip product from Millipore prior to analysis. It is possible to calibrate the fragment masses resulting from the tryptic digest of albumin using trypsin autolysis peak masses, when the trypsin peaks appear in the MALDI-TOF mass spectrum.

F. ICP-MS Experiments (not including HPLC)

Before each experimental run, the "daily performance" check was conducted as described in the Elan 6000 manual on page 3-14. Gold standard solutions were prepared in distilled water as follows. The concentration of the gold standard purchased from Alfa Aesar was 1000 parts per million. A 1000 parts per billion (ppb) standard was made by diluting 100 μL of the purchased standard to 100 mL with distilled water using a volumetric flask. Generally, six standard solutions were made from the 1000 ppb standard and were between 0.5 ppb and 100 ppb depending on the expected concentration to be analyzed. Sample was introduced via the peristaltic pump which was set at 15 rpm (approximately 0.6 mL/min). The instrument was set to collect data at m/z 197 at one sweep per reading, one reading per replicate and 20 replicates were averaged to yield the average number of counts per second (cps) and a standard deviation for that set of data. Individual replicates were analyzed for precision and accuracy using the "Q test for bad data" as described by Harris.[18] This method uses the ratio of the gap in the data, between the outlier and the nearest point, compared to the entire range of the data. Points that are above the ratio listed in the table are discarded.[18 (p. 71)] All standards and samples were analyzed using this method. For each set of standards, a blank that contained only the water used to make the dilutions was analyzed (150 cps average) and subtracted from the average cps from each standard solution. The most dilute standard analyzed contained 0.5 ppb gold and averaged 2500 cps. In this case, the blank intensity was 6% of the standard intensity. The average cps for each standard was plotted against the concentration of each standard. Once all of the data from the standards was plotted, a best-fit line was drawn and used to calibrate the samples analyzed during a particular run. In this way, the concentration of gold in each sample was determined. Standard solutions were analyzed at the beginning of the run and selected standards were re-

analyzed at the conclusion of the run. For each set of protein samples analyzed (either ultrafiltered or digested), a blank that contained protein but no gold was also analyzed and the average cps for this sample was subtracted from the average cps from the other samples in the set. The average value determined for the buffered protein solutions was 3000 cps and the average value determined for a sample set was 35000 cps (the representative sample set was comparatively low in its concentration of gold). The sample blank intensity was 9% of the sample intensity.

G. Binding Constants: Ultrafiltration

Buffer B was used in this experiment (10 mM Na_2HPO_4, pH 7.40). The protein solution for incubation with $KAu(CN)_2$ was made by dissolving 1.6870 g human serum albumin in 35 mL of buffer B (6.16×10^{-4} M HSA). To 25 mL of buffer B, 0.0016 g $KAu(CN)_2$ was added (0.000324 M). This dicyanogold(I) solution was diluted by adding 1.0 mL of the solution to a 25 mL volumetric flask and filling the flask with water (1.30×10^{-5} M) Four incubated solutions were made by combining 5 mL portions of the HSA solution with 1.0 mL of $KAu(CN)_2$ solution. Additionally, 1.0 mL of buffer was added to 5 mL of HSA as a control that contained no gold. These solutions were incubated at room temperature for 30 minutes. A 0.2 mL aliquot of each solution was diluted to 2 mL and the concentration of the protein was determined by recording the UV absorbance at 280 nm (36600 $M^{-1}cm^{-1}$)[14]. The initial concentration of $KAu(CN)_2$ was determined by diluting 1 mL of each incubated solution and the control to 5 mL with buffer (except for the solution that contains the most gold which was diluted to 10 mL) then 1 mL of each dilute solution was combined with 2 mL 2% nitric acid in a microwave digestion bomb.

The bomb was sealed and microwaved at high power for 30 seconds then allowed to cool for 30 minutes before opening. All digested samples were diluted 100-fold with 2% nitric acid for ICP-MS analysis.

Approximately 2 mL of each incubated solution was placed in a 2 mL ultrafilter with a 30000 NMWL regenerated cellulose membrane. The ultrafilters were centrifuged at approximately 1200 rpm for 70 minutes. The filtrate was diluted by a factor of 2.5 with 2% nitric acid. The two lower concentration solutions and the no gold added solution were further diluted 50-fold while the higher concentration solutions were further diluted 100-fold with 2% nitric acid before ICP-MS analysis. Note that bovine serum albumin was used for comparing binding constants obtained using ultrafiltration to those obtained using Penefsky chromatography, human serum albumin was used for the remainder of the experiments discussed in this work.

When using low concentrations of $KAu(CN)_2$, the following procedure was used to obtain binding constants via ultrafiltration. The incubated protein solution, 2 mL, was placed in a 30000 NMWL ultrafilter. The ultrafilter was placed in the Sorvall centrifuge and spun for 35 minutes at 22ºC at 4500 rpm (2500 x g), unless otherwise noted. The filtrate was analyzed by direct aspiration into the ICP-MS for gold content; no dilutions were performed unless specifically noted. The concentration of gold in each sample was calculated using the calibration data collected on the day of the ICP-MS run.

H. Reversibility of dicyanogold(I) binding

Buffer C was used for this experiment (100 mM $NaHCO_3$ and 50 mM NaCl, pH 7.40). A stock solution of $KAu(CN)_2$ was made by dissolving 0.0034 g (1.18×10^{-5} mol) $KAu(CN)_2$ in 25 mL distilled water. The gold stock solution was diluted from 1 mL to 125 mL with buffer C (3.776×10^{-6} M $KAu(CN)_2$). HSA and HSA•AA solutions were approximately 4.6×10^{-4} M prepared in buffer A. The total volume of the reaction solutions was 5 mL; 3 mL of protein plus 2 mL of one of the dilute dicyanogold(I) solutions. A gold only solution that contained 3 mL of buffer plus 2 mL of the dilute dicyanogold(I) solution was prepared, then it was diluted 10-fold, 50-fold and 100-fold with distilled water. A blank solution that contained 3 mL of protein plus 2 mL of buffer was prepared as a control. The reaction solutions were incubated at room temperature for 30 minutes. The initial concentration of protein in the incubated solution was determined by diluting an aliquot of the solution 10-fold and recording the absorbance at 280 nm (ε_{280}= 36600 $M^{-1}cm^{-1}$)[14]. The dilute gold only solutions were analyzed for initial gold concentration by direct aspiration into the ICP-MS. A 2 mL portion of each incubated solution was used to determine the binding constant via ultrafiltration as described for low concentrations of $KAu(CN)_2$. The remainder of the solution was used to continue with the next part of the experiment.

The Penefsky columns (see Appendix A) were prepared for use by soaking overnight in water and centrifuging for 2 minutes immediately before sample introduction. The remainder of the incubated solution was placed in the Penefsky column and the apparatus was immediately centrifuged for 1 minute. The eluent was allowed to re-equilibrate at room temperature for 30 minutes. The total gold concentration was determine by removing 0.5 mL of the re-

equilibrated solution and performing a microwave digestion as described previously using 1 mL of 2% nitric acid and subsequently analyzed for gold concentration by direct aspiration into the ICP-MS. Another aliquot of the re-equilibrated solution was diluted 10-fold and the concentration determined using the UV absorbance at 280 nm. The remainder of the re-equilibrated solution was placed in a 2 mL, 30000 NMWL ultrafilter and centrifuged at 4500 rpm (2500 x g) for 35 minutes at room temperature. Half of the filtrate was analyzed for gold concentration using the ICP-MS. The other half of the filtrate was analyzed by reverse phase ion-pairing chromatography.

The mobile phase (1 L) used for ion-pairing chromatography was 50/50 (buffer D)/methanol, 10 mM $NaHCO_3$ (pH 7.40) plus 1.39 g (5 mmol) tetrabutylammonium chloride. The HPLC system included a Spectra-Physics SP8800 pump (flow rate: 1 mL/min), a Rheodyne injector with a 50 μL loop and a 25 cm C_{18} reverse phase analytical column with the ICP-MS as the detector. Retention time and peak shape from the incubated samples were compared to those from $KAu(CN)_2$ standards. The $KAu(CN)_2$ standards were the diluted gold only solutions that were analyzed in the first part of this experiment.

I. Changing the equilibrium conditions

Experiment 1: varying the concentration of $KAu(CN)_2$ added to the HSA solution.

Buffer C was used for this experiment (100 mM $NaHCO_3$, 50 mM NaCl, pH 7.40). A stock solution of $KAu(CN)_2$ was made by dissolving 3.0 mg of $KAu(CN)_2$ in 5 mL of distilled water. The stock solution of gold was diluted 400-fold (low concentration), 40-fold (middle concentration) and 4-fold (high concentration) with buffer C. The concentration of the normal, glutathione treated HSA was approximately 3.16×10^{-4} M and the concentration of the blocked, glutathione treated HSA was approximately 2.77×10^{-4} M. Each sample set contained 4 protein plus gold samples, 1 protein plus buffer sample (background) and 1 buffer plus $KAu(CN)_2$ sample (gold only). Samples were prepared by combining 1 mL of HSA/buffer with 0.3 mL $KAu(CN)_2$/buffer solution so that the total volume was 1.3 mL. Samples were incubated for 30 minutes at room temperature. An aliquot of incubated solution was taken from each set of samples and diluted 11-fold and the concentration of HSA determined by recording the UV absorbance at 280 nm. The incubated solutions were placed in 2 mL ultrafilters then centrifuged at 4500 rpm (2500 x g) for 35 minutes at room temperature. The filtrate solutions were diluted with distilled water, 625-fold (high) and 101-fold (middle). The filtrate for the low concentration samples was analyzed without dilution. The gold only solutions were diluted with distilled water 1000-fold (high), 250-fold (middle) and 25-fold (low). All solutions were analyzed for gold concentration using ICP-MS.

Experiment 2: Varying the ionic strength of the incubated solutions

Three buffer solutions were used for this experiment: low, middle and high ionic strength. The low ionic strength buffer (75 mM $NaHCO_3$) was prepared by dissolving 0.63 g (7.5 mmol) $NaHCO_3$ in 100 mL distilled water and adjusting the pH to 7.40 by dropwise addition of HCL (10% solution). The middle ionic strength buffer (100 mM $NaHCO_3$, 10 mM NaCl) was prepared dissolving 0.84 g (10 mmol) $NaHCO_3$ and 0.058 g (1 mmol) NaCl in 100 mL distilled water and adjusting the pH to 7.40 by dropwise addition of HCL (10% solution). The high ionic strength buffer used in this experiment was buffer C (100 mM $NaHCO_3$, 50 mM NaCl, pH 7.40).

A stock solution of $KAu(CN)_2$ was made by dissolving 3.0 mg of $KAu(CN)_2$ in 5 mL of distilled water. The stock solution of gold was diluted 400-fold with each buffer. The concentration of the normal, glutathione treated HSA was approximately 3×10^{-4} M and the concentration of the blocked, glutathione treated HSA was approximately 2.7×10^{-4} M. As a result of sample treatment, the actual concentration of HSA varied slightly among sets. Each sample set contained four protein plus gold samples, one protein plus buffer sample (background) and one buffer plus $KAu(CN)_2$ sample (gold only). Samples were prepared by combining 1 mL of HSA/buffer with 0.3 mL $KAu(CN)_2$/buffer solution so that the total volume was 1.3 mL. Samples were incubated for 30 minutes at room temperature. An aliquot of incubated solution was taken from each set of samples and diluted 11-fold and the concentration of HSA determined by recording the UV absorbance at 280 nm. The incubated solutions were placed in 2 mL ultrafilters then centrifuged at 4500 rpm (2500 x g) for 35 minutes at room temperature. The filtrate solutions were diluted with distilled water 5-fold (HSA•AA, high and middle samples) and 2-fold (HSA, high and middle samples). The filtrate for the low

concentration samples was analyzed without dilution. The gold only solutions were diluted with distilled water 25-fold. All solutions were analyzed for gold concentration using ICP-MS.

Experiment 3: Varying the temperature of the incubated solutions

Buffer C was used for this experiment (100 mM $NaHCO_3$, 50 mM NaCl, pH 7.40). A stock solution of $KAu(CN)_2$ was made by dissolving 3.0 mg of $KAu(CN)_2$ in 5 mL of distilled water. The stock solution of gold was diluted 400-fold with buffer C. The concentration of the normal, glutathione treated HSA was approximately 3.7×10^{-4} M and the concentration of the blocked, glutathione treated HSA was approximately 3.9×10^{-4} M. Each sample set contained 4 protein plus gold samples, one protein plus buffer sample (background) and one buffer plus $KAu(CN)_2$ sample (gold only). Samples were prepared by combining 1 mL of HSA/buffer with 0.3 mL $KAu(CN)_2$/buffer solution so that the total volume was 1.3 mL, and the ratio of dicyanogold(I) added to albumin was approximately 0.003. The gold/protein solutions were incubated for 30 minutes then placed in 2 mL ultrafilters and centrifuged for 35 minutes at 4 temperatures: 37°C, 22°C, 14°C, and 4°C. The actual temperature of each sample set was determined by measuring the temperature of a buffer solution incubated and centrifuged with the gold/protein solutions using a tenth-degree mercury thermometer. The temperatures appear reproducible ±0.2 °C. An aliquot of incubated solution was taken from each set of samples and diluted 11-fold and the concentration of HSA determined by recording the UV absorbance at 280 nm. The filtrate from HSA•AA samples was diluted with distilled water 5-fold (37°C), 3-fold (14°C) and 2-fold (4°C). The gold only samples were diluted 25-fold with distilled water. The resulting solutions were analyzed for gold concentration using ICP-MS.

Chapter 3:

Results and Discussion

A. FT-ICR-MS as a tool for studying HSA

As was previously discussed, FT-ICR-MS can be used to characterize large proteins by adding enough protons to bring the mass to charge ratio of the molecular ion into the 400-2500 range. This is accomplished with human serum albumin by diluting the protein with a 1% formic acid solution and electrospray ionization to add 45-60 protons (positive charges). The resulting peak distribution contains clusters of peaks at regular intervals that represent the protein in different charge states. Each individual peak represents the m/z value for the chemical mass of the molecule, which is the average mass of all of the isotopic contributions, rather than representing the m/z value for a specific isotopic composition of the molecule. For this reason, it is likely that some peaks within the mass spectrum of HSA, upon close inspection, may appear asymmetric. The charge of each cluster is determined using the following equations. Where peak 1 and peak 2 are corresponding peaks in adjacent clusters in the mass spectrum and peak 1 has a lower mass to charge ratio than peak 2.

$$M/z_1 = m_1 \qquad \text{and} \qquad M/(z_1\text{-}1) = m_2 \qquad \text{(eq. 8)}$$

Where M is the actual mass, z_1 is the charge on peak 1 and m_1 is the m/z value. Because peak 1 and peak 2 arise from different charge states of the same protein, the actual mass (M) is the same for both peaks. Solving each equation for M and setting the equations equal to each other:

$$m_1\ (z_1) = (m_2\ z_1)\ -(m_2)$$

$$z_1 = m_2/(m_2 - m_1) \qquad \text{(eq. 9)}$$

This calculation can be used on any two corresponding peaks in adjacent charge clusters. The mass of any given peak in the mass spectrum can be calculated using the following equation.

$$\text{Mass} = (m_1/z_1 - 1)\, z_1 \qquad \text{(eq. 10)}$$

Where m_1/z_1 is the mass to charge ratio of the peak of interest and z_1 is the charge on the cluster of interest. Because the charge on the protein was generated by the addition of protons, the mass of a proton, 1, is subtracted from m/z before multiplying by the charge state so that the calculated mass is the mass of the native protein and not the protein plus 45 to 60 protons. Figure 19 shows a typical FT-ICR mass spectrum of HSA-purchased where each cluster of peaks representing a charge state has been numbered 1 through 13. Using equation 10, the charge states contained in this mass spectrum range from 57 to 45. The charge state information, the m/z value for each major peak and the calculated mass for each major peak are contained in columns 2, 3 and 4, respectively, in Table 1. The average mass of HSA-purchased calculated from this mass spectrum is 66437 ± 3 Daltons which agrees closely with the value calculated from the amino acid composition of HSA, 66438 Daltons.[10 (p. 25)]

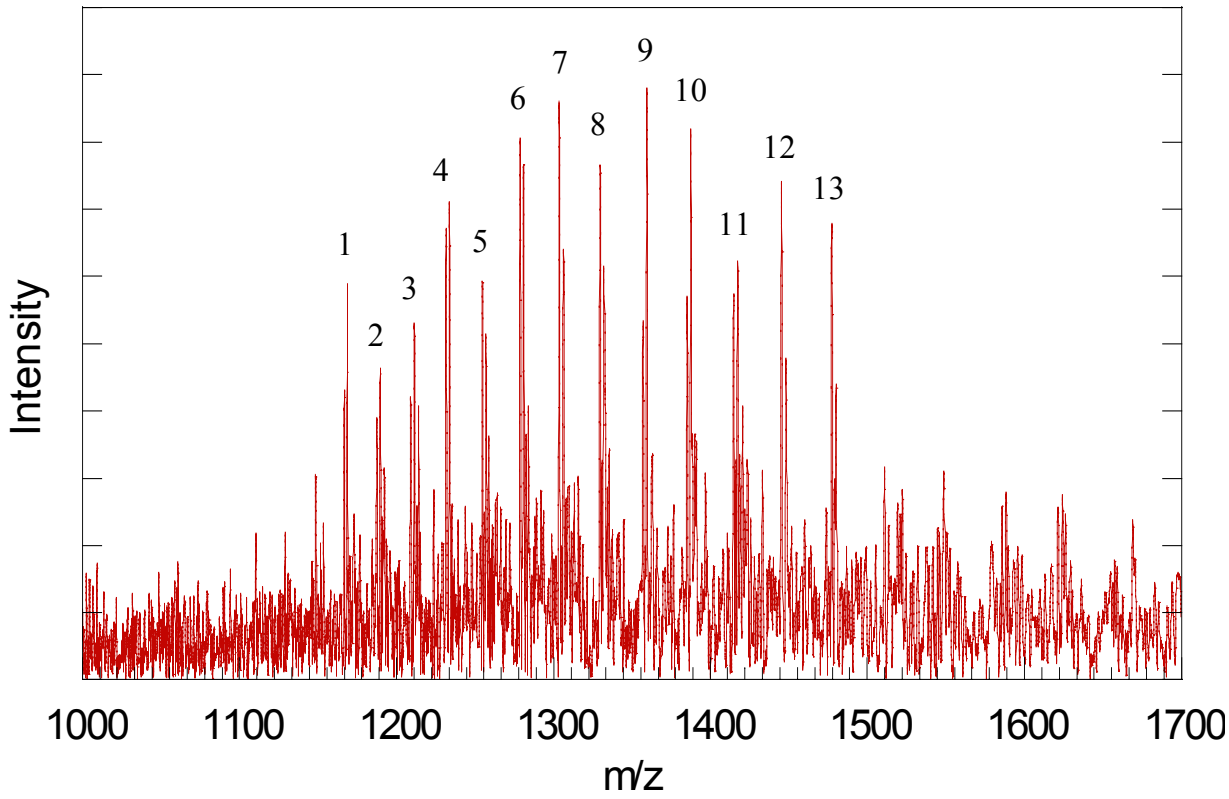

Figure 19. FT-ICR-MS of HSA-bottle, not treated with glutathione.

Table 1. Charge states, m/z values and calculated masses corresponding to the HSA-bottle peaks labeled in Figure 19.

peak #	z	m/z	mass
1	57	1166.5907	66438.6699
2	56	1187.3496	66435.5776
3	55	1208.8545	66431.9975
4	54	1231.3476	66438.7704
5	53	1254.5338	66437.2914
6	52	1278.6712	66438.9024
7	51	1303.5879	66431.9829
8	50	1329.7828	66439.1400
9	49	1356.8374	66436.0326
10	48	1385.1490	66439.1520
11	47	1414.6300	66440.6100
12	46	1445.3826	66441.5996
13	45	1477.3656	66436.4520
		average mass	66437
		standard deviation	+/- 3

B. Reconstitution of cysteine-34 by reaction with glutathione

Commercially available human serum albumin exists as two major forms with respect to cysteine 34: free thiol and cystine disulfide. Previously this has been determined by measuring the SH titre of the protein using Ellman's reagent, 5,5'-dithiobis 2-nitrobenzoic acid (DTNB).[15,22] The methods used to accomplish this rely on quantification of the by-products formed during the reaction rather than direct characterization of the protein. With the use of electrospray ionization, it is now possible to assess more directly the presence of groups bound to the protein.

In the mass spectrum of HSA-purchased that has been de-salted, there are two major peaks within each charge state. The first peak of each group, the average value of which is 66437 ±3 Da, corresponds to the calculated chemical mass of HSA (66438 Da).[10 (p. 25)] The second peak of each group, the average value of which is 66561 ±3 Da, corresponds to the calculated chemical mass of HSA with a cysteine (121 Da) bound to cysteine-34 through disulfide formation (which involves the loss of 2 H's) (66557 Da). A portion of that spectrum has been enlarged in Figure 20, and the calculated masses for the peaks shown, as well as peaks from charge states of that spectrum that are not depicted in Figure 20, are given in Table 2.

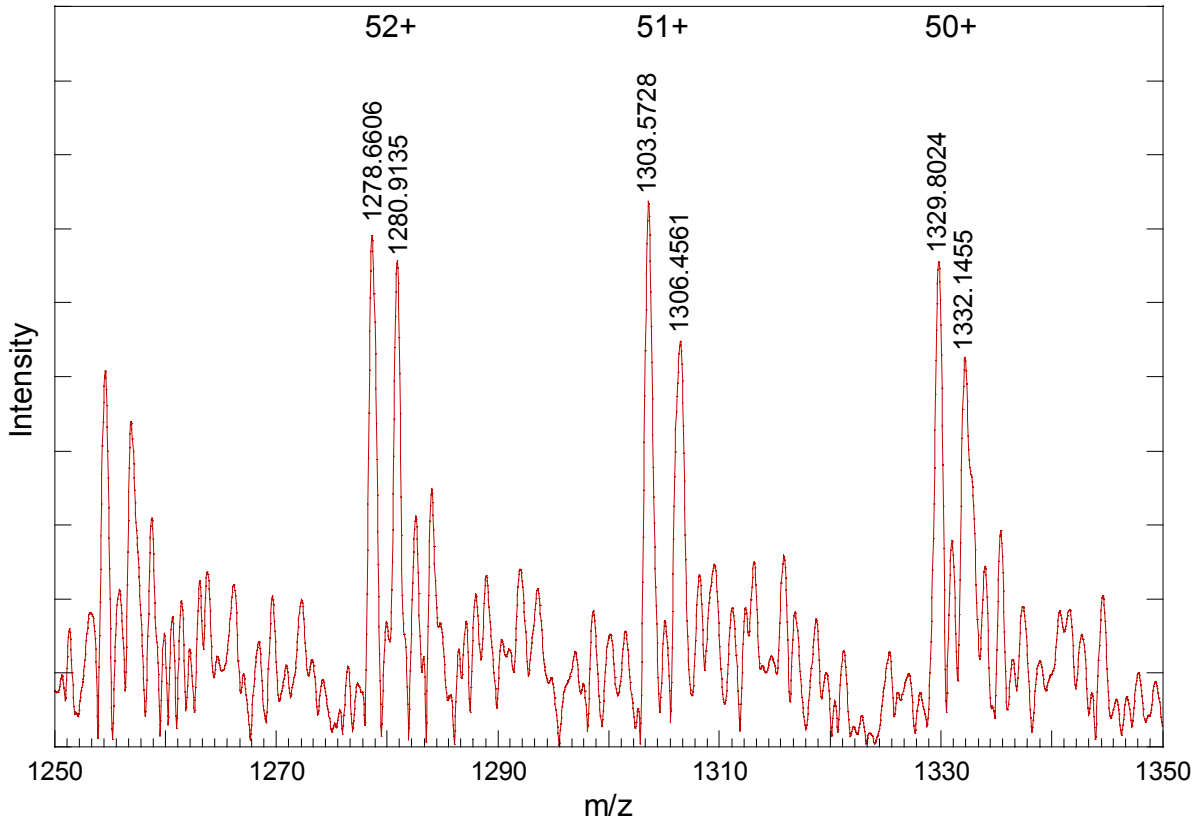

Figure 20. FT-ICR-MS, partial spectrum, of desalted HSA-bottle (not reacted with glutathione).

Table 2. HSA before treatment with glutathione. Charge states, m/z values and calculated masses corresponding to the peaks labeled in Figure 20.

z	m/z	mass	m/z	mass	difference
56	1187.3496	66435.5776	1189.5853	66560.7768	125.1992
55	1208.8545	66431.9975	1211.2003	66561.0165	129.0190
54	1231.3476	66438.7704	1233.6010	66560.4540	121.6836
53	1254.5338	66437.2914	1256.9502	66565.3606	128.0692
52	1278.6712	66438.9024	1280.8979	66554.6908	115.7884
51	1303.5879	66431.9829	1306.3964	66575.2164	143.2335
50	1329.7828	66439.1400	1332.2297	66561.4850	122.3450
49	1356.8374	66436.0326	1359.3269	66558.0181	121.9855
48	1385.1490	66439.1520	1387.6560	66559.4880	120.3360
47	1414.6300	66440.6100	1417.2711	66564.7417	124.1317
46	1445.3826	66441.5996	1447.9592	66560.1232	118.5236
45	1477.3656	66436.4520	1480.1682	66562.5690	126.1170
Average		66437		66561	123
Standard deviation		3		3	4

In the mass spectrum of HSA-purchased, which has been de-salted and treated with glutathione, there are two major peaks within each charge state. A portion of that spectrum has been enlarged in Figure 21. The first peak of each group, the average value of which is 66440 ± 3 Da, corresponds to the calculated chemical mass of HSA (66438 Da). The second peak of each group, the average value of which is 66537 ± 5 Da, corresponds to the calculated chemical mass of HSA plus a phosphate group, H_2PO_4 (66534 Da). The peak in the untreated spectrum (Figure 20) that corresponds to the HSA plus cysteine species is no longer present after treatment

with glutathione (Figure 21). The masses of the two major peaks of each cluster in the mass spectrum of HSA (pretreated with glutathione) are calculated in Table 3.

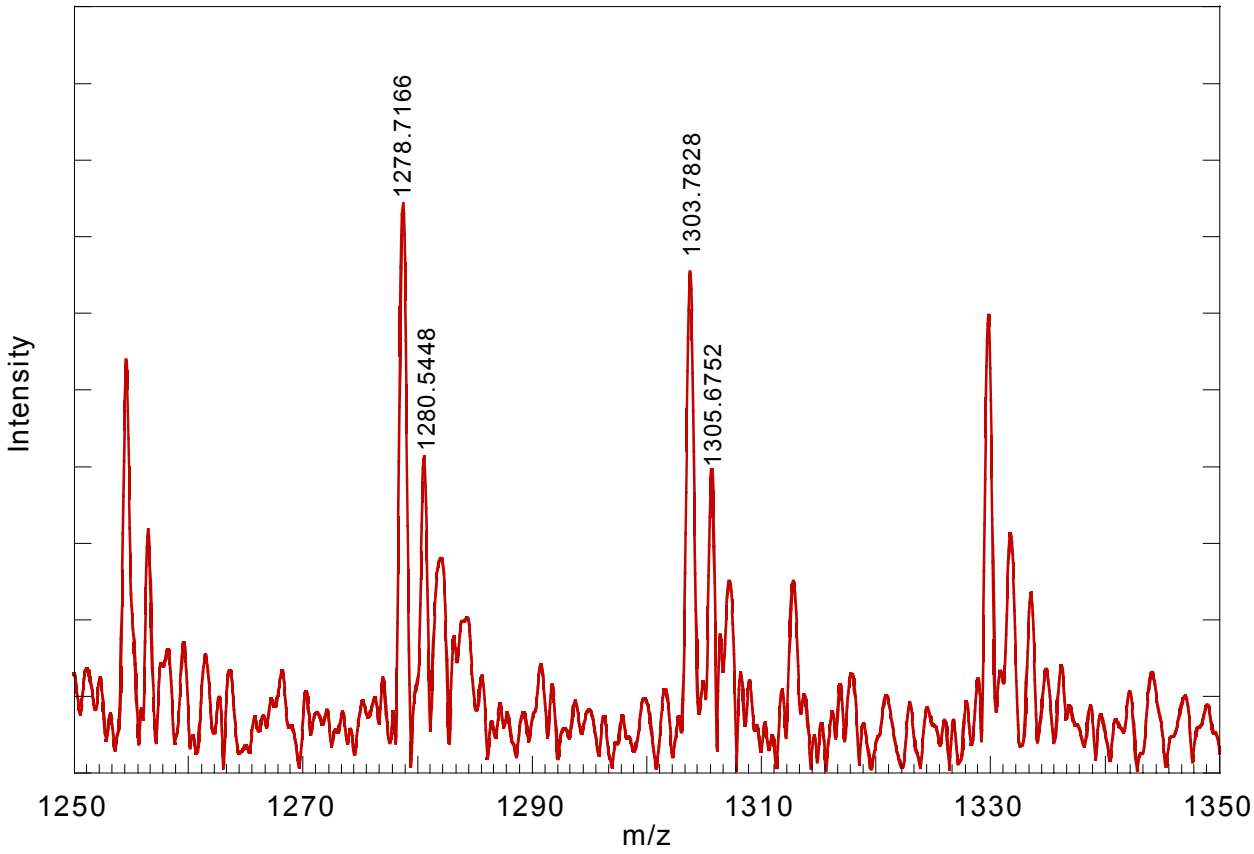

Figure 21. FT-ICR-MS, partial spectrum, of desalted HSA (pretreated with glutathione).

Table 3. HSA after treatment with glutathione. Charge states, m/z values and calculated masses corresponding to the peaks labeled in Figure 21.

z	m/z	mass	m/z	mass	difference
56	1187.4266	66439.8896	1189.1439	66536.0584	96.1688
55	1208.9332	66436.3260	1210.8006	66539.0330	102.7070
54	1231.2776	66434.9904	1233.0636	66531.4344	96.4440
53	1254.5588	66438.6164	1256.4891	66540.9223	102.3059
52	1278.7166	66441.2632	1280.5488	66536.5376	95.2744
51	1303.7828	66441.9228	1305.4336	66526.1136	84.1908
50	1329.8126	66440.6300	1331.7624	66538.1200	97.4900
49	1356.9381	66440.9669	1358.8484	66534.5716	93.6047
48	1385.2124	66442.1952	1387.3720	66545.8560	103.6608
47	1414.5796	66438.2412	1416.6588	66535.9636	97.7224
46	1445.3433	66439.7918	1447.5582	66541.6772	101.8854
45	1477.5593	66445.1685	1479.6422	66538.8990	93.7305
Average mass		66440		66537	97
Standard deviation		3		5	5

C. Alkylation of cysteine-34

Both the glutathione-treated and untreated forms of HSA were alkylated with iodoacetamide in order to chemically block cysteine-34. In the mass spectrum of HSA-purchased that has been reacted with iodoacetamide and de-salted, there are three major peaks within each charge state. A portion of that spectrum has been enlarged in Figure 22, and the masses of the first two peaks have been calculated in Table 4.

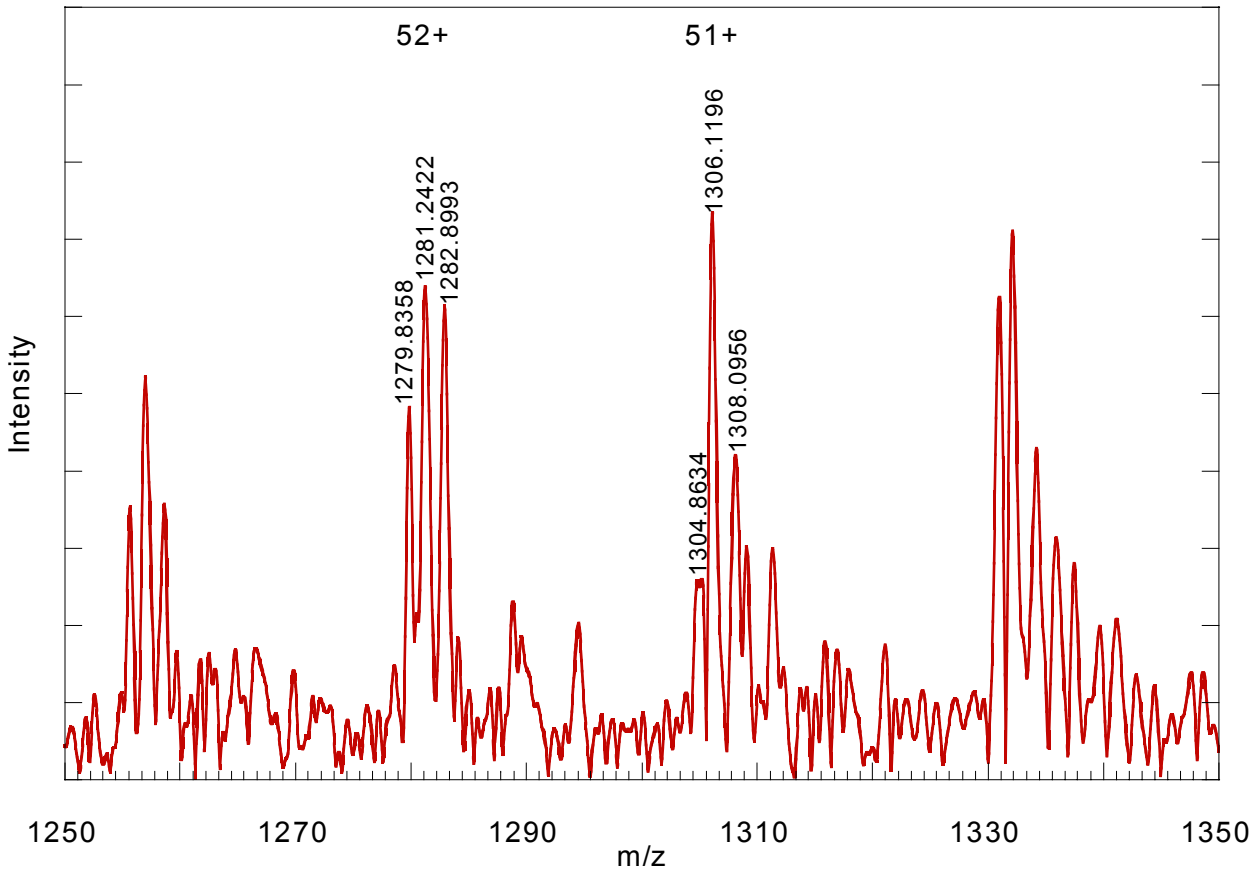

Figure 22. FT-ICR-MS of desalted HSA•AA, not reacted with glutathione.

Table 4. HSA•AA before treatment with glutathione. Charge states, m/z values and calculated masses corresponding to the peaks labeled in Figure 22.

z	m/z	mass	m/z	mass	difference
55	1210.1124	66501.1820	1211.0850	66554.6750	53.4930
54	1232.4285	66497.1390	1233.6387	66562.4898	65.3508
53	1255.6611	66497.0383	1257.0021	66568.1113	71.0730
52	1279.8358	66499.4616	1281.2422	66572.5944	73.1328
51	1304.8634	66497.0334	1306.1196	66561.0996	64.0662
50	1330.9397	66496.9850	1332.1324	66556.6200	59.6350
49	1357.9453	66490.3197	1359.3254	66557.9446	67.6249
48	1386.4038	66499.3824	1387.6343	66558.4464	59.0640
47	1416.0571	66507.6837	1417.3277	66567.4019	59.7182
46	1446.6809	66501.3214	1448.0519	66564.3874	63.0660
45	1478.7459	66498.5655	1479.9310	66551.8950	53.3295
Average mass		66499		66560	61
Standard deviation		4		5	7

The first peak of each group, the average value of which is 66499 ± 4 Da, corresponds to the calculated chemical mass of HSA•AA, where the acetamide group is bound through the sulfur of cysteine-34 (66495 Da). The second peak of each group, the average value of which is 66560 ± 5 Da, corresponds to the calculated chemical mass of HSA with a cysteine bound to cysteine-34 (66557 Da). The average difference between these two peaks is 61 ± 7 Da and the calculated difference between the chemical mass of HSA•AA and HSA•cys is 62 Da. The third

peak of each group corresponds to the addition of 97 ± 8 Da to the second peak, which corresponds to the mass of HSA•cys plus a single phosphate group (95 Da).

In the mass spectrum of HSA (pretreated with glutathione) that has been reacted with iodoacetamide, and de-salted, there is a single major peak within each charge state. A portion of that spectrum has been enlarged in Figure 23, and the masses of the major peak and the next discernable peak have been calculated in Table 5. The first peak, the average value of which is 66497 ± 2 Da, corresponds to the calculated chemical mass of HSA•AA (66495 Da). The average difference between the main peak and the next discernable peak is 162 ± 6 Da and does not corresponds to and addition of any of the species in question here. It can be seen in the FT-ICR mass spectrum that only a single acetamide has been added to the HSA. (Figure 23.)

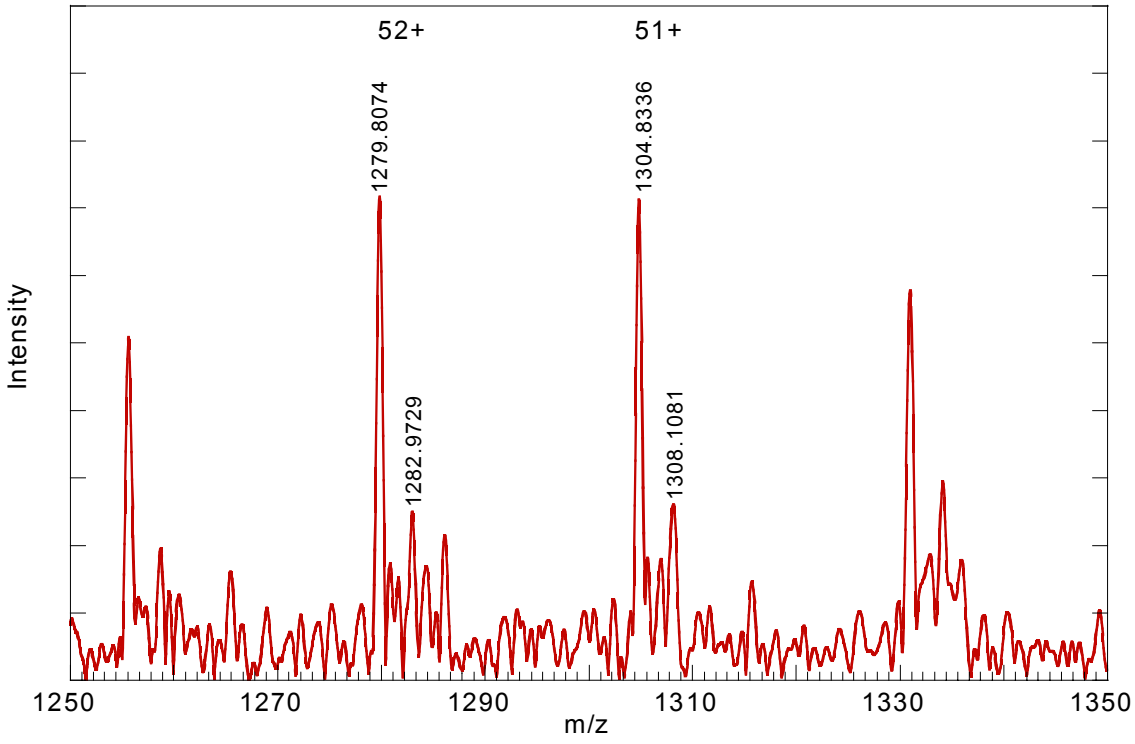

Figure 23. FT-ICR-MS of HSA•AA pre-treated with glutathione.

Table 5. HSA•AA after treatment with glutathione. Charge states, m/z values and calculated masses corresponding to the peaks labeled in Figure 23.

z	m/z	mass	m/z	mass	difference
56	1188.4732	66498.4992	1191.2845	66655.9320	157.4328
55	1210.0247	66496.3585	1213.0035	66660.1925	163.8340
54	1232.3873	66494.9142	1235.4883	66662.3682	167.4540
53	1255.6243	66495.0879	1258.6950	66657.8350	162.7471
52	1279.8074	66497.9848	1282.9729	66662.5908	164.6060
51	1304.8336	66495.5136	1308.1081	66662.5131	166.9995
50	1330.9501	66497.5050	1334.0955	66654.7750	157.2700
49	1358.0766	66496.7534	1361.2781	66653.6269	156.8735
48	1386.3124	66494.9952	1389.7345	66659.2560	164.2608
47	1415.8493	66497.9171	1419.5600	66672.3200	174.4029
46	1446.6344	66499.1824	1449.9081	66649.7726	150.5902
45	1478.7209	66497.4405	1482.2581	66656.6145	159.1740
Average		66497		66659	162
Standard deviation		2		6	6

D. Tryptic digest and MALDI-TOF-MS analysis of HSA

Tryptic digests of proteins, in which trypsin "cuts" the protein after lysine and arginine residues, are generally well-characterized and the fragments produced typically lie within the range that is easily resolved in MALDI-TOF-MS. The sensitivity of the instrument coupled with the smaller masses of the fragments, compared to the whole protein, produce mass peaks with isotopic resolution. Performing a tryptic digest on HSA•AA, with analysis using MALDI-TOF-

MS, provides information about the composition of specific protein fragments.

Programs that are available to calculate the expected masses of fragments resulting from MALDI-TOF-MS analysis of a tryptic digest of HSA are typically used for protein identification, but in this work such programs are used only to predict the masses of some of the expected fragments. The most common tryptic digests involve denaturation of the protein by reduction and alkylation of the disulfide bonds. Since cysteine-34 lies within a 21 peptide digest region that contains no disulfide bonds, it is unnecessary to denature the HSA. As a result, many of the fragments are still bound to other fragments through a disulfide bridge that was present in the intact protein, and are not readily recognizable by digest calculation programs, though the masses of the fragments can be calculated. The amino acid sequence for the first 103 residues of human serum albumin is shown in Figure 24. The following are labeled: trypsin cuts, disulfide bonds and cysteine-34. In the segment that contains amino acids 74 through 103, there are two disulfide bonds linking different digest fragments to each other, though these fragments are not seen in the MALDI-TOF mass spectra in Figures 25 and 26. The expected mass of the segment that contains amino acids 74-81 without disulfide linking is 877.1 Da. The mass of that segment linked to the following segment (amino acids 82-93) through the disulfide bond between cys-75 and cys-91 is 2198.6 Da. A third possibility is that the disulfide bond between cys-90 and cys-101 also remains intact resulting in a fragment that has a mass of 3217.8 Da.

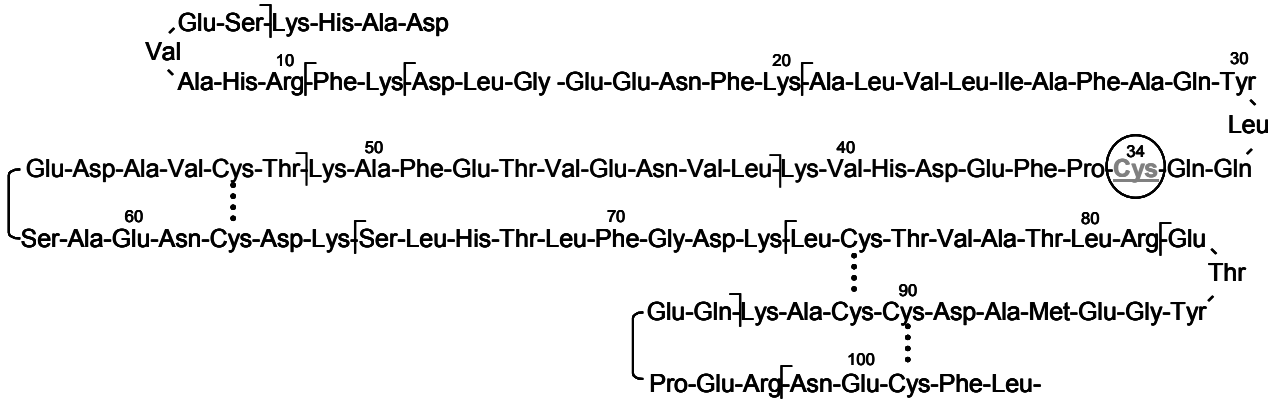

Figure 24. Amino acid sequence of HSA. ⌈-cut made during tryptic digest. … - disulfide bonds. Cysteine-34 is circled.

Figures 25 and 26 show the entire MALDI-TOF mass spectra collected for both HSA and HSA•AA. The spectra contain many common peaks such as 927 Da, 962 Da, 1468 Da, 1895 Da, and 2041 Da. These correspond to the calculated masses of tryptic digest fragments of HSA. Table 6 lists the calculated masses for selected fragments expected from a tryptic digest of HSA. Many of the fragments listed can be observed in the MALDI-TOF mass spectrum of HSA and HSA•AA. Reading from left to right, Table 6 contains the monoisotopic masses of the calculated fragments, which is the mass peak corresponding to the structure that contains only the most abundant isotopes, in the first column, the average masses of the fragments, which is the average mass calculated using the isotopic peaks, in the second column, the portion of the amino acid sequence contained in the fragment in the third column, and the number of missed digest cleavages that give rise to that mass in the last column. The term "missed cleavage" refers to a situation where the protein was not completely digested, leaving some adjacent pieces linked

together by a lysine or arginine. The most significant difference between the two spectra is the appearance of a peak at 2492 Da in the spectrum of HSA•AA. Some of the expected tryptic digest fragments and their expected masses are summarized in Table 6. A closer look at these spectra is given in Figures 27 and 28.

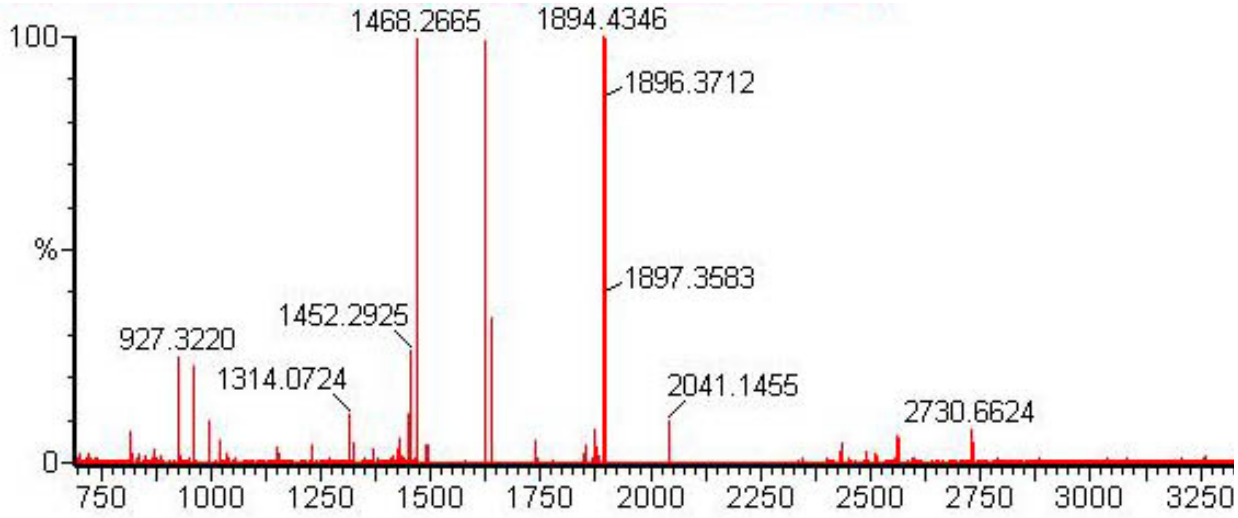

Figure 25. MALDI-TOF mass spectrum of HSA.

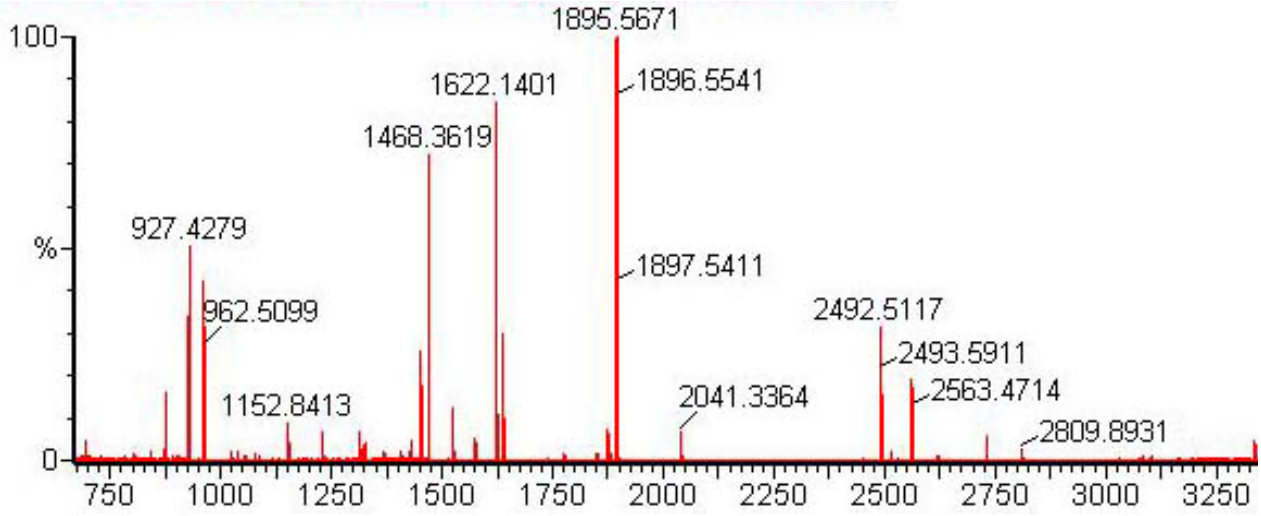

Figure 26. MALDI-TOF mass spectrum of HSA•AA.

Table 6. Calculated m/z values for selected fragments resulting from a tryptic digest of HSA. (mi = monoisotopic mass, avg = average mass, fragment = amino acid composition, and missed = the number of missed cleavages.

m/z (mi)	m/z (avg)	fragment	missed
927.4940	928.0828	138-144	0
1311.7452	1312.5647	338-348	0
1467.8436	1468.7533	337-348	1
1623.8771	1624.9111	324-336	0
1898.9958	1900.2478	146-160	1
2045.0959	2046.3863	373-389	0
2433.2641	2434.8812	21-41	0
2560.2726	2562.0667	445-466	1

The calculated average mass of the HSA fragment containing cysteine-34 is 2434.8812 Da and the calculated monoisotopic mass is 2433.2641 Da. In the mass spectrum of a tryptic digest of HSA, the fragment containing cysteine-34 is represented by a cluster of isotope peaks separated by one mass unit. Figure 27 shows the partial MALDI-TOF mass spectrum of HSA after it has been digested with trypsin. The sample was analyzed using the Micromass MALDI-TOF-MS available in the University of Cincinnati Mass Spectrometry Facility. The spectrum is expanded in the region around the expected mass of the cysteine-34 trypsin digest fragment. The peak cluster that begins with 2432.756 corresponds to the expected mass of the cysteine-34 fragment.

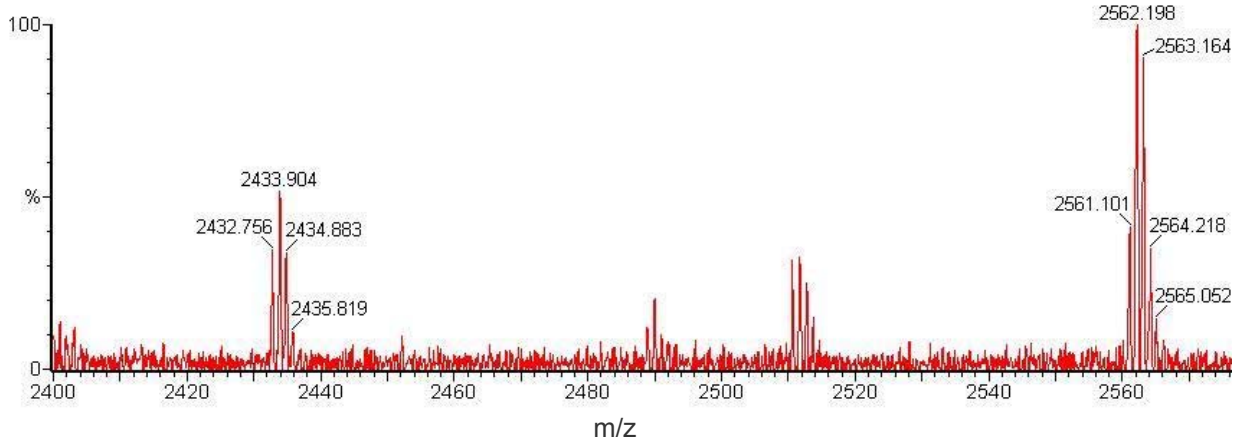

Figure 27. Partial MALDI-TOF mass spectrum of HSA, focusing on the fragment containing cysteine-34.

The calculated average mass of the HSA-purchased fragment containing cysteine-34 plus another cysteine is 2552.8812 Da and the calculated monoisotopic mass is 2551.2641 Da. In the mass spectrum of a tryptic digest of HSA-purchased, the fragment containing cysteine-34 is represented by a cluster of isotope peaks separated by one mass unit. Figure 28 shows the partial MALDI-TOF mass spectrum of HSA-purchased after it has been digested with trypsin. This sample was analyzed using the Bruker Daltronics reflex IV MALDI-TOF-MS and was made available through the UC-MS facility by Dr. Patrick Limbach. The spectrum is expanded in the region around the expected mass of the cysteine-34 plus cysteine trypsin digest fragment. The peak at m/z 2552.8843 corresponds to the expected mass of the cysteine-34 fragment with an additional cysteine bound. The difference in the visual quality between Figures 27 and 28 lies with the capability of each instrument to collect and combine the signal from the mass spectrometer for a specific length of time. The Micromass MALDI-TOF-MS is able to average spectra collected during a certain period of time, where the Bruker instrument was not operated using that option.

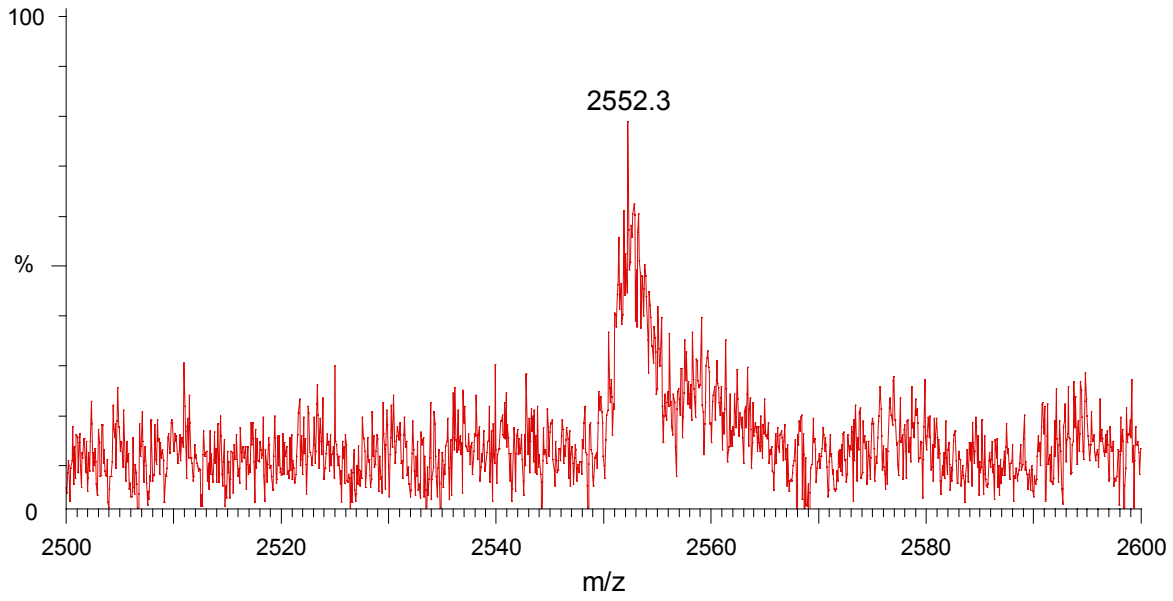

Figure 28. Partial MALDI-TOF mass spectrum of HSA-purchased showing the region that contains the 21 amino acid sequence surrounding cysteine-34.

The calculated average mass of the HSA•AA fragment containing cysteine-34 is 2491.9334 Da and the calculated monoisotopic mass is 2490.2855 Da. In the mass spectrum of a tryptic digest of HSA•AA, the fragment containing cysteine-34 is represented by a cluster of isotope peaks separated by one mass unit. Figure 29 shows the MALDI-TOF mass spectrum of HSA•AA after it has been digested with trypsin. The spectrum is expanded in the region around the expected mass of the cysteine-34 trypsin digest fragment. In the mass spectrum of HSA•AA, the peak cluster that begins with 2489.076 corresponds to the expected mass of the fragment containing cysteine-34 plus the mass of an acetamide (57 Da).

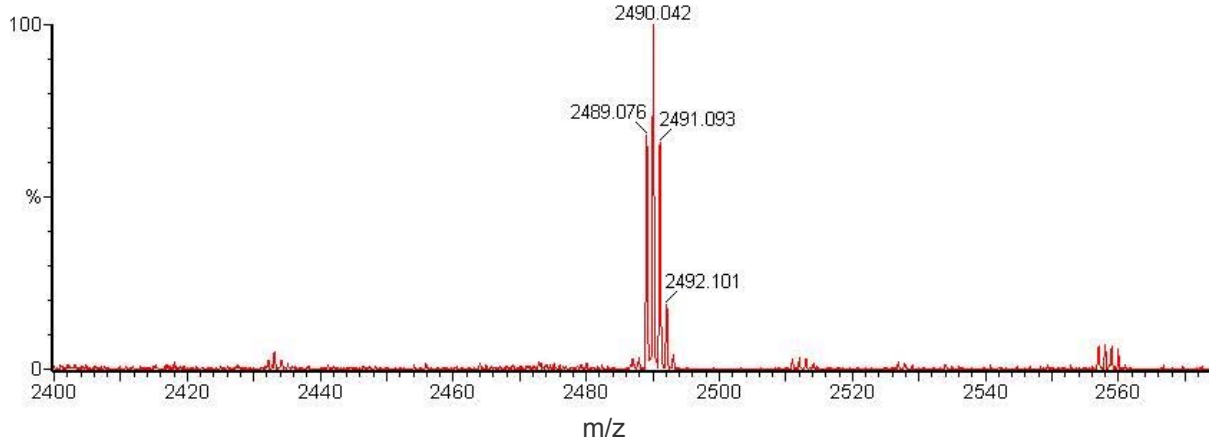

Figure 29. MALDI-TOF mass spectrum of HSA•AA, focusing on the fragment containing cysteine-34.

E. Binding Constants via Ultrafiltration

Ultrafiltration is a more direct and accurate way to measure the binding constant of the dicyanogold(I)-serum albumin system than Penefsky size-exclusion chromatography (see Appendix A for discussion of Penefsky chromatography). The equilibrium established between the bound and unbound species in solution is maintained throughout the process of ultrafiltration, so that the concentration of gold present in the sample at equilibrium is measured. The binding constants obtained using ultrafiltration are, as expected, higher than those obtained from Penefsky chromatography (Table 7). In the latter method, the amount of gold bound to the protein at "equilibrium" is measured, which is less than the actual equilibrium value (and is discussed in Appendix A). In ultrafiltration, the filtrate can be analyzed for the equilibrium concentration of dicyanogold(I) directly using the ICP-MS with no digestion and, at most, one dilution step using the following equation.

$$K_{eq} = \frac{[HSA \bullet Au(CN)_2^-]_{eq}}{[HSA]_{eq}\,[Au(CN)_2^-]_{eq}} \qquad \text{(eq. 11)}$$

Since the initial and equilibrium concentrations of dicyanogold(I) can be measured, the equilibrium concentration of dicyanogold(I) bound to albumin can be calculated.

$$[albumin \bullet Au(CN)_2^-]_{eq} = [Au(CN)_2^-]_{initial} - [Au(CN)_2^-]_{eq} \qquad \text{(eq. 12)}$$

Since the initial concentration of albumin can also be measured, the equilibrium concentration of unbound albumin can be calculated.

$$[albumin]_{eq} = [albumin]_{initial} - [albumin \bullet Au(CN)_2^-]_{eq} \quad \text{(eq. 13)}$$

The ultrafiltration sample 1 in Table 7 was calculated as follows.

$$[Au(CN)_2^-]_{initial} = 1.523\ (\pm 0.02) \times 10^{-6}\ M$$

$$[albumin]_{initial} = 4.613\ (\pm 0.1) \times 10^{-4}\ M$$

$$[Au(CN)_2^-]_{eq} = 5.859\ (\pm 0.1) \times 10^{-8}\ M$$

$$[albumin \bullet Au(CN)_2^-]_{eq} = (1.523\ (\pm 0.02) \times 10^{-6}\ M) - (5.859\ (\pm 0.1) \times 10^{-8}\ M)$$

$$[albumin]_{eq} = (4.613\ (\pm 0.1) \times 10^{-4}\ M) - (1.464\ (\pm 0.02) \times 10^{-6}\ M)$$

$$K_{eq} = (1.464\ (\pm 0.02) \times 10^{-6}\ M)/(4.598\ (\pm 0.1) \times 10^{-4}\ M)(5.859\ (\pm 0.1) \times 10^{-8}\ M)$$

$$K_{eq} = 5.9\ (\pm 0.2) \times 10^{4}\ M^{-1}$$

According to Harris[18], p. 88, the concentrations reported in the equilibrium constant equations are relative to their standard state. The standard state of the solute in this solution is 1M. As a result, the concentration units of K_{eq} are mathematically eliminated making K_{eq} a unitless quantity and will be reported as such from this point. The values reported in Table 7 are the calculated binding constants for bovine serum albumin and dicyanogold(I) using either Penefsky chromatography or ultrafiltration. Additionally, the standard deviations reported in Table 7 refer to the variance in the four values listed for K_{eq}.

Table 7. Comparison of binding constants obtained via Penefsky chromatography and ultrafiltration.

Penefsky		**Ultrafiltration**	
Sample	K_{eq}	Sample	K_{eq}
1	3.0×10^4	1	5.9×10^4
2	1.7×10^4	2	5.7×10^4
3	2.1×10^4	3	6.1×10^4
4	3.8×10^4	4	6.2×10^4
avg	2.7×10^4	avg	6.0×10^4
SD	0.9×10^4	SD	0.2×10^4

F. Reversibility of dicyanogold-HSA Binding

This experiment tested the reversibility of the binding interaction between dicyanogold(I) and HSA through the removal of the unbound dicyanogold(I) present at equilibrium using Penefsky chromatography. In Penefsky chromatography protein-containing components of the solution are eluted while free dicyanogold(I) is retained in the column packing material. Subsequently the equilibrium is allowed to re-establish and ultrafiltration is used to determine the binding constant, K_{eq}. The binding constant, $K_{re\text{-}eq}$, measures the binding interaction between HSA and dicyanogold(I) after the small molecule gold is removed and the solution is allowed to re-equilibrate. The data for both HSA and HSA•AA (Table 8) show that K_{eq} is equal to $K_{re\text{-}eq}$, indicating that the system is not losing small molecule gold through irreversible covalent binding. The standard deviation of K_{eq} and $K_{re\text{-}eq}$ is based on the variance of the binding constant within a set of four individual samples treated in the same way, so that there were four replicates within each experiment.

Table 8. The binding constants for normal and acetamide-blocked HSA both before and after re-equilibration.

	K_{eq}	SD	$K_{re\text{-}eq}$	SD
HSA	3.5×10^5	0.5	4.0×10^5	0.2
HSA·AA	1.3×10^4	0.1	1.28×10^4	0.05

The second step in exploring reversibility involves speciation of the small molecule gold released by the protein during re-equilibration. Reverse phase ion pairing chromatography of the filtrate from re-equilibrated samples shows that there is a single gold-containing species released from HSA. Comparing the chromatograms of samples to those of dicyanogold(I) standards, one can see that the retention time and peak shape are the same. (Figure 30)

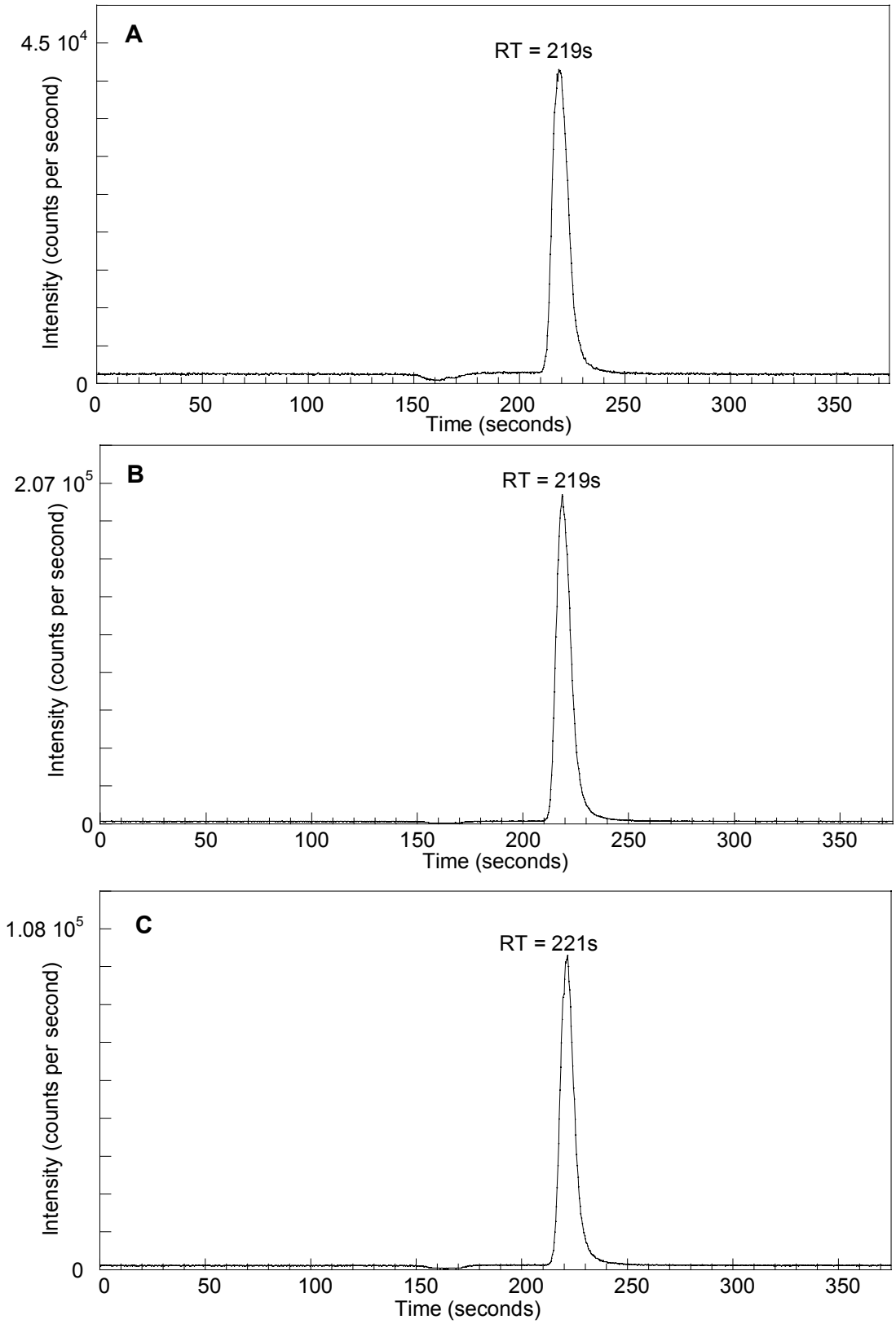

Figure 30. Gold species released from HSA. (**A**) normal HSA, (**B**) AA blocked HSA, (**C**) $[Au(CN)_2]^-$ standard. (5mM TBAC, 50% MeOH, 50% water, 5mM phosphate buffer adjusted to pH 7.4)

It is possible to quantify the amount of gold represented by a particular dicyanogold(I) chromatographic peak by determining the area under the peak and comparing that area to chromatographic data collected from dicyanogold(I) standards. By integrating the area under the peak of the chromatograms of the dicyanogold(I) standards, a calibration line can be constructed similar to those constructed for other ICP-MS experiments. In order to calculate concentrations from the chromatographic data, it is essential that the same portion of the chromatogram is integrated for each sample. To do this the peak maximum of the widest chromatographic peak is found and a window of data is selected that contains the entire peak. The number of data points before and after the peak maximum is recorded and the same range of data points is integrated for each chromatographic peak. Figure 31 shows a sample chromatogram. The area under the peak is integrated from 26 data points before the peak maximum to 120 data points after the peak maximum. All of the chromatograms from a given day are analyzed in this way. The areas calculated for each peak can be compared to the calibration data and concentrations of gold in each sample can be determined. Chromatograms that resulted from injecting the buffer solution that the protein was dissolved in were also analyzed in this way and the area under the blank peak was subtracted from the area under the sample peaks. Table 9 compares the total amount of gold released by the protein to the amount of gold determined to be dicyanogold(I) for both HSA and HSA•AA. Each value reported in Table 9 represents four individually-prepared replicate samples.

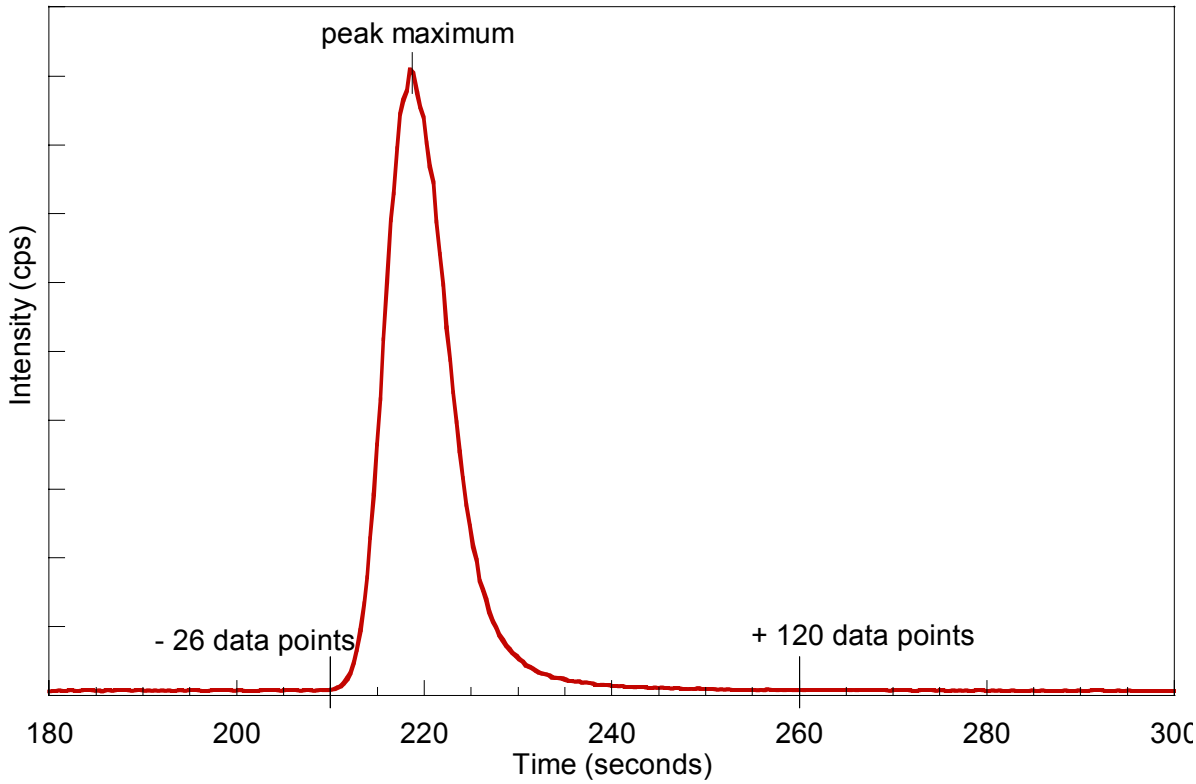

Figure 31. Sample chromatogram showing the data range used to determine the area under the peak.

Table 9. Reverse phase ion pairing chromatography of the gold containing species released by human serum albumin. Total gold represents the concentration in parts per billion of gold found in the ultrafiltrate as determined by direct aspiration into the ICP-MS. HPLC gold represents the concentration in parts per billion of dicyanogold(I) found in the ultrafiltrate as determined from the chromatograms.

HSA		**HSA·AA**	
total gold	HPLC gold	total gold	HPLC gold
13.8 ± 0.1	14.2 ± 0.2	50.1 ± 0.9	49.8 ± 0.4
12.8 ± 0.1	13.8 ± 0.3	45.6 ± 0.7	44.4 ± 0.5
13.2 ± 0.2	13.7 ± 0.1	47.6 ± 0.9	46.4 ± 0.5

In both HSA and HSA•AA, all of the gold that is released by the protein is in the form of dicyanogold(I). Through these experiments, we have shown that dicyanogold(I) binds as an intact anion to normal HSA and acetamide-blocked HSA, and that the binding is reversible, which means it can be approached from either direction. In one direction free dicyanogold(I) is added to HSA and an equilibrium is established. In the other direction HSA with bound dicyanogold(I) is allowed to dissociate, releasing dicyanogold(I) in order to maintain equilibrium. Additionally, it can be seen that the binding interaction between dicyanogold(I) and human serum albumin is stronger than that between dicyanogold(I) and human serum albumin blocked at cysteine-34 with iodoacetamide.

G. Changing the equilibrium conditions

1. Varying the initial concentration of $KAu(CN)_2$

In this set of experiments, the initial concentration of $KAu(CN)_2$ was varied while the concentration of HSA was held constant. Though the focus of this work is to study the probable binding scenario at physiological levels, which includes concentrations of dicyanogold(I) at or below 1.5 μM, the initial ratios for this experiment were allowed to far exceed gold concentrations that are possible *in vivo* so that more information about the binding site could be gathered. The data for HSA show that as the initial concentration of $KAu(CN)_2$ increases, the binding constant decreases. Similar behavior is seen in the acetamide-blocked HSA, though the change in the observed binding constant is not as dramatic. For both HSA and HSA•AA the percent change in the binding constant decreases as the initial concentration of dicyanogold(I) increases. Table 10 lists the initial ratio of dicyanogold(I) to HSA, the measured equilibrium constant (K_{eq}) and the standard deviation of K_{eq} for both HSA and HSA•AA. The standard deviations for K_{eq} throughout this section arise from the variance that occurred within each sample set, i.e. each binding constant reported is the average of four binding constants calculated from four experimental samples and SD is the standard deviation associated with that average. Though the temperature of each sample in this set of experiments was not determined, the experiments were conducted at room temperature (22-24ºC) and the centrifuge was set at 22ºC, which generally operates at 1-2ºC above the programmed temperature.

Traditional analysis of these data employs a method for linearizing the data followed by a linear regression analysis of the resulting data. Two linear regression analyses were used to study these data: Scatchard (reciprocal plot) and Klotz (double reciprocal plot) methods. Both of these methods of analysis involve first operating on the data so that one can draw a line of best

fit, and then visually determining if one line (single-site binding) or multiple lines (multiple-site binding) can be drawn through the data. These methods, which rely on a visual assessment of the data, were designed for the purpose of characterizing a single binding site. Both methods show that the data appear linear when a single binding site is present and a distinct deviation from linearity when multiple binding sites are occupied. Thus, these analyses are most quantitative in the case where a single site is occupied, but they are also useful in determining whether the binding occurs at a single site or multiple sites.

In addition to the methods mentioned above, a third technique that has become a standard analysis for binding data is non-linear regression. In this type of analysis the data is plotted without mathematical treatment to linearize the data. Since this method does not rely on visual assessment of the data, it lacks the ambiguity of the linear methods when distinguishing the number of different kinds of binding sites that are occupied.

Table 10. Concentration dependence of K_{eq} on the initial dicyanogold(I):HSA ratio.

HSA			**HSA·AA**		
Ratio	K_{eq}	SD	Ratio	K_{eq}	SD
0.0027	2.62×10^5	0.04	0.0032	1.10×10^4	0.03
0.0053	2.3×10^5	0.1	0.0060	2.41×10^4	0.06
0.0112	2.92×10^4	0.07	0.054	5.3×10^3	0.2
0.047	1.5×10^4	0.1	0.119	4.87×10^3	0.09
0.51	6.8×10^3	0.5	0.59	6.8×10^3	0.2
0.769	8.6×10^3	0.3	0.884	8.1×10^3	0.1

The data from this experiment was initially analyzed using the Scatchard method. In the Scatchard method, the ratio of protein-bound gold (Au_b) to HSA at equilibrium, or the fraction of albumin which has gold bound to it (labeled B), is plotted on the x-axis and $B/[Au]_{free}$, where $[Au]_{free}$ is the equilibrium concentration of free gold in solution, is plotted on the y-axis. Table 11 lists the values used to construct the Scatchard plot in Figure 32. A line of best fit can be drawn through the resulting data points. In situations where more than one kind of binding site is available, the data points do not lie on a straight line, instead they are arranged so that more than one line can be drawn. Each line represents a different kind of binding site, though it is possible to have multiple binding sites of the same kind. The slope of each line represents the negative value of the estimated binding constant while the x-intercept represents the number of binding sites per molecule. Plotting the data in this way, it can be seen that more than one line of data points may be present on a single plot. The Scatchard plot for glutathione treated HSA, in fact, reveals that there are two kinds of dicyanogold(I) binding sites present on HSA, even though all initial Au:HSA ratios were less than 1:1. The first binding site is a high affinity site, where $K = 1.88 \times 10^7$ calculated from the slope of the line. There are only 0.014 of these sites per molecule of albumin as calculated from the x-intercept of the line. (Figure 32) The second binding site is a lower affinity site, $K = 2.22 \times 10^4$, though it occurs more frequently per molecule of albumin, 0.590 sites per molecule. The equations for the lines are

$$y = (-1.88 \times 10^7)(x) + (2.55 \times 10^5) \quad \text{(high affinity)} \qquad \text{(eq. 14)}$$

$$y = (-2.22 \times 10^4)(x) + (1.31 \times 10^4) \quad \text{(low affinity)} \qquad \text{(eq. 15)}$$

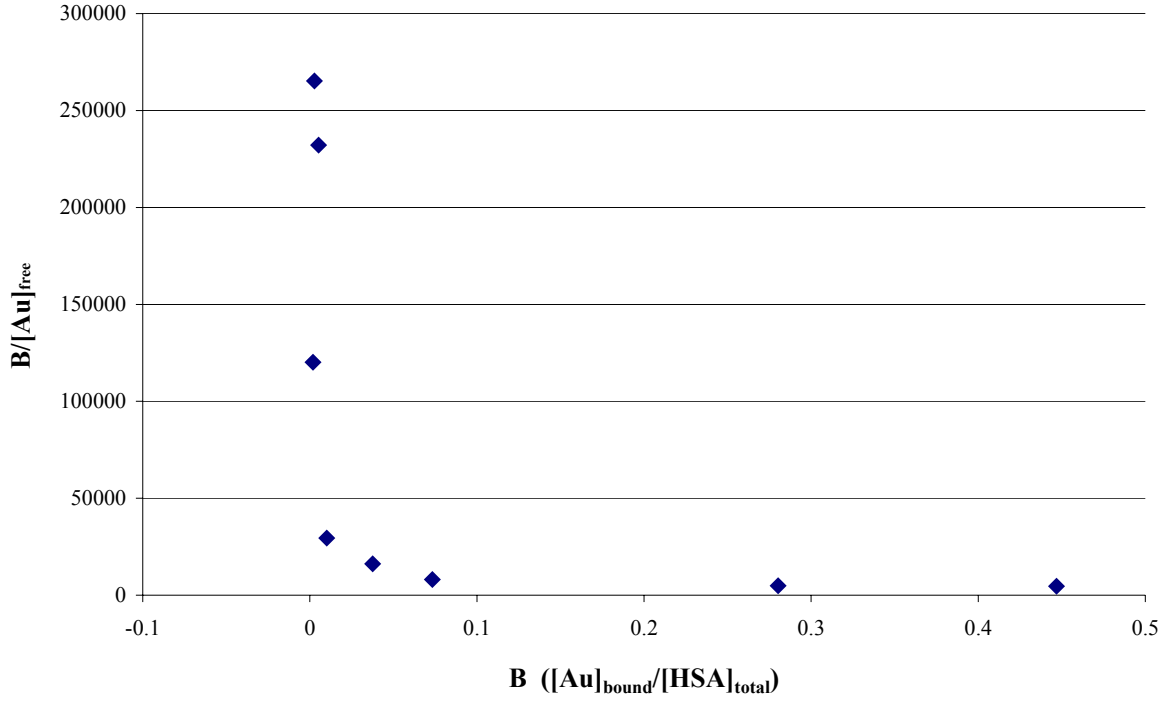

Figure 32. Scatchard plot for HSA and dicyanogold(I).

Table 11. Data from which the Scatchard plot of HSA was constructed, where B is the ratio of gold atoms bound per each albumin molecule at equilibrium.

B	$[Au]_{free}$ (M)	$B/[Au]_{free}$
0.0019	1.58×10^{-8}	1.20×10^{5}
0.0027	1.02×10^{-8}	2.65×10^{5}
0.0052	2.24×10^{-8}	2.32×10^{5}
0.0101	3.43×10^{-7}	2.95×10^{4}
0.0376	2.33×10^{-6}	1.61×10^{4}
0.0733	9.02×10^{-6}	8.12×10^{3}
0.2802	5.71×10^{-5}	4.91×10^{3}
0.4469	9.62×10^{-5}	4.65×10^{3}

Similarly, the Scatchard plot for the acetamide-blocked HSA data reveals that there are two dicyanogold(I) binding sites on each molecule of albumin. The first binding site is a high affinity site, but there are only 0.043 of these sites per molecule of albumin determined from the x-intercept of the line representing the high affinity site. (Figure 33) Table 12 lists the values used to construct the Scatchard plot in Figure 33. The estimated binding constant for the site can be calculated from the slope of that line, $K = 4.1 \times 10^{5}$. The second binding site is a lower affinity site though it occurs more frequently, 3.90 sites per molecule of albumin. The equilibrium constant calculated for the low affinity site is 1.3×10^{3}. Though the plots for HSA and HSA•AA appear to be similar, the number of low affinity binding sites, and the binding constants for both types of sites on HSA•AA, are significantly different from the sites on HSA. The equations for the lines are

$$y = (-4.06 \times 10^{5})(x) + (1.75 \times 10^{4}) \quad \text{(high affinity)} \qquad \text{(eq. 16)}$$

$$y = (-1.28 \times 10^{3})(x) + (5.00 \times 10^{3}) \quad \text{(low affinity)} \qquad \text{(eq. 17)}$$

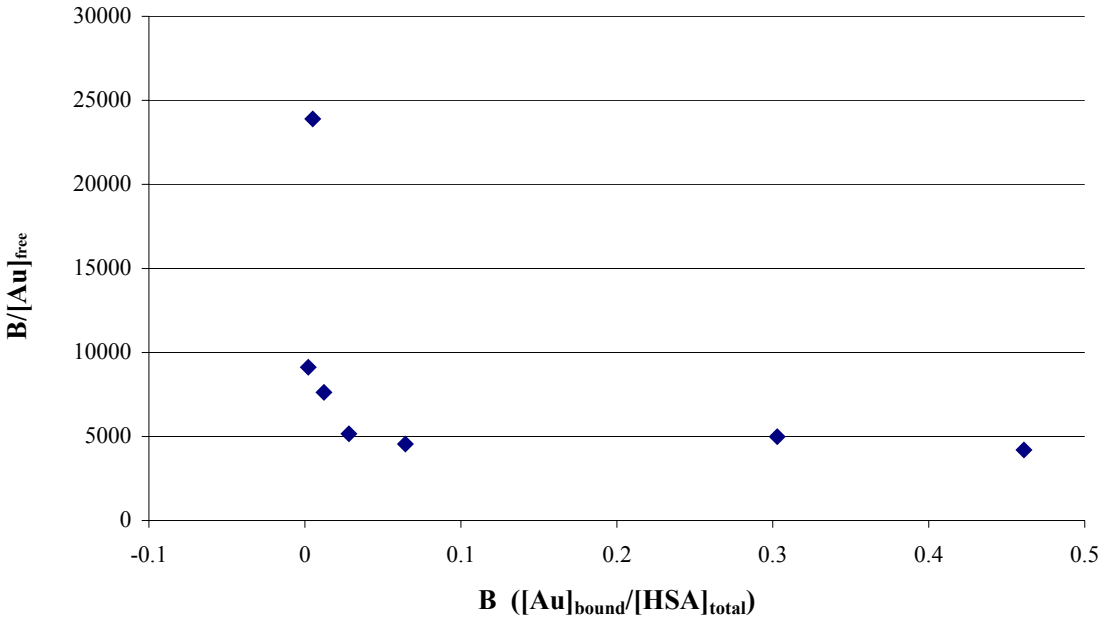

Figure 33. Scatchard plot of HSA•AA and dicyanogold(I).

Table 12. Data from which the Scatchard plot of HSA•AA was constructed, where B is the ratio of gold atoms bound per each albumin molecule.

B	$[Au]_{free}$ (M)	$B/[Au]_{free}$
0.0022	2.41×10^{-7}	9.12×10^{3}
0.005	2.09×10^{-7}	2.39×10^{4}
0.0122	1.60×10^{-6}	7.63×10^{3}
0.0282	5.46×10^{-6}	5.16×10^{3}
0.0644	1.42×10^{-5}	4.55×10^{3}
0.3028	6.07×10^{-5}	4.99×10^{3}
0.461	1.10×10^{-4}	4.20×10^{3}

The binding data obtained from varying the initial concentration of dicyanogold(I) can also be analyzed using a reciprocal analysis of the data, also referred to as a Klotz plot[22]. In this method, the reciprocal of the concentration of free dicyanogold(I) ([Au] free) present at equilibrium is plotted on the x-axis and the reciprocal of the ratio of bound gold to total albumin (B) is plotted on the y-axis. Figure 34 is the reciprocal plot representing the binding interaction between dicyanogold(I) and HSA. The data used to construct the plot in Figure 34 are contained in Table 13. A line of best fit can be drawn through the resulting data points, or in this case two lines, each representing a type of binding site.

$$1/B = 1/n + 1/nK[Au]_{free} \qquad \text{(eq. 18)}$$

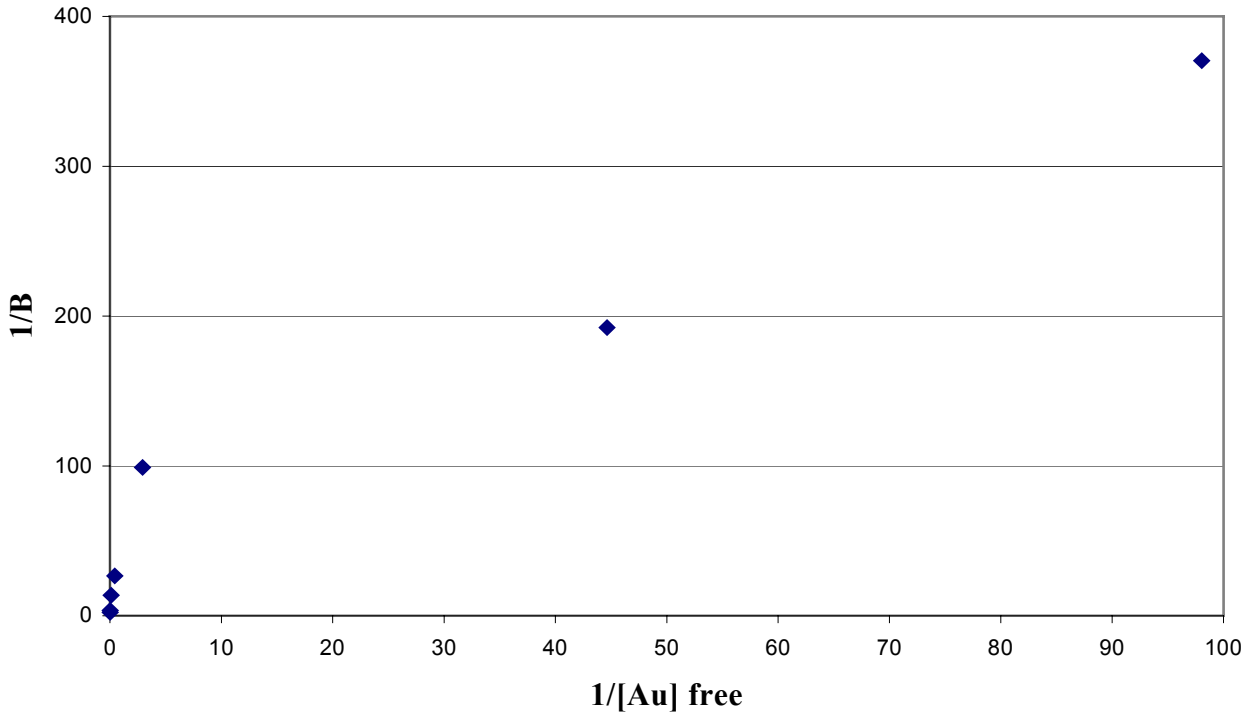

Figure 34. Double-reciprocal plot for the binding of dicyanogold(I) to HSA.

Table 13. Data used to construct the double-reciprocal plot for the binding of dicyanogold(I) to HSA, concentrations are μM.

$1/Au_{free}$	1/B
0.010	2.238
0.018	3.569
0.111	13.643
0.429	26.596
2.915	99.010
44.643	192.308
98.039	370.370

As with the Scatchard analysis, the data appear to form two different straight lines, each representing a different type of binding site. A line drawn through the first three points represents the low affinity site. The equation of this line is

$$y = (1.11 \times 10^{-4})\, x + 1.343 \qquad \text{(eq. 19)}$$

A line drawn through the last three points represents the high affinity site. The equation of this line is

$$y = (2.87 \times 10^{-6})\, x + 81.045 \qquad \text{(eq. 20)}$$

Calculating the binding constants and number of binding sites for each line, K_{eq} for the low affinity site is 1.21×10^{4} with n = 0.745 binding sites per molecule and K_{eq} for the high affinity site is 2.90×10^{7} with n = 0.012 binding sites per molecule.

The data for the HSA•AA case also appear to form two different straight lines, each representing a different type of binding site, though the effect is not as dramatic as with the HSA system. The data used to construct the plot in Figure 35 are contained in Table 14. Figure 35 is the double reciprocal plot representing the binding interaction between dicyanogold(I) and HSA•AA and contains six data points. A line drawn through the first four points, where the first two points seem to appear as one, represents the low affinity site. The equation of this line is

$$y = (1.92 \times 10^{-4})\, x + 0.695 \qquad \text{(eq. 21)}$$

A line drawn through the last two points represents the high affinity site. The equation of this line is

$$y = (2.80 \times 10^{-5})\, x + 64.213 \qquad \text{(eq. 22)}$$

Calculating the binding constants and number of binding sites for each line, K_{eq} for the low affinity site is 3.62×10^{3} with n = 1.440 binding sites per molecule and K_{eq} for the high affinity site is 2.23×10^{6} with n = 0.016 binding sites per molecule.

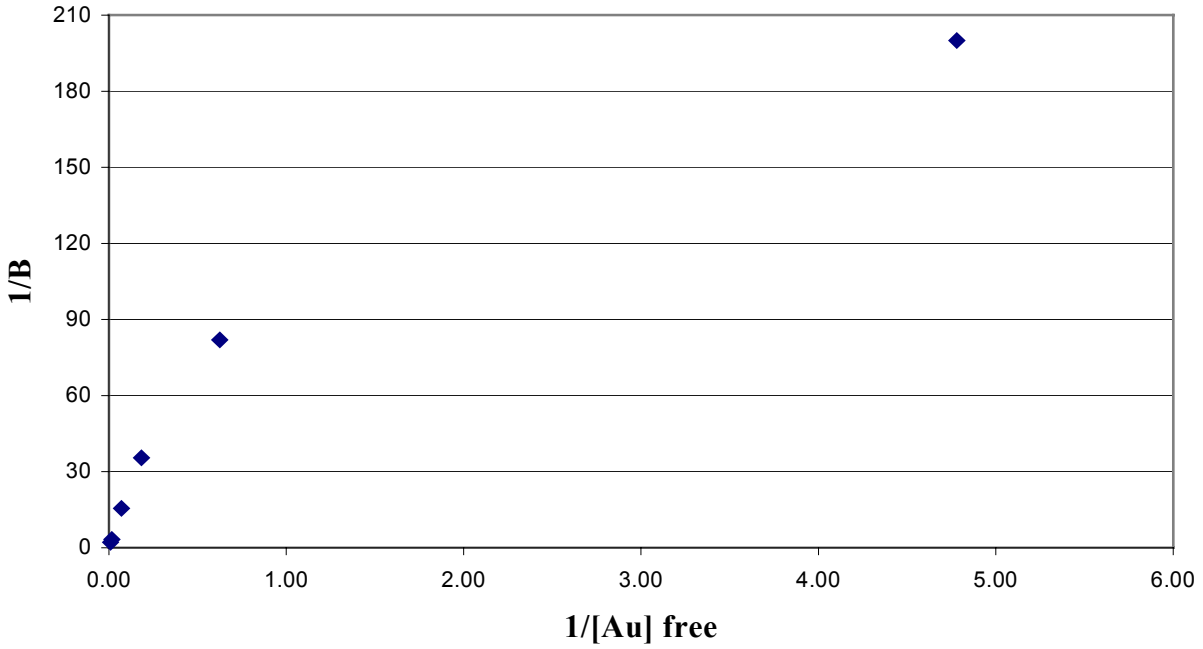

Figure 35. Reciprocal plot for the binding of dicyanogold(I) to HSA•AA.

Table 14. Data used to construct the reciprocal plot for the binding of dicyanogold(I) to HSA•AA, concentrations are μM.

$1/Au_{free}$	1/B
0.009	2.169
0.016	3.303
0.071	15.528
0.183	35.461
0.625	81.967
4.780	200.000

The final method used to analyze the binding data from this series of experiments was non-linear regression. Because this type of analysis does not require a linear transformation of the data, it is a more reliable method for analyzing binding data that involves multiple binding sites. The data from the dicyanogold(I)-HSA system was analyzed using a built-in two site hyperbola fit within the GraphPad Prism software. Figure 36 contains the non-linear regression fit ($R^2 = 0.9999$) for the dicyanogold(I)-HSA binding data. The binding constant for the high affinity site was 9.89×10^5 and there were 0.0390 of this type of binding site per molecule of albumin. The data for the second site indicated non-specific binding with a binding constant of approximately 1 and more than 4000 binding sites per molecule of albumin. The apparent non-specific behavior of the low-affinity site is due to the lack of data available at higher dicyanogold(I) concentrations.

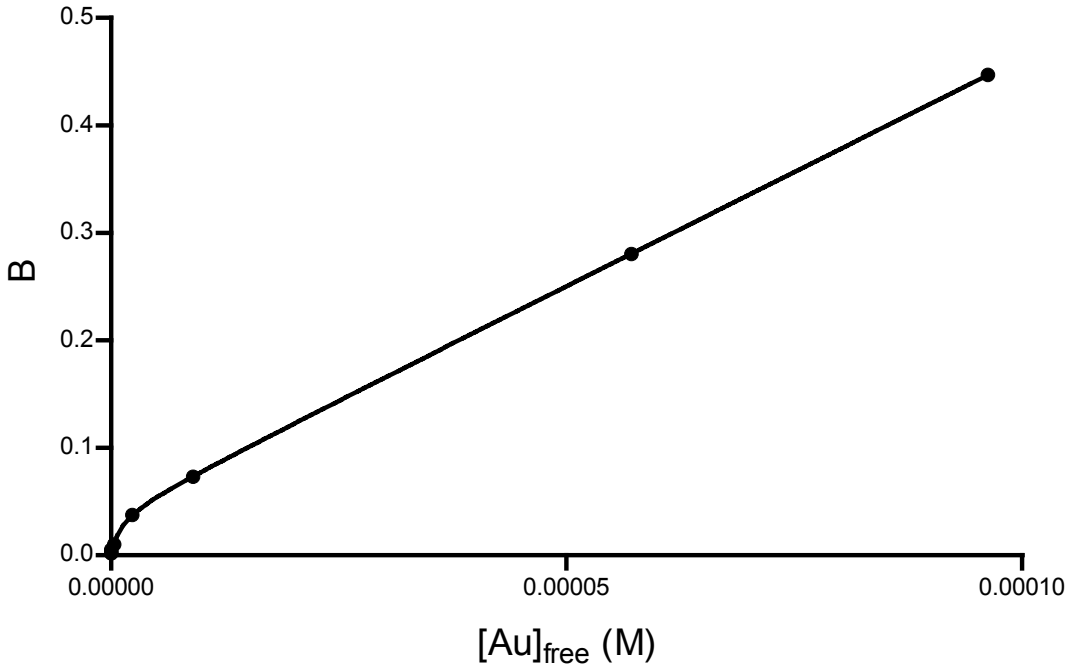

Figure 36. Non-linear regression fit of the binding data for dicyanogold(I)-HSA binding.

The data from the dicyanogold(I)-HSA•AA system were analyzed using both the single site hyperbola and the built-in two site hyperbola fit within the GraphPad Prism software. Figure 37 contains the non-linear regression fits (single site $R^2 = 0.9982$, two site $R^2 = 0.9823$) for the dicyanogold(I)-HSA•AA binding data. For the two-site fit, the binding constant for the high affinity site was 1.01×10^4 and there were 0.3957 sites of this type per molecule of albumin. The binding constant for the low affinity site was 9823 and there were 0.4332 sites of this type per molecule of albumin. For the single-site fit, the binding constant was 3546 and there were 1.655 sites of this type per molecule of albumin. The ambiguity associated with the non-linear regression of the binding data for the dicyanogold(I)-HSA•AA system, is due to the lack of data collected in general, as well as the lack of data at higher dicyanogold(I) concentrations. Also, the increasingly poor fit for two sites versus one site is likely a breakdown in how the software analyzes the available data.

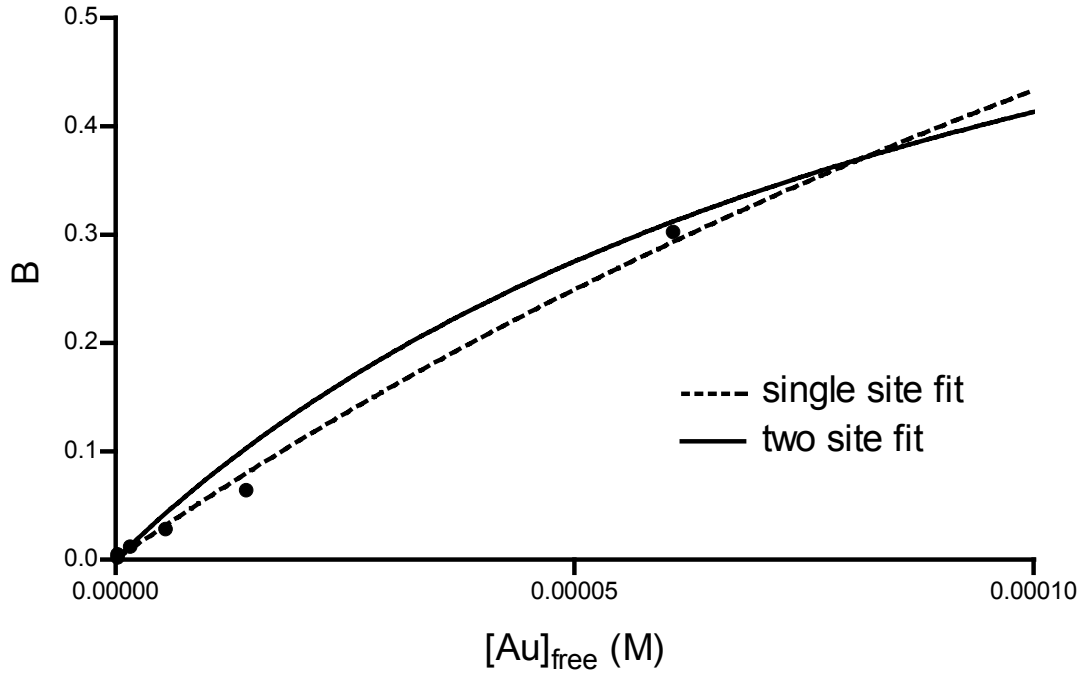

Figure 37. Non-linear regression fit of the binding data for dicyanogold(I)-HSA•AA binding.

The binding constants determined using each of the data analysis methods are compiled in Table 15. Recall that both the Scatchard and Klotz analyses were intended for use in system with only one type of binding site. While the data seems inconsistent, the result is the same for both forms of the protein in both of the analyses; that is, in each case there are two different kinds of binding sites. There is a high affinity site that occurs rarely and a low affinity site that occurs frequently. Though lacking in high concentration data, the non-linear regression for HSA also shows that there is a high affinity site that also occurs rarely. It is clear that at physiological levels, where the initial gold to HSA ratio is less than 0.01, the only site that is actively populated is this high affinity site. So, while it is interesting to observe the low affinity site, it is not necessary to fully characterize this site for the purpose of this study, which focuses on the interaction between dicyanogold(I) and HSA at physiologically relevant concentrations.

Table 15. Comparison of the binding constants obtained through different methods of data analysis.

	HSA		**HSA·AA**	
	K_{eq}	no. of sites	K_{eq}	no. of sites
Scatchard	1.88×10^{7}	0.014	4.1×10^{5}	0.043
	2.22×10^{4}	0.59	1.3×10^{3}	3.9
Klotz	2.90×10^{7}	0.012	2.23×10^{6}	0.016
	1.21×10^{4}	0.745	3.62×10^{3}	1.44
Non-linear	9.89×10^{5}	0.039	1.01×10^{4}	0.396
	1	4000	9.82×10^{3}	0.433

2. Varying the ionic strength of the solution

The second series of experiments tested the effect of ionic strength on the binding interaction between dicyanogold(I) and albumin, both HSA and HSA•AA. The ionic strength solutions were chosen so that the buffer strength remained essentially constant while the amount of added salt was varied. Other variables, such as initial concentrations of $KAu(CN)_2$ and HSA, were held constant. The binding constants for the normal HSA increase with increasing ionic strength, as shown in Table 16. Conversely, the binding constants for the acetamide-blocked HSA remain relatively constant, or increase slightly, with increasing ionic strength, as shown in Table 17.

Table 16. The dependence of K_{eq} on the ionic strength of the HSA solution, where each solution contains 100 mM $NaHCO_3$ buffer plus the concentration of salt listed.

		HSA	
Au:HSA	NaCl	K_{eq}	SD
0.00273	100 mM	4.4×10^5	0.1
0.00274	50 mM	2.7×10^5	0.1
0.00273	0 mM	2.1×10^5	0.3

Table 17. The dependence of K_{eq} on the ionic strength of the HSA•AA solution, where each solution contains 100 mM $NaHCO_3$ buffer plus the concentration of salt listed.

HSA·AA			
Au:HSA	NaCl	K_{eq}	SD
0.00312	100 mM	1.43×10^4	0.05
0.00320	50 mM	0.92×10^4	0.01
0.00321	0 mM	1.10×10^4	0.03

In general, the ionic environment of the binding site is directly related to the ionic strength of the solution around the binding site. Increasing the ionic strength effectively increases the number of ions, both positive and negative, located near a particular binding site. Increasing the charge at an electrostatic binding site will screen some of the charge effects of that binding site.[21 (p. 46)] In this case, the effect of the ionic atmosphere around the binding site of HSA is larger than the effect of the same ionic atmosphere around the binding site of HSA•AA. Also, the observed effect of increasing the ionic strength around the binding of dicyanogold(I) is the reverse of that expected for an interaction between oppositely charged species.

3. Temperature dependence of $KAu(CN)_2$ binding to HSA

The final series of experiments presented in this section explored the effects of temperature on the binding interaction between $KAu(CN)_2$ and albumin, both HSA and HSA•AA. The temperatures chosen were within the range of temperatures tolerated by albumin without major structural changes.[10] For HSA, as the incubation temperature increases the binding constant also increases, as shown in Table 18. For HSA•AA, as the incubation

temperature increases the binding constant decreases, indicating that the binding interaction seen here is different than in HSA, as shown in Table 19.

Table 18. Temperature and calculated binding constants for HSA.

HSA			
T (°C)	Au:HSA $_{(initial)}$	K	SD
4.5	0.0037	1.11×10^5	0.04
14.1	0.0037	1.39×10^5	0.05
20.3	0.0054	2.3×10^5	0.1
26.15	0.00273	2.62×10^5	0.04
33.9	0.00273	4.54×10^5	0.09
37.4	0.0037	5.8×10^5	0.6

Table 19. Temperature and calculated binding constants for HSA•AA.

HSA·AA			
T (°C)	Au:HSA (initial)	K	SD
3.90	0.0035	3.16×10^4	0.06
9.80	0.0032	1.42×10^4	0.02
15.10	0.0035	1.71×10^4	0.05
26.80	0.0032	9.2×10^3	0.1
34.15	0.0032	9.7×10^3	0.4
38.30	0.0035	9.6×10^3	0.2

A van't Hoff plot[23] can be constructed using these data from which the enthalpy and entropy of binding can be extracted. A van't Hoff plot is constructed by plotting 1/T (Kelvin) on the x-axis and lnK on the y-axis. A line of best fit can be drawn through the data points. The slope of the resulting line is used to determine the enthalpy of binding while the y-intercept is used to determine the entropy as follows.

$$\Delta G = \Delta H - T\Delta S$$

$$\Delta G = -RT\ (\ln K)$$

$$-RT\ (\ln K) = \Delta H - T\Delta S$$

$$\ln K = (-\Delta H/R)(1/T) + (\Delta S/R) \qquad \text{(eq. 23)}$$

$$-\Delta H/R = \text{slope} \qquad \text{(eq. 24)}$$

$$\Delta S/R = \text{y-intercept} \qquad \text{(eq. 25)}$$

The van't Hoff plot constructed for HSA are shown in Figure 38, and the data used to construct this plot are presented in Table 20. The line drawn through the points has a negative slope, which is indicative of a positive enthalpy change upon binding (36.7 KJ/mol or 8.8 Kcal/mol). The entropy change upon binding, as it is determined from the intercept, is also positive for dicyanogold(I) binding to normal HSA (228 J/mol·K or 54.4 cal/mol·K). The equation for this line:

$$y = -4417.5x + 27.385 \qquad \text{(eq. 26)}$$

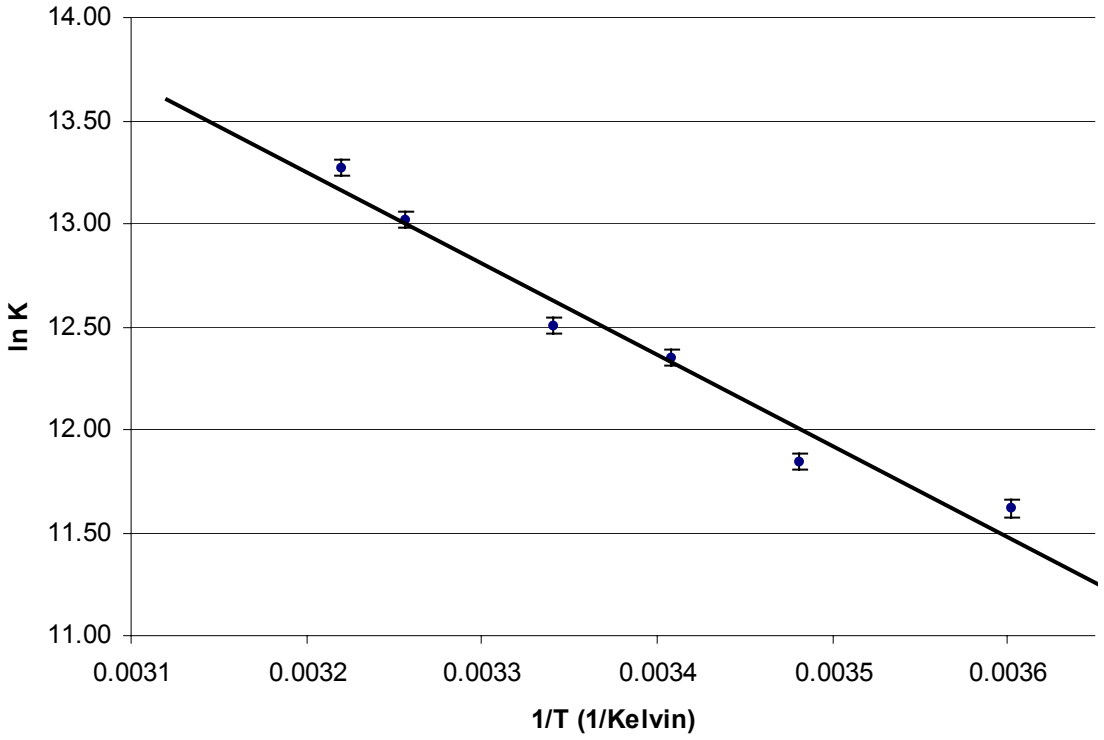

Figure 38. Van't Hoff plot of HSA.

Table 20. Temperature and binding constants from which the van't Hoff plot for HSA and dicyanogold(I) was constructed.

T	1/T	K	SD	lnK	SD	ΔG
277.65	0.003602	1.11×10^5	0.04	11.62	0.04	-26.8 kJ (-6.41 kcal)
287.25	0.003481	1.39×10^5	0.05	11.84	0.04	-28.3 kJ (-6.76 kcal)
293.45	0.003408	2.30×10^5	0.1	12.35	0.05	-30.1 kJ (-7.20 kcal)
299.30	0.003341	2.62×10^5	0.04	12.48	0.02	-31.1 kJ (-7.42 kcal)
307.05	0.003257	4.54×10^5	0.09	13.03	0.02	-33.3 kJ (-7.95 kcal)
310.55	0.003220	5.8×10^5	0.1	13.71	0.12	-35.4 kJ (-8.46 kcal)

The van't Hoff plot constructed for HSA•AA is shown in Figure 39, and the data used to construct this plot are presented in Table 21. The data reveal an opposite trend to the one observed in the HSA plot. In the HSA•AA plot, the line drawn through the data points has a positive slope indicating that the enthalpy change upon binding is now negative (-20.9 KJ/mol or –5.0 Kcal/mol). The entropy change upon binding is much less positive in the blocked HSA than in the normal HSA (8.0 J/mol·K or 1.9 cal/mol·K). The equation for this line:

$$y = 2511.4x + 0.9638 \qquad \text{(eq. 27)}$$

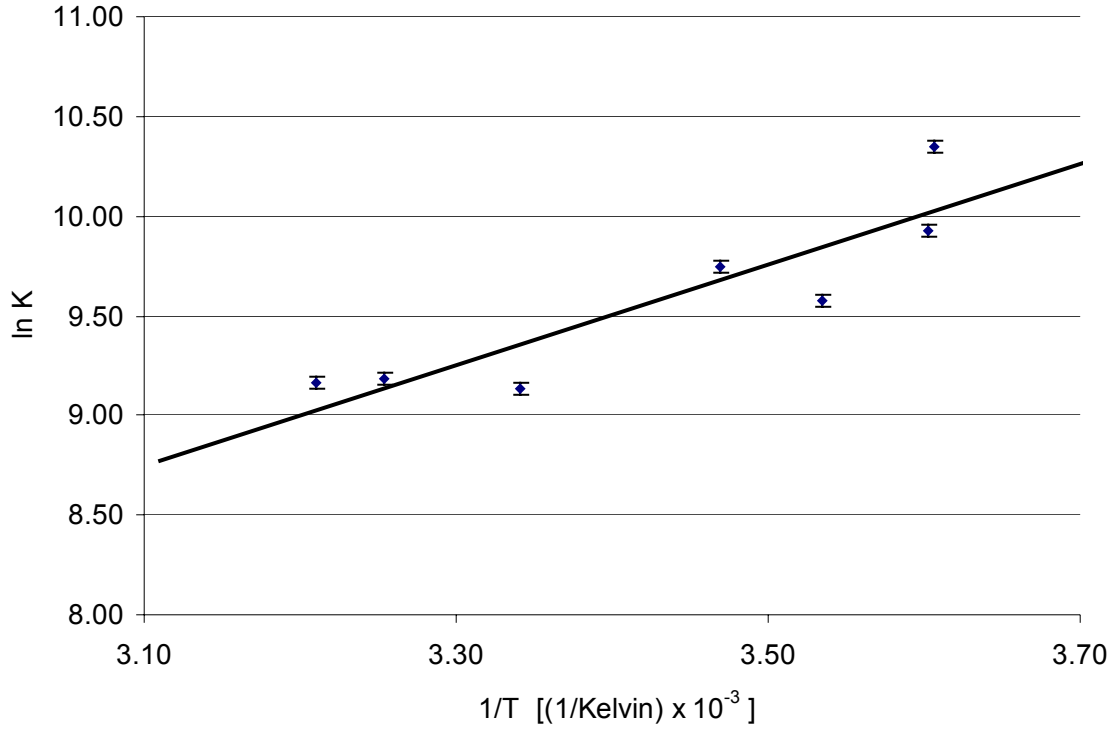

Figure 39. Van't Hoff plot of HSA•AA.

Table 21. Temperature and binding constants from which the van't Hoff plot for HSA•AA and dicyanogold(I) was constructed.

T	1/T	K	SD	lnK	SD	ΔG
277.05	0.003609	3.11×10^4	0.06	10.34	0.02	-23.8 kJ (-5.7 kcal)
277.60	0.003602	2.04×10^4	0.09	9.92	0.04	-22.9 kJ (-5.7 kcal)
282.95	0.003534	1.44×10^4	0.02	9.57	0.01	-22.5 kJ (-5.38 kcal)
288.25	0.003469	1.71×10^4	0.05	9.75	0.03	-23.4 kJ (-5.58 kcal)
299.95	0.003334	9.3×10^3	0.1	9.14	0.01	-22.8 kJ (-5.44 kcal)
307.30	0.003254	9.7×10^3	0.4	9.18	0.04	-23.5 kJ (-5.61 kcal)
311.45	0.003211	9.5×10^3	0.2	9.16	0.02	-23.7 kJ (-5.68 kcal)

Table 22 summarizes the enthalpy and entropy change upon binding of dicyanogold(I) to human serum albumin. The interaction between dicyanogold(I) and HSA is an entropically favored process in which both ΔH and ΔS have positive values. If an entropically dominated process is spontaneous, that is ΔG has a negative value, it occurs because the system in question is sufficiently more disordered after reaction than before so that the entropy term becomes larger than the enthaply term in the free energy equation. Specifically, in this case, upon binding of dicyanogold(I) to HSA, the disorder of the dicyanogold(I)-HSA system has increased. Also, because ΔH is positive the process of binding dicyanogold(I) to HSA is endothermic, so that when energy in the form of heat is added to the system the binding increases. Conversely, the interaction between dicyanogold(I) and HSA•AA is an enthalpically dominated process in which ΔH has a negative value. In this case, the binding of dicyanogold(I) to HSA that has been blocked at cysteine-34 with the addition of an acetamide group is an exothermic process. The

data from these experiments reveal that upon alkylation, the binding changed from an entropically favored process to and enthalpically favored process. This change suggests that alkylation of cysteine-34 alters the binding site.

Table 22. Comparison of calculated values for enthalpy and entropy of dicyanogold(I) binding to HSA and HSA•AA.

	HSA	HSA·AA
ΔH	42.6 KJ/mol (10.2 Kcal/mol)	-20.8 KJ/mol (-5.0 Kcal/mol)
ΔS	248 J/mol*K (59.3 cal/mol*K)	8.1 J/mol*K (1.9 cal/mol*K)

Chapter 4:

Conclusions

A. About the protein

In the course of this work, three forms of human serum albumin (HSA) have been studied using both FT-ICR-MS and MALDI-TOF-MS. The results of these experiments established that the HSA purchased from Sigma Chemicals is contaminated with a significant amount of protein containing an extra cysteine. Treatment with glutathione removes the extra cysteine and restores the HSA protein to the native form. Characterization of the HSA-purchased sample using MALDI-TOF-MS shows that this extra cysteine is bound to the 21-amino acid fragment (from the tryptic digest of HSA) that contains cysteine-34. Comparison of these results to the mass spectral data obtained from HSA that has been treated with glutathione reveals that the restoration of cysteine-34 was successful. In this case, the mass spectrum not only showed that the extra cysteine was removed from the HSA but that the excess glutathione in solution did not react with the HSA. Subsequent treatment with iodoacetamide results in addition of a single acetamide group to the protein along the 21 amino acid fragment containing cysteine-34. It is probable that the acetamide is bound to the sulfur atom of cysteine-34. In order to work with homogeneous protein sample, subsequent binding studies were carried out using glutathione treated samples (HSA) and iodoacetamide treated samples (HSA•AA). These two forms of HSA only differ in composition at cysteine-34.

With respect to the form of cysteine-34, recall that the pK of the thiol is significantly lower as it occurs in HSA (about 5.5) compared to the free amino acid (above 8). This becomes important because at the pH of blood, 7.4, a significant portion of the albumin (98.7%) is present in the thiolate form. This means that even in a sample of "homogeneous" albumin there are actually two forms of the protein present at any given moment. Because cysteine-34 resides near a hydrophobic crevice, it is expected that the difference between negatively charged sulfur and

neutral sulfur may, in fact, have a significant impact on that environment. Additionally, since cysteine-34 lies within a loop near the surface of the protein, its movement is somewhat unrestricted relative to the rest of the protein.

B. Binding studies

The binding studies involving dicyanogold(I) were carried out concurrently using both HSA and HSA•AA. The difference in the binding constants between the two systems must be attributed to the difference in the protein structure at cysteine-34 upon alkylation with iodoacetamide. The lower binding constant for the HSA•AA and dicyanogold(I) system leads to two observations. First, the binding of dicyanogold(I) to HSA•AA is significantly affected by the addition of an acetamide group to cysteine-34. Second, the binding of dicyanogold(I) to HSA•AA is not prevented by the addition of this acetamide group. These results indicate that the binding site for dicyanogold(I) on HSA is, in fact, altered by the addition of an acetamide group. Thus, the binding site must lie in close proximity to cysteine-34 or is in a location that is directly influenced by cysteine-34.

The rest of this chapter focuses on the discussion of the interaction between dicyanogold(I) and human serum albumin. First, a thermodynamic model for discussing binding is developed. Subsequently, the interaction between dicyanogold(I) and HSA is explored based on the data obtained through binding constant experiments and without making comparisons to the behavior observed in the acetamide-blocked system. Next, the interaction between dicyanogold(I) and HSA•AA is explored without making comparisons to the unblocked case. Finally, after presenting a case for the individual systems, the behavior observed in each system, HSA and HSA•AA, is compared.

1. thermodynamics of binding

A useful two-state model for interpreting the results of the binding studies is the reversible reaction of A and B to form the complex AB:

$$A + B \leftrightarrow AB \qquad (1)$$

The reaction is favorable and proceeds in the forward direction if the free energy of the associated product is less than the free energy of the reactants, *i.e.*, if the free energy of the reaction ($\Delta G'$) is negative. The free energy of the reaction is given by the general expression:

$$\Delta G' = \Delta H' - T\Delta S' \qquad (2)$$

where $\Delta H'$ is the enthalpy of reaction, $\Delta S'$ is the entropy of reaction and T is the temperature. $\Delta G'$ is related to the standard free energy of reaction ΔG by:

$$\Delta G' = \Delta G + RT\ln(Q) \qquad (3)$$

where Q is the reaction quotient. At equilibrium the free energy of reaction ($\Delta G'$) is zero and Q equals the value of the equilibrium constant (K_{eq}). The ΔG values reported here derive from the measured binding constant according to:

$$\Delta G = -RT\ln(K_{eq}) \qquad (4)$$

where R is the gas constant. Therefore, the corresponding values of ΔH and ΔS calculated using equation (2) are the standard enthalpy and entropy of binding, respectively. These values describe reaction of A and B at standard pressure, temperature and concentration. It is noteworthy that when binding is favorable, K_{eq} is greater than one, ΔG is negative and the equilibrium in equation (1) lies to the right.

Assuming that the entropy of the model system decreases when A binds to B, binding is only favorable if the enthalpy term is sufficiently large and negative to overcome the positive entropy

term (-TΔS) of equation (2). In that case, the reaction is described as being enthalpically driven. However, it is not necessarily the case that ΔS is negative. For example, solvent may be highly organized around free A and/or B, but less so around the AB complex, resulting in a positive ΔS. In that case, the free energy of reaction may be negative, despite ΔH being positive, and the reaction is described as being entropically driven. In either case, the binding constant is greater than one.

2. the binding site in HSA

It is likely that the water molecules surrounding the thiolate of cysteine-34 will orient themselves around the negatively charged sulfur in a reasonably ordered manner. The dicyanogold(I) anion is negatively charged, linear and non-polar. Thus, the dicyanogold(I) anion also has associated water molecules oriented around the anion. The interaction of dicyanogold(I) with HSA likely involves loss or rearrangement of water molecules at the binding site. As this description more accurately depicts the composition of the interacting HSA-dicyanogold(I) system, it becomes clear that the thermodynamic quantities that have been measured experimentally represent the energy of binding which is associated not only with the formation of the gold-protein complex, but also with the release and/or rearrangement of the water molecules in or around the binding site (Table 23). In particular, this energy picture also includes any local conformational changes that occur as a result of gold binding to the protein. In the case of the HSA-dicyanogold(I) complex, it is apparent from the large positive value of ΔS for binding that the solvent and/or protein conformation are less organized than in the case of the dissociated components.

Table 23. K_{eq} and ΔG at 37°C and thermodynamic quantities for the HSA-dicyanogold(I) system.

	HSA
K_{eq}	5.8×10^5
ΔG	-35.4 kJ (-8.46 kcal)
ΔH	42.6 KJ/mol (10.2 Kcal/mol)
ΔS	248 J/mol*K (59.3 cal/mol*K)

For the purposes of understanding the thermodynamic contributions to enthalpy, the binding of dicyanogold(I) to HSA can be regarded as a two-step process. The first step is endothermic ($\Delta H>0$), involving rupture of specific solvent-protein and solvent-dicyanogold(I) interactions. The second step is exothermic ($\Delta H<0$) since it involves formation of the dicyanogold(I)-protein interactions. The positive enthalpy of binding observed for the dicyanogold(I)-HAS system indicates that the formation of favorable dicyanogold(I)-protein interactions does not entirely compensate for the loss of stabilizing solvent-protein and solvent-dicyanogold(I) interactions. The fact that ΔG is nevertheless negative is consistent with ΔS being sufficiently large to overcome ΔH in equation (2), shifting the equilibrium to the right.

Having explored some of the consequences of including water in the binding scenario, it is logical, at this point, to also include the ions that contribute to the ionic strength of the system. Ions migrate in solution so that they occupy the space near oppositely charged species. In this case, positively charged sodium ions tend to be clustered around the negatively charged sulfur of cysteine-34 and the dicyanogold(I) anion. So, at high ionic strengths, the apparent charge of an ion is effectively lowered. This means that either the attractive force between specific,

oppositely charged ions or the repulsive force between two ions of like charge is reduced. In the dicyanogold(I)-HSA system, the dicyanogold(I) is negatively charged and binds to HSA. Since the binding constant increases with increasing ionic strength, the dicyanogold(I) binding site is most likely close to or influenced by a negative charge on cysteine-34. In order to definitively elucidate the enthalpic and entropic origins of the increase in binding, data at several different temperatures are needed for each ionic strength solution.

3. the binding site in HSA•AA

In this case, the binding of dicyanogold(I) to HSA•AA is enthalpically driven, indicating that the formation of favorable dicyanogold(I)-protein interactions more than offsets the loss of solvent-protein and solvent-dicyanogold(I) interactions. While ΔH is negative and dominates the free energy equation, the entropy change upon binding of dicyanogold(I) to HSA•AA is positive, though much smaller in magnitude compared to the HSA-dicyanogold(I) system. As previously discussed, both the protein and the dicyanogold(I) anion are likely to have water molecules oriented around them. Therefore, the positive value for ΔS is consistent with one or more of the water molecules surrounding the binding site of the protein and/or the dicyanogold(I) anion being released and/or rearranged as a result of binding.

Table 24. K_{eq} and ΔG at 37°C and thermodynamic quantities for the HSA•AA-dicyanogold(I) system.

	HSA
K_{eq}	9.5×10^3
ΔG	-23.7 kJ (-5.68 kcal)
ΔH	-20.8 KJ/mol (-5.0 Kcal/mol)
ΔS	8.1 J/mol*K (1.9 cal/mol*K)

The ionic strength data show that K_{eq} remains reasonably constant with changing ionic strength. Since the binding appears to be unaffected within the range of ionic strengths tested, there is little or no change in the effective charge screening between dicyanogold(I) and the binding site on the protein by the ionic atmosphere. It is likely that the dicyanogold(I) binding site on HSA•AA is influenced by removal of the negative charge on cysteine-34.

5. comparing the binding sites in HSA and HSA•AA

Whereas the binding constants are somewhat similar, the thermodynamic data for binding of dicyanogold(I) to each of the forms of albumin, are distinctly different. Binding to HSA is entropically driven, whereas binding to HSA•AA is enthalpically driven. Since a non-covalent interaction between dicyanogold(I) and the protein is implicated in both cases, it is reasonable to suggest that the differences in binding are associated with differences between the two forms of the protein. The accumulated evidence suggests that the two forms are structurally identical with the exception of the local environment around cysteine-34. These differences can be summarized as follows. First, the sulfur of cysteine-34, which is a thiolate at the pH of blood, is

involved in a covalent bond with a carbon atom of the acetamide group transforming the previously negatively charged sulfur to neutral sulfur. Second, in order for the protein to accommodate the steric bulk of the added acetamide group the local conformation of the protein may change. Third, in accommodating the addition of the acetamide, cysteine-34 and the loop in which it is contained may "flip-out" and subsequently become locked into a single conformation (chapter 1, section E). Fourth, the acetamide group may introduce additional hydrogen bonding interactions to this portion of the protein.

In the case of HSA, an increase in entropy upon binding dicyanogold(I) dominates the free energy equation (2) causing the binding equilibrium in equation (1) to lie to the right. Whereas, in the case of HSA•AA, the increase in entropy has become so small that the free energy of binding dicyanogold(I) to the protein is essentially unaffected by temperature changes. This difference in ΔS can be attributed to two basic differences in the proteins: the conformational flexibility of the protein and the number of ordered water molecules that reside in or around the binding site. The first possibility is simply due to the added bulk of the acetamide group on cysteine-34, and the second possibility can be attributed to the presence or absence of the thiolate.

As the observed values for entropy of binding dicyanogold(I) to each form of albumin were vastly different, so were the observed values for the enthalpy of binding. For HSA the enthalpy of binding was positive while for HSA•AA the enthalpy of binding was negative. These properties, as well, can be explained in terms of the enthalpy associated with changing the local environment in order to bind dicyanogold(I). In the HSA-dicyanogold(I) system, it is possible that enough water molecules were released or rearranged so that the energy needed to accomplish this task exceeded the amount of enthalpic energy released upon binding of

dicyanogold(I) to HSA. In the HSA•AA-dicyanogold(I) system, it is possible that fewer specific solvent-solute interactions were disrupted, or more likely, the favorable protein-dicyanogold(I) interaction energy exceeded that of the HSA case. As a consequence, the free energy for binding dicyanogold(I) to HSA•AA was dominated by enthalpy rather than entropy.

In the HSA-dicyanogold(I) system, K_{eq} increases as ionic strength increases, whereas in the HSA•AA-dicyanogold(I) system, K_{eq} is relatively insensitive to changes in ionic strength. These results are consistent with a more concentrated ionic atmosphere in solution, favoring HSA-dicyanogold(I) interaction. This phenomenon can be generally attributed to screening of the interaction between two "macro-ions" of like charge. The absence of this increase in K_{eq} as a result of increased ionic strength in the HSA•AA-dicyanogold(I) system suggests that this form of albumin lacks the negative charge that is being screened in the HSA-dicyanogold(I) system. Since the only difference between the two systems, with respect to the charge state of the protein, is whether or not the sulfur of cysteine-34 is blocked with acetamide or present as a thiolate, then the binding of dicyanogold(I) to HSA must involve a reasonably close encounter with cysteine-34.

Focusing on the influence of the thiolate on the binding of dicyanogold(I) to HSA, it becomes possible to construct an explanation for the behavior observed in the binding studies conducted as a function of gold concentration. In both the Scatchard (reciprocal) and Klotz (double reciprocal) analyses two distinct binding sites were revealed. In each case there was a very high affinity site that occurred in about 1.2-1.4% of the total protein present and a lower affinity site that occurred in about 60-70% of the total protein present. The occurrence of this high affinity site correlates roughly to the amount of protein that is present with cysteine-34 in the thiol form at the pH of blood (about 1.3%; Chapter 1, Section E). Linking the binding

interaction between dicyanogold(I) and HSA to the presence of cysteine-34 in the thiolate form, indicates that the binding is influenced by the presence of cysteine-34 in the thiol form. It follows that since the binding constant increased as the ionic strength increased for the HSA-dicyanogold system, then the binding constant should increase to a greater degree if the protein remains unchanged except for the addition of a single proton, which presumably neutralizes the charge on the sulfur without changing the conformation of the region or changing the ability of the protein to adopt different conformations.

6. Future studies

In order to fully understand and characterize the binding interaction between dicyanogold(I) and human serum albumin, further experiments could be designed to explore this interaction. First, in order accurately analyze the concentration dependence of binding many more data points are required. In general, non-linear regression works best when there are at least 15 data points to fit, preferably more. Another interesting series of experiments would involve further exploration of the effect of ionic strength on binding. Obviously, a wider range of ionic strengths with more concentrations studied would fill in currently sparse data, but performing these experiments over a range of temperatures would yield more thermodynamic information about the binding interaction. Finally, other experiments could explore the effects of different groups being used to block the thiolate of cysteine-34.

Appendix A:
Penefsky chromatography

1. Introduction

Penefsky chromatography is similar to conventional size exclusion chromatography in that the stationary phase is generally Sephadex size exclusion material. The difference between Penefsky and conventional chromatography is that Penefsky chromatography couples the principles of size exclusion chromatography with fast elution times. By using centrifugal force to quickly elute the sample, the interaction between sample and the stationary phase of the column is reduced so that the small molecules in the sample partition into the Sephadex while the much larger protein molecules are completely excluded. This method offers an advantage over conventional size exclusion chromatography for binding constant determination because in the system under investigation the equilibrium will shift as free dicyanogold(I) is removed from the solution. So, for binding constant determination the quantity measured after separation via Penefsky chromatography is the concentration of the dicyanogold(I)-HSA complex at equilibrium. In this experiment, the goal was to compare the accuracy and precision associated with determining the binding constant using either Penefsky chromatography or ultrafiltration.

2. Experimental

To prepare Sephadex for use, it was soaked for several hours in distilled water. Once the Sephadex had swelled, the Penefsky size exclusion columns were prepared. A porous filter disc was fitted over the outlet of a syringe whose barrel measured approximately 1 cm in diameter and 6 cm in length. The swelled Sephadex was added to the syringe, filling it about ¾ full. Water was added to fill the rest of the syringe, the syringe was placed inside a test tube so that the syringe rested on the lip of the tube and the entire apparatus was centrifuged, using a Clay-Adams desktop centrifuge, for 2 minutes at 1200 rpm and room temperature. Sephadex and

water were added, followed by centrifugation until the length of the packed Sephadex was 2 cm. When the column was the appropriate length, the syringe was filled with water for storage. Immediately prior to use the columns were centrifuged, then the sample was introduced and, within 30 seconds, centrifuged again. After use the columns were cleaned by adding distilled water and centrifuging, repeating this step several times.

Buffer B was used in this experiment (10 mM Na_2HPO_4, pH 7.40). The protein solution for incubation with $KAu(CN)_2$ was made by dissolving 1.6255 g bovine serum albumin in 40 mL of buffer B (6.16×10^{-4} M BSA). To 5 mL of buffer B, 0.0146 g $KAu(CN)_2$ was added (0.0101 M). Four incubated solutions were made by combining 6 mL portions of the BSA solution with 0.1 mL, 0.2 mL, 0.3 mL, or 0.6 mL of $KAu(CN)_2$ solution and 0.5 mL, 0.4 mL, 0.3 mL, and 0.0 mL of buffer respectively so that the total volume of the incubated solutions was 6.6 mL. Additionally, 0.6 mL of buffer was added to 6 mL of BSA as a control that contained no gold. These solutions were incubated at room temperature for 30 minutes. A 0.2 mL aliquot of each solution was diluted to 2 mL and the concentration was determined by recording the UV absorbance at 278 nm (39600 $M^{-1}cm^{-1}$). The initial concentration of $KAu(CN)_2$ was determined by diluting 1 mL of each incubated solution and the control to 5 mL with buffer (except for the solution that contains the most gold which was diluted to 10 mL) then 1 mL of each dilute solution was combined with 2 mL 2% nitric acid in a microwave digestion bomb. The bomb was sealed and microwaved at high power for 30 seconds then allowed to cool for 30 minutes before opening. All digested samples were diluted 100-fold with 2% nitric acid for ICP-MS analysis. The Penefsky columns used in this experiment were found to retain 99.9% of the gold in a 5.83×10^{-4} M dicyanogold(I) solution.

Separation of the protein from the unbound $Au(CN)_2^-$ was performed by placing 0.75 mL of the incubated solution in the Penefsky column and adding 0.75 mL of buffer (a two-fold dilution). The Penefsky column was centrifuged at approximately 1200 rpm for 30 seconds. Two 0.75 mL aliquots from each incubated solution were separated in this manner. The eluent was digested as described above using 1mL of eluent and 2 mL of 2% nitric acid. Each of the digested solutions was diluted 100-fold with 2% nitric acid for ICP-MS analysis.

3. Results and discussion

Recall that in Penefsky chromatography the major assumption is that the samples are in contact with the column for so little time that the equilibrium is not shifted during elution of the protein. The deviation from equilibrium is directly related to length of time it takes for a system to reach equilibrium, i.e. systems that are slower to equilibrate are shifted less than systems that reach equilibrium quickly. So, in general, the less time that a sample spends in contact with the size exclusion medium, the more accurate the binding constant will be. It can be seen in the range of calculated binding constants (table 1) that the equilibrium of the dicyanogold(I)-HSA system is very sensitive to removal of dicyanogold(I) from solution as it partitions into the stationary phase of the Penefsky column.

Table A-1. Comparison of binding constants determined using either Penefsky chromatography or ultrafiltration.

Penefsky		**Ultrafiltration**	
Sample	K_{eq}	Sample	K_{eq}
1	3.0×10^4	1	5.9×10^4
2	1.7×10^4	2	5.7×10^4
3	2.1×10^4	3	6.1×10^4
4	3.8×10^3	4	6.2×10^4

The variability in this experiment stems from many sources. The most obvious source of variability is that the columns are not identical. There are minute differences in the amount of Sephadex contained in each column as well as differences in how the particles are packed upon centrifugation. Also there is an increased risk of contamination or sample loss with each dilution step performed. Because the eluent contains protein, it must be digested before it can be analyzed using the ICP-MS, adding both another dilution and the variability associated with the digestion bombs (23 mL Teflon digestion cups manufactured by Parr, Inc.).

While ultrafiltration proved to be a more reliable method for determining binding constants, the characteristic of Penefsky chromatography that prevented its use in binding constant determination was exploited to provide other information. It was found that at the low dicyanogold(I) concentrations used in the HSA-dicyanogold(I) binding experiments, all of the free dicyanogold(I) at equilibrium was removed from the incubated solution as it passed through the Penefsky column. It is also likely that as the equilibrium is disturbed during centrifugation of the Penefsky column gold is released by the protein and subsequently partitioned into the size exclusion material in the column. While this perturbation of the equilibrium was detrimental to the determination of binding constants, the same shift is the equilibrium ensures that after re-

equilibration all of the free gold found in the solution was released by the protein, and not due the residual starting material. So, approaching Penefsky chromatography from this perspective it was an essential method of separation for measuring the reversibility of the binding interaction between dicyanogold(I) and human serum albumin.

Appendix B:
Linear regression analysis of binding data

In many of the experiments discussed in this work, I have studied the binding interaction between dicyanogold(I) and human serum albumin. Proteins are complex systems in which there is ample opportunity for chemical interactions. This means that a protein may contain multiple binding sites for a small molecule. We have seen evidence for a binding site at low ligand concentration that interacts strongly with the ligand. At higher ligand concentrations there may be secondary binding sites as well. There are many analyses currently in use for graphically determining binding constants and numbers of binding sites for small molecule-protein interactions. Two often-used linear regression analyses are discussed below.

Changing the initial concentration of reactants such as the experiment described in chapter 1, section L-1, can be graphically analyzed to reveal the binding constant and number of binding sites. Traditionally, the Scatchard method is most often applied and has been used to analyze the binding of dicyanogold(I) to bovine serum albumin by Shaw and co-workers.[15] In the Scatchard method, the binding data are transformed into a linear representation by plotting the ratio of bound dicyanogold(I) to total HSA (B) on the x-axis and the equilibrium concentration of free dicyanogold(I) divided into that ratio ($B/[Au]_{free}$) on the y-axis. If there is a single binding site, the data will fall on a straight line, whereas, if there are multiple binding sites available, the data will fit a curved line.

The equation that represents the equilibrium constant, K_{eq}, is

$$K_{eq} = \frac{[HSA \bullet Au(CN)_2^-]_{eq}}{[HSA]_{eq}\,[Au(CN)_2^-]_{eq}} \qquad \text{(eq. B1)}$$

and, according to Rosenthal[26], it can be re-written,

$$K_{eq} = \frac{[\text{concentration of bound complex}]}{[\text{concentration of free binding sites}]\,[Au]_{free}} \qquad \text{(eq. B2)}$$

and subsequently rearranged,

$$K_{eq}[\text{concentration of free binding sites}] = \frac{[\text{concentration of bound complex}]}{[Au]_{free}} \quad \text{(eq. B3)}$$

It follows that the concentration of free binding sites can be represented as follows where n is the number of binding sites per molecule, $[P_0]$ is the initial concentration of protein and b is the concentration of bound complex.

$$[\text{concentration of free binding sites}] = (n\,[P_0]) - b \quad \text{(eq. B4)}$$

Re-writing equation B3,

$$n\,K_{eq}\,[P_0] - b\,K_{eq} = \frac{b}{[Au]_{free}} \quad \text{(eq. B5)}$$

Dividing each side of equation B5 by $[P_0]$,

$$n\,K_{eq} - \frac{b\,K_{eq}}{[P_0]} = \frac{b}{[P_0]\,[Au]_{free}} \quad \text{(eq. B6)}$$

Since the bound fraction, B, is the ratio of the bound complex to total protein ($B = b/[P_0]$), then equation B6 becomes the Scatchard equation used to plot the binding data mentioned above.

$$n\,K_{eq} - B\,K_{eq} = \frac{B}{[Au]_{free}} \quad \text{(eq. B7)}$$

It can now be seen in equation B7 that both the binding constant and the number of binding sites per molecule of protein can be determined. The slope of the line is equal to the negative binding constant, $-K_{eq}$, and the x-intercept is equal to the number of binding sites per molecule of protein, n.

The appeal of the Scatchard plot is that it is, in general, easier for the human eye to detect deviation from a line than it is to detect deviation from complex curve. In fact, when multiple binding sites are present, it is theoretically possible to include more than one best-fit line such that each separate line represents a class of binding sites. The deviation from linearity is easily visible in a Scatchard plot, but quantifying that deviation, i.e. determining specific values for K

and n for each class of binding site, can be difficult and involves significant error.[25] It follows that the larger the difference is between the binding constants of the two different sites causes the data to lie more distinctly along two or more straight lines.

Klotz[25] developed a second method for transforming the data to yield a linear plot using a double reciprocal treatment of the data. This second type of graphical analysis of binding data involves plotting the reciprocal of the equilibrium concentration of free dicyanogold(I) ($1/[Au]_{free}$) on the x-axis and the reciprocal of the ratio of bound dicyanogold(I) to total HSA (1/B) on the y-axis. A line of best fit drawn through the data can be used to determine the binding constant as well as the number of binding sites.

Starting with equation B2,

$$K_{eq} = \frac{[\text{concentration of bound complex}]}{[Au]_{free}\ [\text{concentration of free binding sites}]} \qquad \text{(eq. B2)}$$

and taking the reciprocal of each side,

$$\frac{1}{K_{eq}} = \frac{[Au]_{free}\ [\text{concentration of free binding sites}]}{[\text{concentration of bound complex}]} \qquad \text{(eq. B8)}$$

Substituting the values from equation B4,

$$\frac{1}{K_{eq}} = \frac{[Au]_{free}\ ((n\ [P_0]) - b)}{b} \qquad \text{(eq. B9)}$$

Rearranging,

$$b = n\ K_{eq}\ [Au]_{free}\ [P_0] - b\ K_{eq}\ [Au]_{free} \qquad \text{(eq. B10)}$$

Dividing by b,

$$1 = n\ K_{eq}\ [Au]_{free}\ [P_0]/b - K_{eq}\ [Au]_{free} \qquad \text{(eq. B11)}$$

$$n\ K_{eq}\ [Au]_{free}\ [P_0]/b = K_{eq}\ [Au]_{free} + 1 \qquad \text{(eq. B12)}$$

$$[P_0]/b = 1/n + 1/n\ K_{eq}\ [Au]_{free} \qquad \text{(eq. B13)}$$

Since the $b/[P_0]$ is the bound fraction, B, then equation B13 becomes the reciprocal equation used to plot the data mentioned above.

$$1/B = 1/n + 1/n\, K_{eq}\, [Au]_{free} \qquad \text{(eq. B14)}$$

It can now be seen in equation B14 that both the binding constant and the number of binding sites per molecule of protein can be determined from the reciprocal plot as well. The slope of the line is equal to the reciprocal of the number of binding sites per molecule multiplied by the binding constant ($1/nK_{eq}$) and the y-intercept is equal to the reciprocal of the number of binding sites per molecule of protein, 1/n. Because the reciprocal plot is also a linear transformation of the binding data, the same arguments for the validity of the Scatchard method can be used here.

Appendix C:
Studies of possible covalent bonding between cysteine-34 and gold drugs with various types of mass spectrometry

1. Introduction

Two of the three kinds of mass spectrometry used in this dissertation have been discussed previously with respect to characterization of the protein. Specifically, FT-ICR-MS was used to identify if iodoacetamide successfully alkylated the protein and how many of these groups were added. It was found that only a single acetamide group was present bound to the HSA. Using a combination of a tryptic digest followed by MALDI-TOF-MS, I showed that the acetamide group was, in fact, bound to the 21 amino acid digest fragment that contained cysteine-34. While these experiments do not reveal any direct evidence of a covalent bond between the acetamide and cysteine-34, it is possible to focus on the 21 amino acid sequence that contains the acetamide rather than continuing to consider the entire protein, which contains 535 amino acids. The progression of these experiments suggests that the technique developed here could be applied to other systems in which there is specific binding of a ligand to some amino acid.

Studies have been reported in the literature involving the reactions of gold drugs with serum albumin.[11, 27] Auranofin was shown to bind to serum albumin through cysteine-34 via conformational changes in the protein, and the proposed mechanism states that the acetylthioglucose ligand is lost and the remaining species, triethylphosphine gold, binds to the protein. In this work, preliminary studies using these methods described above for analyzing HSA-gold drug complexes were conducted. Both Auranofin and Myochrysine were used in these experiments; the structures of these drugs are shown in figure C-1.

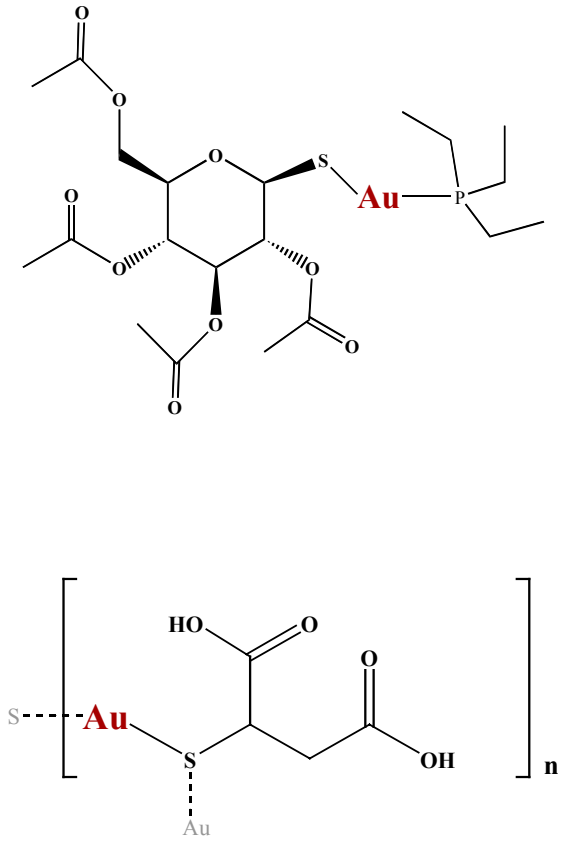

Figure C-1. Auranofin (top) and Myochrysine (bottom).

2. Experimental

In each case, approximately equimolar solutions of HSA and either Myochrysine or Auranofin were prepared in 40 mM $NaHCO_3$ buffer (pH 7.4), where the concentration of HSA and the gold drugs were approximately 3.5 x 10^{-8} mol/mL. The samples were made by combining 0.5 mL of HSA solution with 0.5 mL of gold drug solution and incubating at 37ºC for 3 hours. Following incubation, the sample solutions were desalted, as described in chapter 2, via dilution with water and ultrafiltration. A portion of each sample was digested with trypsin (see chapter 2 for protocol) and submitted to the University of Cincinnati Mass Spectrometry facility for MALDI-TOF-MS analysis. An undigested portion of each sample was analyzed using the Q-TOF instrument with electrospray ionization available in the UCMS facility.

3. Results and discussion

The data from the Q-TOF are very similar to the data from the FT-ICR-MS used previously in this work. Both instruments use electrospray ionization, which allows protonation of the protein to yield charge states up to 65+. The Q-TOF mass spectrum for HSA with Auranofin bound (figure C-2) shows a species with a molecular weight calculated to be 66,754 Da, which is 316 Da larger than the mass of HSA with no Auranofin added. Table C-1 lists the reported m/z values for each peak, the charge state for each peak and the calculated molecular mass for each peak. There are three Auranofin-HSA complexes that might be present in the reaction mixture: HSA plus Auranofin (646 Da), HSA plus tetraacetylthioglucose gold(I) (528 Da) and HSA plus triethylphosphine gold(I) (315 Da). The calculated mass of HSA with triethylphosphine gold(I) bound is 66,753 Da, which agrees with experimental value of 66,754 Da. The most straightforward interpretation is that only one Auranofin molecule has reacted per albumin and that the Auranofin has undergone thiol exchange with cysteine-34 to lose tetraacetylthioglucose and bind triethylphosphinegold(I)at cysteine-34.

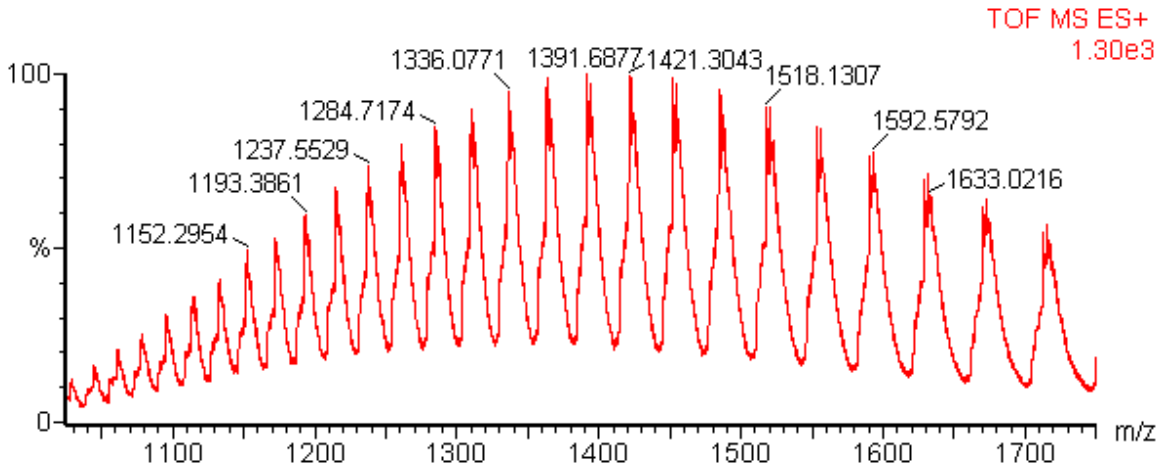

Figure C-2. Q-TOF mass spectrum of HSA-auranofin complex.

Table C-1. Peak table for Q-TOF-MS of HSA-auranofin complex.

z	m/z	mass	m/z	mass	difference	m/z	mass	difference
53	1260.5388	66755.556	1262.2799	66847.835	92.2783	1263.53	66914.02	158.4647
52	1284.7174	66753.305	1286.5045	66846.234	92.9292	1287.78	66912.53	159.2292
51	1309.8649	66752.110	1311.7581	66848.663	96.5532	1313.05	66914.33	162.2208
50	1336.0771	66753.855	1337.9594	66847.970	94.1150	1339.24	66912.24	158.3850
49	1363.3486	66755.081	1365.2649	66848.980	93.8987	1366.62	66915.58	160.4946
48	1391.6877	66753.010	1393.6698	66848.150	95.1408	1395.10	66916.98	163.9728
47	1421.3043	66754.302	1423.3226	66849.162	94.8601	1424.62	66910.03	155.7298
46	1452.1820	66754.372	1454.2222	66848.221	93.8492	1455.64	66913.45	159.0818
44	1518.1307	66753.751	1520.3282	66850.441	96.6900			
43	1553.3846	66752.538	1555.6077	66848.131	95.5933	1556.99	66907.73	155.1913
42	1590.3790	66753.918	1592.5792	66846.326	92.4084	1594.08	66909.34	155.4252
41	1629.1277	66753.236	1631.4701	66849.274	96.0384	1633.02	66912.89	159.6499
40	1669.8115	66752.460	1672.2163	66848.652	96.1920			
39	1712.5858	66751.846	1715.1565	66852.104	100.2573	1716.71	66912.83	160.9842
Average		66754		66849	95		66913	159
Standard Dev.		1		1	2		3	3

The Q-TOF mass spectrum for HSA with Myochrysine bound (figure C-3) shows a species with a molecular weight of approximately 66,785 Da, which is 347 Da larger than the mass of HSA with no Myochrysine (M.W. = 345 Da) added. Table C-2 lists the reported m/z values for each peak, the charge state for each peak and the calculated molecular mass for each peak. While these results are less conclusive than those for Auranofin, they indicate that the monomeric unit of gold(I)thiomalic acid likely has added in place of the proton on cysteine-34.

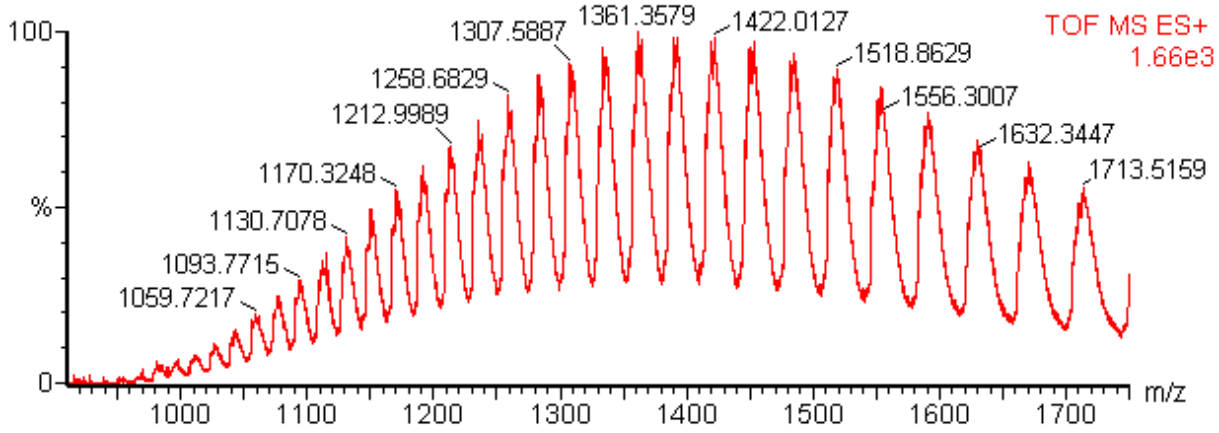

Figure C-3. Q-TOF mass spectrum of HSA-myochrysine complex.

Table C-2. Peak table for Q-TOF-MS of HSA-myochrysine complex.

z	m/z	mass	m/z	mass	difference
53	1258.6829	66657.194	1261.1482	66787.855	130.6609
52	1282.3756	66631.531	1285.3179	66784.531	152.9996
51	1307.5887	66636.024	1310.3676	66777.748	141.7239
50	1334.0769	66653.845	1336.6147	66780.735	126.8900
49	1361.3579	66657.537	1364.1028	66792.037	134.5001
48	1389.5092	66648.442	1392.2975	66782.280	133.8384
47	1419.2258	66656.613	1422.0127	66787.597	130.9843
46	1450.0499	66656.295	1452.9137	66788.030	131.7348
45	1481.6770	66630.465	1485.0599	66782.696	152.2305
44	1515.3942	66633.345	1518.8629	66785.968	152.6228
Average		66646		66785	139
Standard Dev.		12		4	10

The examination of the tryptic digests was made to see if the same gold moiety that had added to the albumin as a whole as shown by Q-TOF could be seen added to the fragment (21-41) expected from the digestion. The results for the MALDI-TOF analysis of both protein-gold drug complexes were negative. The fragment of interest, amino acids 21-41 with a mass of 2433 Da, did not appear in any of the spectra obtained and there were no other peaks that could be identified as gold-bound fragments. The absence of this peak does not necessarily mean that the fragment does not exist, but it is more likely that the fragment does not ionize easily.

A number of changes could be made to the procedures used to characterize the gold drug-protein complex in order to increase the likelihood of success. Techniques involving LC-MS and LC-MS-MS could be used to study the tryptic digest fragments of these complexes using the Q-TOF-MS with electrospray ionization rather than MALDI-TOF-MS. There are also protocols available for derivatizing the ends of the tryptic digest pieces that would increase the ability of the piece to be ionized via MALDI, and thereby increasing the possibility that the fragment of interest will appear in the MALDI-TOF mass spectrum. There are also other enzymes available to digest proteins which will result is different fragments. This would allow for a comparison between tryptic digest pieces and digest pieces (from other enzymes) that contain cysteine-34 as well as an opportunity to observe the appropriate fragment in the MALDI-TOF mass spectrum. Ideally, it is necessary to identify all of the digest fragments and subsequently check for possible gold drug binding to each fragment, which can be done using either MALDI-TOF-MS or LC-MS using the Q-TOF (with electrospray ionization).

(1) Forestier, J. *J. Lab. Clin. Med.* **1935**, *20*, 827-840.

(2) Srinivasan, R.; Miller, B.; Paulus, H. *Arth. Rheum.* **1979**, *22*, 105.

(3) Zhang, Y.; Hess, E.; Pryhuber, K.; Dorsey, J.; Tepperman, K.; Elder, R. C. *Inorganica Chimica Acta* **1995**, *229*, 271-280.

(4) Felson, D.; Anderson, J.; Meenan, R. *Arth. Rheum*. **1990**, *33*, 1449-1461.

(5) Elder, R. C.; Zhao, Z.; Zhang, Y.; Dorsey, J.; Hess, E.; Tepperman, K. *J. Rheum.* **1993**, *20*, 268-272.

(6) Zhang, Y. Ph.D. Thesis, University of Cincinnati, Cincinnati, OH, 1996.

(7) Rudkowski, R.; Graham, G.; Champion, G. D.; Ziegler, J. *Biochem. Pharm*. **1990**, *39*, 1687-1695.

(8) Shaw, C. F., III; Isab, A.; Coffer, M.; Mirabellis, K. *Biochem. Pharm*. **1990**, *40*, 1227-1234.

(9) Guo, Z.; Sadler, P. *Angew. Chem. Int. Ed.* **1999**, *38*, 1512-1531.

(10) Peters, T., Jr *All About Albumin: Biochemistry, Genetics, and Medical Applications*; Academic Press: San Diego, California, 1996.

(11) Christdoulou, J.; Sadler, P.; Tucker, A. *FEBS Letters* **1995**, *376*, 1-5.

(12) Cleland, W. *Biochemistry* **1964**, *3*, 480.

(13) Isles, T.; Jocelyn, P. *Biochem. J.* **1963**, *88*, 84-88.

(14) Moreano, F.; Gonzalez-Jimenez, J. *Chemico-Biol. Interactions* **1999**, *121*, 237-252.

(15) Canumalla, A.; Schraa, S.; Isab, A.; Shaw, C. F., III; Gleichmann, E.; Dunemann, L. *J. Biol. Inorg. Chem.* **1998**, *3*, 9-17.

(16) Boyde, T. R. C. *J. Chem. Soc. (C)* **1968**, 2751-2753.

(17) Ultrafiltration (I can't seem to find this one right now…)

(18) Harris, D. C. *Quantitative Chemical Analysis, 4th Ed.* W. H. Freeman and Company: New York, 1995.

(19) Canumalla, A.; Shaw, C. F., III; Wagner, F. *Inorg. Chem.* **1999**, *38*, 3268-3269.

(20) Stubhardt, J. *The Proteins II, 2nd Ed.* Neurath, H., Ed. Academic Press, New York, 1964; 139-304.

(21) Mathews, C.; van Holde, K. *Biochemistry, 2nd Ed*. Scanlan-Rohrer, Ed. Benjamin/Cummings Publishing Company, Inc. 1996; 46-48.

(22) I. M. Klotz, D. L. Hunston, *Biochemistry* **1971**, *10*, 3065.

(23) Atkins, P. W. *Physical Chemistry, 4th Ed.* W. H. Freeman and Company: New York, 1990, 219-221.

(24) Hendrickson, C. L.; Emmett, M. R. *Annual Review of Physical Chemistry* **1999**, 50, 517.

(25) Limbach, P. A. *Spectroscopy* **1998**, 13, 16.

(26) Clauser K. R., Baker P. R. and Burlingame A. L., *Analytical Chemistry*, **1999**, 71, 14, 2871.

(27) Walker, J. M., ed. *The Protein Protocols Handbook*; Chapter 71, pp. 415-425 Humana Press: Totowa, N.J., 1996.